Understanding the winter flounder (Pseudopleuronectes americanus) Southern New England / Mid-Atlantic stock through historical trawl surveys and monitoring cross continental shelf...

Thesis · May 2015

DOI: 10.7282/T35T3NBD

1 author:

Kaycee E Coleman

U.S. Fish and Wildlife Service

4 PUBLICATIONS **12** CITATIONS

SEE PROFILE

UNDERSTANDING THE WINTER FLOUNDER (*PSEUDOPLEURONECTES AMERICANUS*) SOUTHERN NEW ENGLAND / MID-ATLANTIC STOCK THROUGH HISTORICAL TRAWL SURVEYS AND MONITORING CROSS CONTINENTAL SHELF MOVEMENT

by

KAYCEE E. COLEMAN

A thesis submitted to the

Graduate School – New Brunswick

Rutgers, The State University of New Jersey

In partial fulfillment of the requirements

For the degree of

Master of Science

Graduate Program in Oceanography

Written under the direction of

Thomas M. Grothues

and approved by

_____

_____

_____

New Brunswick, New Jersey

May, 2015

ABSTRACT OF THE THESIS

Understanding the winter flounder (*Pseudopleuronectes americanus*) Southern New England / Mid-Atlantic stock through historical trawl surveys and monitoring cross continental shelf movement

By KAYCEE E. COLEMAN

Thesis Director:
Thomas M. Grothues

The goal of this study was to better understand where adult winter flounder (*Pseudopleuronectes americanus*) are, both in distribution and while seasonally spawning in the central to southern Mid-Atlantic Bight, through the use of historic datasets and tagging and tracking methods. I accomplished this with the use of three historic bottom trawl surveys to investigate if there was a shift in the distribution of winter flounder at the southern extend of the their range. In addition, the relationship between ocean temperatures and winter flounder centers of biomass and abundance was tested to see if temperature was a driver. To characterize seasonal migration, adult winter flounder (n=231) were tagged with three tag types. I targeted adult fish, using fish length and the gonadosomatic index as an indicator. To reconstructing an individual's location using the environmental data recorded from a data logging archival tag, three state space models were developed and tested for model accuracy.

I subsampled the trawl data and used data below the Hudson Valley and found that the distribution of winter flounder has shifted over the last few decades. A distributional shift north along the continental shelf was the most common trend across surveys, but there were several other changes in the distribution (e.g., across shelf location and depth) that

were season and survey specific. These spatial shifts, along with abundance, were not temporally similar to an increase in ocean temperatures.

While the tagging efforts were successful, I had a low recapture rate. Most of the tagged fish were female and mature. I observed two movement behaviors in the fall of 2012, including two individuals that moved inshore and north from the release site and two offshore.

The recovery of one archival tag helped inform the three state space models developed. I used two data matching and simulation state space models and one particle filter model to reconstruct fish location. All of the models were tested on simulated known fish paths, and while they performed similarly on short time scales, at larger time scales the particle filter outperformed the data matching and simulation state space models.

ACKNOWLEDGEMENTS

I thank T. M. Grothues, K. W. Able, O. Jensen, J. Wilkin, M. Pinsky, J. Dobarro, R. Petreca, N. Giraldi, E. Hunter, E. Curchitser, W. Bajwa, and K. Bekris for support and advise; the captains and crew of the *R/V SeaWolf, F/V Viking II, M/V Venture III*, and *M/V Fin-Ominal* for their assistance in tagging efforts; the National Marine Fisheries Service, the Northeast Area Monitoring and Assessment Program, and the American Littoral Society (especially J. Dement) for their cooperation with data; the New Jersey Department of Environmental Protection (especially G. Hinks and L. Barry) for their cooperation with data and allowing me to participate in their groundfish surveys; the Manasquan River Marlin and Tuna Club, George Burlew Scholarship and Rutgers University Marine Field Station Scholarship for funding; and most importantly the New Jersey SeaGrant (especially M. Danko) for funding and assistance.

I would also like to thank T. Young, M. Provost, N. Waite, A. Lopez, S. Lietzke, C. Haskins, C. Denisevich, C. Van Pelt, J. Valenti, R. Speiser, and my family for their support and encouragement.

TABLE OF CONTENTS

ABSTRACT OF THE THESIS……*ii*

ACKNOWLEDGEMENTS ……*iv*

TABLE OF CONTENTS ……*v*

LIST OF TABLES ……*vii*

LIST OF FIGURES ……*xi*

Chapter 1: General Introduction ……1

Chapter 2: Changes in the distribution, abundance, and weight of southern Mid-Atlantic Bight winter flounder: is temperature responsible?

Abstract……8

2.1 Introduction ……8

2.2 Methods ……13

2.3 Results ……15

2.4 Discussion ……19

Chapter 3: Tagging and tracking winter flounder: Multiple approaches used in the Mid-Atlantic

Abstract……41

3.1 Introduction ……41

3.2 Methods ……47

3.3 Results ……53

3.4 Discussion ……55

Chapter 4: Path reconstruction for tagged Mid-Atlantic fish

Abstract……80

4.1 Introduction ……80

4.2 Methods ……82

4.3 Results ……95

4.4 Discussion ……98

Chapter 5: General Conclusions ……116

Literature Cited ……119

LIST OF TABLES

– Chapter 2 –

Table 1. Winter flounder collection methods for DEP, NEAMAP, and NEFSC bottom trawl surveys, including areas covered, and range of temperatures and depths sampled. See Figure 1 for sampling area.

Table 2. Regression results of winter flounder spatial, size, and abundance metrics, as well as, an environmental variable to time, by season and for yearly average, as observed in the DEP survey. Significant ($\alpha = 0.05$) results are in bold. See Figure 1 for sampling area.

Table 3. Regression results of winter flounder spatial, size, and abundance metrics, as well as, an environmental variable to time, by season and for yearly average, as observed in the NEFSC offshore survey. Significant ($\alpha = 0.05$) results are in bold. See Figure 1 for sampling area.

Table 4. Regression results of winter flounder spatial, size, and abundance metrics, as well as, an environmental variable to time, by season and for yearly average, as observed in the NEFSC inshore survey. Significant ($\alpha = 0.05$) results are in bold. See Figure 1 for sampling area.

Table 5. Regression results of winter flounder spatial, size, and abundance metrics, as well as, an environmental variable to time, by season and for yearly average, as observed in the NEAMAP survey. Significant ($\alpha = 0.05$) results are in bold. See Figure 1 for sampling area.

Table 6. Cross correlation coefficient (C), at zero-lag, of the geometric mean catch of winter

flounder and average bottom water temperature observed by each survey for each year, by season and for yearly average, after the respective means have been subtracted. Significant ($\alpha = 0.05$) results are in bold (P). Number of years used is defined by N.

Table 7. Results of two general linear models modeling winter flounder catch-per-tow, each with a Poisson distribution link function. All variables are significant at $\alpha = 0.001$ level. The Akaike information criterion (AIC) is listed. Model 1 does not include temperature as an explanatory variable but Model 2 does.

Table 8. Results of ANOCOVA comparing winter flounder spatial, size, and abundance metrics, as well as, an environmental variable across surveys (DEP, NEFSC offshore, NEFSC inshore, and NEAMAP) for all seasons sampled and the yearly average. Significant ($\alpha = 0.05$) results are in bold.

Table 9. Results of Tukey's honest significant difference test on pairwise comparisons testing which surveys (DEP, NEFSC offshore, NEFSC inshore, and NEAMAP) had significantly different results for winter flounder and environmental metrics tested. Only variables that were significant in the ANOCOVA are included in this table. Significant ($\alpha = 0.05$) results are in bold.

– Chapter 3 –

Table 3.1. All acoustically tagged winter flounder were caught by trawl 8 on 9/7/12 and released at the Mud Hole (40.1588, -73.6842). Released fish were selected based on a condition rating high enough to likely survive after being tagged. See Figure 1 for location.

Table 3.2. Winter flounder with archival tags were caught on Sept. 6 and 7, 2012 at the Mud Hole (by trawls 1-7), as well as, in October 2012 and January 2013 off of northern New Jersey with the New Jersey Department of Environmental Protection (DEP). Tag 6663 occurs twice because the tag was reused after recapture and the data record was removed. Released fish were selected based on a condition rating high enough to likely survive after being tagged. See Figure 1 for location.

Table 3.3. Winter flounder with American Littoral Society (ALS) marker tags were released across the whole study period (at the Mud Hole and ranging the coast of New Jersey, from June 2012 - May 2014). One tag (ID no. 825083) remained unused since it was used in a tank study on tag retention.

Table 3.4. Winter flounder gonad data was collected on Sept. 6, 2012 at the Mud Hole and used to identify the sex of the winter flounder and the proportion of mature individuals. This was determined by visual inspection of the gonad and weighing the total body mass of the individual and the gonad mass separate from the body. A gonadosomatic index (GSI) in addition to comparing the individual's length to literature defining size at maturing for the Mid-Atlantic Bight and Southern New England sector was used to determine maturity.

– Chapter 4 –

Table 4.1. Pseudocode for the data matching and simulation model

Table 4.2. Pseudocode for particle filter model

Table 4.3. Path reconstruction results using the data matching and simulation Righton and Mills (2008) method. I defined each simulated known path by the path number (1-20) and the subsample of the time series used is denoted by days (11, 31, or 92). The residuals and standard deviation (STDEV) here are calculated using the kernel density method. The number of successfully reconstructed paths is out of 100,000 possible paths. The time in which the model took to run (successful or not) is recorded in seconds.

Table 4.4. Path reconstruction results using the data matching and simulation Ådlandsvik *et al.,* (2007) method. I defined each simulated known path by the path number (1-20) and the subsample of the time series used is denoted by days (11, 31, or 92). The residuals and standard deviation (STDEV) here are calculated using the kernel density and the arithmetic mean method. The number of successfully reconstructed paths is out of 10,000 or 100,000 possible paths. The time in which the model took to run (successful or not) is recorded in seconds.

Table 4.5. Path reconstruction results using the particle filter method. I defined each simulated known path by the path number (1-20) and the subsample of the time series used is denoted by days (11, 31, or 92). The residuals and standard deviation (STDEV) here are calculated using the kernel density and the arithmetic mean method. The number of successfully reconstructed paths is out of 100 or 1,000 plausible states kept at each time step. The time in which the model took to run (successful or not) is recorded in seconds.

LIST OF FIGURES

– Chapter 2 –

Figure 2.1. Areas sampled for winter flounder in each survey with the Northeastern Fisheries Science Center (NEFSC) in blue, Northeastern Fisheries Science Center inshore (NEFSC inshore) portion in green, the Northeastern Area Monitoring and Assessment Program (NEAMAP) in yellow, and the Department of environmental Protection (DEP) in red. The coastline is denoted in black. Inshore surveys (DEP, NEFSC inshore, and NEAMAP) all overlap off of NJ. The NEFSC inshore and NEAMAP surveys overlap spatially for the whole costal study area. The NEFSC offshore survey has minor overlap off of southern NJ with other surveys but is mainly focused offshore.

Figure 2.2. Fall centers of biomass for winter flounder in each survey with the Northeastern Fisheries Science Center (NEFSC) in blue, Northeastern Fisheries Science Center inshore (NEFSC inshore) portion in green, and the Department of environmental Protection (DEP) in red.

Figure 2.3. The spawning stock biomass yearly average centers of biomass for winter flounder in each survey with the Northeastern Fisheries Science Center (NEFSC) in blue, Northeastern Fisheries Science Center inshore (NEFSC inshore) portion in green, the Northeastern Area Monitoring and Assessment Program (NEAMAP) in yellow, and the Department of environmental Protection (DEP) in red.

– Chapter 3 –

Figure 3.1. Distribution of tagged winter flounder released during 2012-2013 (see Tables 1, 2, and 3 for addition details) including American Littoral Society (ALS), Archival, and

Acoustic tags. The bathymetry is shaded in blue with dark blue denoting deeper and light blue denoting shallower and the coastline marked in green. The Mud Hole is a portion of the Hudson Shelf Valley. The hydrophones (denoted by purple stars) were set near the mouths of the Manasquan River, Navesink River, and Shark River to detect movement into New Jersey estuaries.

Figure 3.2. The length (cm) frequency distributions for winter flounder by each tag type including American Littoral Society (ALS), Archival, and Acoustic tags.

Figure 3.3. (A) An example of the search pattern to track acoustically tagged winter flounder used for the AUV (red) as well as the search pattern used by the boat (blue) on Sept. 7, 2012. (B) A subset map includes the initial acoustic tag distribution in relation to the release point (green) and the boat GPS track, which is used to pinpoint position. Fish are denoted in pink with tag identification number underneath.

Figure 3.4. Recovered winter flounder with archival tag (ID no. 6663), dorsal and ventral views.

Figure 3.5. Graph of a spectral analysis used to determine the most influential tidal state experienced by the fish so that tide can be removed from the archival tag depth data. The period is in hours and the power determines the dominant signal.

Figure 3.6. Graph of a depth record from a winter flounder tagged with an archival tag. The raw depth data (in blue) and the depth data with the tidal signal removed (in green), using a nyquist frequency (ns) of 24 to maintain as much of the time series as possible.

Figure 3.7. The daily averaged and raw temperature recorded of a winter flounder with archival tag ID no. 6663. This tag was release and recaptured out near the Mud Hole in September 2012.

Figure 3.8. The daily averaged salinity observed by a winter flounder with archival tag ID no. 6663. This tag was release and recaptured out near the Mud Hole in September 2012.

Figure 3.9. Temperature range experienced by tag ID no. 6663 as recorded every 24 minutes, with error of ±0.1°C. This tag was release and recaptured out near the Mud Hole in September 2012.

Figure 3.10. Salinity range experienced by tag ID no. 6663 as recorded every 24 minutes, with error of ±1. This tag was release and recaptured out near the Mud Hole in September 2012.

– Chapter 4 –

Figure 4.1. The model domain on the Northeastern U.S. shelf for the ROMS ESPreSSO data, including grid and bathymetry. This image is from http://www.myroms.org/espresso/espresso_grid.png.

Figure 4.2. An illustration of the State Space Model framework used, including the measurements (Y), our unknown (X) across time (T).

Figure 4.3. Simulated paths for 11, 31, and 92 days in the New York Bight (off of New Jersey and below Long Island, New York) with the New Jersey coastline, different paths are denoted by the change in color. Release was on Sept. 6, 2012.

– Chapter 1 –

GENERAL INTRODUCTION

Statement of Problem

The Magnuson-Stevens Act (1996) recognizes that there is an urgent need for habitat-related fisheries management to protect 'Essential Fish Habitat' for all life stages (Stoner *et al.*, 2001). There are two problems inherently critical to the management of winter flounder (*Pseudopleuronectes americanus,* Walbaum 1792) and their habitat. First, the species is in marked decline, as recognized by fishery managers, fishers and other resource managers (Mayo and Terceiro, 2005). Second, the status of winter flounder influences how we manage many habitats in New Jersey and elsewhere in the northeastern U. S. since several regulations focus on winter flounder, especially relative to dredging. Resolving these issues will enhance managers' ability to manage this species and the estuarine and continental shelf habitat that winter flounder rely upon.

Dredging, a common practice on the east coast, is performed in estuaries to maintain navigation channels for local commerce and recreation as well as on the inner continental shelf for beach replenishment (Maa *et al.,* 2004; Diaz *et al.,* 2004; Kelley *et al.,* 2004; Nairn *et al.,* 2004). The concern is that these dredging activities may negatively influence habitat quality in these ecosystems. Most attempts to evaluate the effects of dredging on important finfish resources assume that they are stationary in space and time. Unlike most other marine finfish, winter flounder spawn demersal, adhesive eggs (Pearcy 1962; Scarlett and Allen, 1992), leaving the egg stage highly susceptible to benthic disturbances such as dredging. A current definition of winter flounder 'spawning habitat' as strictly estuarine results in denial of many winter-spring dredging permits in estuaries of New England and the Mid-Atlantic states and subsequently impacts maritime industries. However, accumulating evidence suggests this species is quite mobile, that its movements

are variable, and that spawning may take place in estuaries and on the inner continental shelf (DeCelles and Cadrin, 2010; Fairchild *et al.,* 2013; Wuenschel *et al.,* 2009). Current attempts to define the time and location of dredging activities do not take these dynamics into consideration. The validity of the current spawning habitat definition thus remains unclear, with the implication that legal mechanisms for winter flounder protection are either too restrictive or too lax. This is most evident in the New Jersey and New York portions of New York Harbor as well as in Cape May, New Jersey.

Background

Winter flounder, a recreationally and commercially important pleuronectid, are found in the northeastern part of North America, ranging from Labrador to Georgia (Bigelow and Schroder, 1953), but are most abundant from the Gulf of St. Lawrence to Chesapeake Bay and are rarely found below this point (Able and Fahay, 1998). There are three defined stocks in the northeastern United States: the Southern New England/ Mid-Atlantic Bight (SNE/MAB) stock, Gulf of Maine (GOM) stock, and Georges Bank (GB) stock (ASMF, 2005). Commercial landings for the winter flounder SNE/MAB stock peaked in 1981 and then sharply declined in the following decade due to overfishing (Mayo and Terceiro, 2005). An increase in estuarine temperature compounded the impacts of overfishing inhibiting stock recovery (Bell *et al.*, 2014a).

Winter flounder are often found in several substrates including muddy sand, patchy eelgrass, clay, sand, pebbles, and gravel (Pereira *et al.,* 1999; Collette and Klein-MacPhee, 2002, Young *et al.,* 2004) as well as sediments mixed with shell or wood debris (Howell and Molnar, 1995). They have an upper lethal temperature limit of 26°C (McCracken, 1963) to 31.4°C (Gift and Westman, 1971) and can burry up to 15 cm in the sediment in extreme cold (Fletcher, 1977) or heat (Olla *et al.*, 1969) to thermoregulate. Although it is commonly believed that winter flounder move offshore when inshore temperatures increase during

summer months, adult winter flounder are capable of withstanding warm temperatures through behavioral modifications, including: burial in sediment, reduced swim speeds, and inactivity (Olla *et al.,* 1969; He, 2003). By burying 6 cm into the sediment, winter flounder can remain roughly 4°C cooler (Olla *et al.,* 1969). Reported adult temperature avoidance ranges between 20.2°C (McCracken, 1963) to 24°C with movement stopping at 22°C (Olla *et al.,* 1969). At the opposite extreme, to prevent their blood serum from freezing, which occurs between -1.25 and -1.38°C (Fletcher, 1977), another avoidance technique is to relocate to deeper waters during the winter. In New Jersey, the average preferred annual bottom water temperature is 9.5°C (Winton *et al.*, 2014), yet a preferred range of 12-15°C is commonly reported for the species (McCracken, 1963; Pereira *et al.,* 1999).

Since they range between the upper estuaries to the ocean, winter flounder can tolerate a salinity of 15 and higher, with mortality around 8 (Brown *et al.*, 2000). Winter flounder habitat defined in the Navesink River/Sandy Hook Bay estuary, New Jersey, included: newly settled flounder (<25mm) preferred temperatures < 16°C, salinity between 13-23, and sediments with high organic content; juveniles of size 25-55 mm preferred a depth of < 5 meters, salinity between 15-24, with low sediment organic content in high temperatures and high salinity suggesting out river movement in high temperature; and juveniles of >55 mm preferred depths < 2m, temperature 16-27°C, salinity <23, and algal biomass > 3 g m^{-2} (Stoner *et al.*, 2001). Able and Fahay (1998) and others have suggested that young-of-the-year winter flounder are habitat generalists, with no distinct habitat preference due to this wide range (Phelan *et al.,* 2001; Stoner *et al.,* 2001; Goldberg *et al.,* 2002). Since winter flounder do not appear to be substrate-specific spawners, they have been reported to deposit their eggs on gravel bars, algal mats, eelgrass beds, and near freshwater springs (Crawford, 1990). A positive relationship between prey (e.g., Ampeliscidae, Spionidae) abundance and winter flounder abundance is also reported

(Stoner *et al.,* 2001, Phelan *et al.,* 2001; Goldberg *et al.,* 2002). Predators such as birds, fishes, shrimp, and crabs also influence distribution of young winter flounder (Witting and Able, 1995; Manderson *et al.,* 2000; Chambers *et al.,* 2001; Manderson and Pessutti, 2004; Manderson, 2006; Gibson, 2013).

Winter flounder can grow to 580 mm, and live a maximum of 15-20 years (Pereira *et al.,* 1999). Growth rates and maturity vary between stocks with the GB stock having the fastest growth to the largest size and maturing early at a small size, while the GOM stock grows slowest, reaches the smallest size and matures latest at a large size (O'Brien *et al.,* 1993). In the SNE/MAB stock, females mature at three years while males mature at two years of age (Klein-MacPhee, 2002). Specifically in the Mid-Atlantic portion and the Southern New England portion, median female age of maturity is 2.4 (±0.1) years, and 3.1 (±0.1) years, but can range between 1-6 and 1-8 years respectively (McBride *et al.*, 2013).

Winter flounder are iteroparous capital spawners in that they spawn once a year, are synchronous in ovulation, and all of the oocytes ripen at the same time; however, they are behavioral batch spawners in that spawning can happen over multiple events spanning days to weeks laying separate batches of eggs (Stoner *et al.,* 1999; Press *et al.,* 2014). Spawning in the SNE/MAB stock can occur as early as December (offshore of New Jersey) (Chambers *et al.,* 1995; Wuenschel *et al.,* 2009) but peaks in February and can extend until late April (Press *et al.*, 2014).

Winter flounder typically spawn in water between 3-7°C (Chambers *et al.,* 1995; Stoner *et al.,* 1999; Klein-MacPhee, 2002). Spawning and egg survival is temperature-related, with a negative relationship to egg survival and fitness as temperature increases (Keller and Klein-MacPhee, 2000). Poor recruitment can coincide with warm estuarine waters in winter (Bell *et al.*, 2014a), and spring (Able *et al.*, 2014), but is most likely due to changes in timing of predator/prey overlap (Manderson, 2006).

Because spawning is temperature related, ocean temperature change over the last few decades (Friedland and Hare, 2007; Mills *et al.,* 2013), could shift spawning seasonality. In a New York/New Jersey harbor, a shift to later spawning seasonality during severe winters as compared to moderate winters has already been observed (Wilber *et al.*, 2013).

As of late there have been several disputes about where winter flounder are spawning as well as how stocks should be defined. Stocks used to be defined as individual populations for an estuary because of a high return rate to that estuary (i.e. 90% of adults from Green Hill Pond, Rhode Island, returned to the Rhode Island sound)(Salia, 1961). Tagging studies have shown that winter flounder display homing or site fidelity to their spawning grounds (Perlmutter, 1947; Saila, 1961; Phelan, 1992; Fairchild *et al.,* 2013), which could inhibit egg survival but not the act of spawning during unfavorable conditions (Harden Jones, 1968).

Several authors support the existence of local stocks (especially within the SNE/MAB) based on fin ray counts and adult size (Bigelow and Schroeder, 1953), age and size of maturation (Winton *et al.*, 2014) and genetics of young of the year (Buckley *et al.*, 2008), which could confound management. Yet, a recent genetic study by Wirgin *et al.,* (2014) supports the current three stock structure in the United States.

Since dispersal is limited or non-existent in the egg stage, and larvae are often trapped by hydrological features within estuarine spawning areas (Pearcy, 1962; Crawford and Carey, 1985; Chant *et al.,* 2000), for winter flounder, it is most likely that genetic diversity is an adult-mediated process rather than larval-mediated connectivity that is common in other species (Frisk *et al.*, 2014). These same reasons that promote local population structure (e.g. site fidelity) through estuarine spawning, also make young winter flounder vulnerable to human impacts such as dredging, pollution, eutrophication, and elevated temperatures which often occur in estuaries (Nelson *et al.,* 1991).

Winter flounder as a species do not require estuaries as spawning habitat as evidenced by members of the Georges Bank stock, yet for the inshore stocks (SNE/MAB and GB) this has historically been the predominant spawning strategy. We do not know if differences in spawning habitat choice among stocks reflect obligate conditions. In recent studies, location of spawning is varied and includes reported residency in the ocean and estuaries, but also seasonal ocean to estuary movements and the reverse (see *Wuenschel et al.,* 2009; DeCelles and Cadrin, 2010; Able and Fahay, 2010 for reviews). The reasoning behind these differences is not well understood, with behavior, phenotype, or yearly fecundity speculated as the causes in determining the location of spawning (McBride *et al.*, 2013). With the addition of the coastal spawning strategy, winter flounder essential fish habitat boundaries might need to be reconsidered (Fairchild *et al.*, 2013).

Project Goals and Objectives

My goal was to enhance understanding of winter flounder connectivity between estuarine and continental shelf habitats and thus address issues related to the decline of winter flounder and management of its habitats. Specifically, I 1) evaluated the decline in abundance and the distributional response over time and to temperature using historical trawl datasets from the northeastern United States (Northeast Fisheries Science Center and Northeast Area Monitoring and Assessment Program) and off the coast of New Jersey (NJ Department of Environmental Protection), 2) I tagged and in some instances tracked winter flounder, and 3) created and tested models to determine connectivity between estuarine and continental shelf habitats for adults using state-of-the-art archival tags. The combination of archival tags with the examination of the historical data and the secondary tagging techniques (which are location specific) can provide a complimentary, comprehensive view of winter flounder residency and movements. These results, in conjunction with the long-term distribution and abundance data from state/federal

partners will enable more effective management and improved understanding of the decline of this economically and ecologically important species.

– Chap 2 –

CHANGES IN THE DISTRIBUTION, ABUNDANCE, AND WEIGHT OF SOUTHERN MID-ATLANTIC BIGHT WINTER FLOUNDER: IS TEMPERATURE RESPONSIBLE?

Abstract

The goal of this study was to better understand where adult winter flounder are distributed at the southern extend of their range, how their distribution might have shifted over time, and if their distribution was related to bottom water temperatures. I accomplished this with the use of historic bottom trawl survey data (including surveys from the Northeast Fisheries Science Center, Northeast Monitoring and Assessment Program, and the New Jersey Department of Environmental Protection). I subsampled the trawl data and used data points below the Hudson Valley shelf canyon to represent the southern portion of the stock. Additionally I divided the Northeast Fisheries Science Center survey into an offshore and inshore portion. I found that the distribution of winter flounder has shifted over the last few decades within this region. While winter flounder in the majority of bottom trawl surveys analyzed here have shifted north along the continental shelf, there were several other changes in the distribution (e.g., across shelf location and depth at which they were found) that were season and survey specific. These spatial shifts, along with abundance, were not temporally similar to an increase in bottom water temperature for the area.

2.1 Introduction

In the Northeastern U.S., continental shelf waters have warmed over the past few decades (Friedland and Hare, 2007; Mills *et al.,* 2013). Outside of their thermal optima, organisms can experience reduced aerobic scope that negatively influences growth,

reproduction, abundance, and thus survival (Fry, 1947, 1971; Pörtner and Knust, 2007). In response, marine species (including fishes) have shifted their distribution and depth to follow preferred environmental windows in response to climate change (Murawski, 1993; Perry *et al.,* 2005; Weinberg, 2005; Dulvy *et al.,* 2008; Mueter and Litzow, 2008; Overholtz *et al.,* 2011; Pinsky and Fogarty, 2012; Pinsky *et al.,* 2013; Lucey and Nye, 2010; Nye *et al.,* 2009, 2010; Link *et al.,* 2011). The most common shift in distribution has been towards the poles, as documented in the North Atlantic (Rose, 2005), Northeastern U.S. (Nye *et al.,* 2009; Pinsky and Fogarty, 2012), North Sea (Perry *et al.,* 2005; Dulvy *et al.,* 2008), Bering Sea (Mueter and Litzow, 2008), and forecasted in the Northeast U.S. (Drinkwater, 2005) and globally (Cheung *et al.,* 2008; 2009). Shifts are not always poleward, but are often tied to local climatic forcing (Pinsky *et al.*, 2013). Depending on the species, habitat connectivity, and rate of temperature change, the Atlantic Multidecadal Oscillation is correlated with and can intensify poleward shifts in distribution during a positive phase, which has predominated since 1980 (Genner *et al.,* 2004; ter Hofstede *et al.,* 2010; Nye *et al.,* 2014). Aside from change in habitat or temperature, distributional shifts can also be attributed to changes in size and age structure (Radlinski *et al.*, 2013), changes in abundance (Hare *et al.*, 2010), overexploitation (ter Hofstede and Rijnsdorp, 2011; Garrison and Link, 2000), or changes in fishing mortality (Fogarty and Murawski, 1998).

It is projected that shifts in distribution can cause large-scale issues in fisheries productivity (Cheung *et al.,* 2008, 2009) and threaten food security in areas with specialized fisheries that are limited in resources (e.g., social capital and human capital) to adapt (Allison *et al.*, 2009). Distributional shifts can cause challenges for management if a stock contracts, expands past stock boundaries, diverges into smaller groups, if two stocks move parallel to each other (Link *et al.*, 2011), or if they converge with surrounding stocks or subpopulations (Metcalfe, 2006, Link *et al*., 2011). Poleward shifts can be

anthropogenically accelerated at the trailing edge of a species range from an increased effort by harvesters to maintain stable catch levels in the face of local abundance decline (Link *et al*., 2011; Pinsky and Fogarty, 2012; McCay, 2012). In addition, the species can be exploited before being managed at the advancing edge (Link *et al.*, 2011) and if strongly harvested complicates comprehension of the rate of poleward movement.

Winter flounder, a commercially and recreationally valuable species, has demonstrated a shift in its distribution (Nye *et al.,* 2009, 2010; Lucey and Nye 2010; Mills *et al*., 2013); however, depending on the scale analyzed understanding how the winter flounder population is adapting to climate change becomes complex. Winter flounder are managed in the U.S. in three spatially explicit stocks: the Gulf of Maine (GOM) stock, Georges Bank (GB) stock, and the Southern New England/ Mid-Atlantic Bight (SNE/MAB) stock. A recent analysis of the Spring Northeast Fisheries Science Center (NEFSC) trawl data on the West Atlantic continental shelf from 1968 to 2007, indicated that the southern portion of the winter flounder stock (including the SNE/MAB and GB stocks) showed a shift northward in the center of biomass and in minimum latitude, but did not show a strong distributional response on the continental shelf to mean temperature or depth (Nye *et al.*, 2009). Looking solely at the SNE/MAB stock, using this same trawl survey for the spring and fall from 1972 to 2008, the centers of biomass did not demonstrate a spatial shift in either spring or fall (Bell *et al.*, 2014b). Temperature, in addition to abundance or size, was not a significant driver for the location of the centers of biomass of adults (Bell *et al.*, 2014b); however, warmer winter water temperatures did negatively impact the population abundance when considering impacts on early life stages (Bell *et al.*, 2014a).

The detection or quantification of distributional shifts may be sensitive to spatial scale, especially as to whether the area under scrutiny encompasses single or multiple stocks or migratory components. To investigate this distributional shift or lack there of

depending on scale, an emphasis on waters off of New Jersey is especially appropriate because the region is the approximate southern limit of adult winter flounder populations on the continental shelf and experiences some of the broadest seasonal water temperature changes worldwide (Able and Fahay, 2010). In this region, the Hudson Valley shelf canyon divides the Southern New England and Mid-Atlantic Bight (MAB) portions of the stock (Clark and Brown, 1977). The Mid-Atlantic Bight is composed of the equatorward flowing Labrador current (inshore) from the north, the warm Gulf Stream (offshore) from the south that strongly affects temperature but may also entrain freshwater from the Hudson River and the Delaware and Chesapeake Bay plumes. Due to these conditions, the central to southern MAB can become highly stratified with negative effects on bottom water oxygen levels (Hare, 2014; Kemp *et al.*, 1994). This is not an issue for the GB due to strong tidal forces and wind mixing, and is less of an issue for the northern MAB and GOM than for the southern MAB (Hare, 2014).

While there is exchange of adults across the Hudson shelf valley (Phelan, 1992), the Hudson Canyon strongly influences local hydrodynamics and ocean temperatures. Local climate velocities and variability are important in predicting the direction and rate of species shifts (Pinsky *et al.*, 2013). Thus, changes in the spatial distribution within the central to southern MAB may be especially important in interpreting the reasons for the decline in the SNE/MAB stock. In addition, several authors support the existence of local stocks within SNE/MAB (Bigelow and Schroeder, 1953; Klein-MacPhee, 2002, Buckley *et al.,* 2008; and Winton, 2014), along the northeast Atlantic coast (Lobell, 1939; MacPhee ,1978), as well as between bay and offshore residents that could indicate separate populations (Sagarese and Frisk, 2011). While population-wide shifts in distribution are valuable to understand, with the possible existence of local stocks, this stresses the importance of finer scale analysis.

Due to spawning migrations, seasonality can also affect the distribution of winter flounder. The reported patterns of adult winter flounder movements and the location of spawning is varied (see Wuenschel *et al.,* 2009; DeCelles and Cadrin, 2010; Able and Fahay, 2010 for reviews). Numerous authors report that the adults move into estuaries in fall in anticipation of spawning there in the winter, and emigrate to the ocean in late spring (Bigelow and Schroeder, 1953; Perlmutter, 1947; McCracken, 1963; Jeffries and Johnson, 1974; Collette and Klein-MacPhee, 2002). Therefore, seasonal as well as yearly averaged scales are considered in this study. Since migratory species use multiple habitats throughout their lifespan, they can challenge classical fisheries stock assessment and management. Therefore, seasonal geographic distributions for migratory animals should be considered with the understanding that habitat niche patchiness occurs (Oberhauser and Peterson, 2003). Changes in environment (e.g., climate change) can enhance this challenge if a species shifts from its historical range. A shift in timing of seasonal cycles and life history events in response to warmer temperatures has been observed for several species (Hutchings and Myers, 1994; Sims and Wearmouth, 2004; Allison *et al.,* 2009; Mills *et al.,* 2013). This can alter the success of a population and leave lasting effects throughout the ecosystem (Liebhold *et al.*, 2004).

The goal of this study was to quantify spatial changes in distribution and abundance of the southern MAB (SMAB) portion of the SNE/MAB stock using fishery-independent and federal trawl surveys, and their relationship with temperature. This comparison was based on three fishery-independent trawl surveys, one that takes place offshore and two that cover inshore waters. More specifically, I tested these null hypotheses, in order to evaluate spatial changes in the population occurring over time:

$H_0$1: There is no change in the SMAB portion of winter flounder distribution, abundance, or weight-per-fish over time,

$H_0$2: There is no correlation between the SMAB distribution and mean bottom ocean temperature as recorded in the surveys, and

$H_0$3: There is no difference in the results between surveys.

2.2 Methods

I used three bottom trawl data sets: the Northeast Fisheries Science Center (NEFSC), the New Jersey Department of Environmental Protection (DEP), and the Northeast Area Monitoring and Assessment Program (NEAMAP) (Table 1). Trends in distribution and abundance of winter flounder adults were calculated from federal (NEFSC), state (DEP), and a cooperative state/federal data collection program (NEAMAP) for the SMAB portion of the SNE/MAB stock. Both the NEAMAP and NEFSC data were subsampled southwest of the Hudson Shelf Valley (Figure 1). Due to a vessel change in 2009, the NEFSC data is subdivided further into data from consistently sampled strata after this change (offshore) and data from consistently sampled strata inshore before this change (outlined in Table 1), termed here as 'NEFSC offshore' and 'NEFSC inshore'. The NEFSC inshore portion of the survey overlaps with the area surveyed by the NEAMAP as well as a portion surveyed by the DEP (Figure 1). I split the data from the three trawl surveys into winter (January-March), spring (April-June), summer (July-September), and fall (October-December), because while seasonally defined, each organization's seasonal survey had a unique start and end month.

Data used from these surveys included: latitude, longitude, catch-per-tow, depth, weight, and bottom temperature. I used catch-per-tow for each survey to represent abundance and to calculate the centers of biomass. I calculated a yearly arithmetic average for each variable of interest, but the year was defined to associate spawning stock biomass

(SSB) with data from the winter and spring of each year ($year_i$) averaged with the summer and fall of the preceding year ($year_{i-1}$) instead of that calendar year. For this average, only years that had more than one season surveyed for that year were included.

Data Analysis

I used methods described in Nye *et al.,* (2009), including calculating spatial metrics for each year of a) center of biomass using a mean of across-shelf and along-shelf distance weighted by the occurrence (catch-per-tow), b) minimum latitude and longitude, c) maximum latitude and longitude, d) mean depth weighted by occurrence, e) mean temperature weighted by occurrence, f) mean temperature of survey, in addition to g) average weight-per-fish. Across-shelf distance was defined as the distance from the interpolated 200-meter isobath while along-shelf distance was defined as the distance from the southernmost point of the NEFSC trawl survey (approximately 34 degrees N).

As in Nye *et al.,* (2009), I used a linear regression model to determine if there was a trend over time for each variable of interest. I calculated the weighted mean for the center of biomass, along-shelf movement, across-shelf movement, depth, and temperature using:

$$X_j = \frac{\sum_{j=1}^{n} w_i X_{ij}}{\sum w_i} \qquad \textit{Equation 1}$$

where X_j is the variable of interest in year j, w is the abundance for each trawl site i, and n is the number of data points for that year indexed by season. I used minimum and maximum latitude and longitude to determine if there was a range contraction or expansion, in the area below the Hudson Valley shelf canyon.

I ran regressions to determine if there was a significant trend of the variable of interest against time (using the functions *regstats* and *polyfit*). I measured the relationship of abundance, weighted along shelf distance, weighted across shelf distance, and weighted

depth to temperature using a cross correlation (function *corrcoef*). I used a general linear model to examine the effects of along-shelf movement, across-shelf movement, depth, survey, and year interacting with season on catch-per-tow. I compared this model to one with the additional effect of bottom water temperature using Akaike's information criterion (AIC) to find the best model fit. I used an analysis of covariance to test for different means, slopes, and intercepts for variables in question between surveys (using the *aoctools* function), and tested for pairwise survey differences when global tests were significant using a Tukey's honest significant difference. Significance was judged at a 95% confidence interval. I used Matlab (version 2014a) for all analyses.

2.3 Results

Changes in Distribution

There were seasonal changes in the location of the center of biomass for the winter flounder distribution. Based on all three surveys analyzed over the last several decades, the centers of biomass remained north of Chesapeake Bay but extended the furthest south in the fall (Figure 2). Looking at the yearly average, the centers of biomass were most frequently between Delaware Bay and the Hudson Valley shelf canyon (Figure 3). The centers of biomass overlapped for the inshore surveys off of northern New Jersey but the NEFSC offshore survey centers of biomass were further offshore due to area sampled.

It should be noted that there are seasonal changes in the distribution due to migration; however, I am not comparing the spatial metric of one season to another, just to itself over time. That being said, the spatial distribution of the SMAB stock changed over time in the long term DEP, NEFSC offshore, and NEFSC inshore datasets (Table 2, 3, 4), however there was no change in distribution seen in the short duration NEAMAP dataset (Table 5). The depth in which winter flounder were captured in the DEP surveys decreased

for all seasons and for the yearly average (at a rate of 0.2 m yr^{-1}) (Table 2). The depth of occurrence for winter flounder in the NEFSC inshore Jan.-Mar. surveys additionally decreased (at a rate of 0.05 m yr^{-1}) (Table 4).

The centers of biomass for across-shelf distribution shifted inshore in Jan.-Mar. surveys and the yearly average for both the NEFSC offshore and the NEFSC inshore surveys in addition to the Jul.-Sep. surveys for the NEFSC offshore trawl. It shifted offshore in Apr.-Jun. DEP surveys. The minimum change in across-shelf distance, closest to shore where fish were found moved further offshore for both Jan.-Mar. surveys and for the average for the NEFSC offshore and NEFSC inshore surveys, as well as in Jul.-Sep. and Oct.-Dec. NEFSC offshore surveys. The maximum distance offshore where fish were found shifted offshore in Jan.-Mar. in NEFSC inshore surveys, but shifted inshore in Jul.-Sep. DEP surveys and Oct.-Dec. NEFSC offshore surveys.

The centers of biomass for along-shelf distribution shifted north in Jan.-Mar. surveys and for yearly average NEFSC offshore and NEFSC inshore surveys, in addition to, Jul.-Sep. NEFSC offshore surveys and Oct.-Dec. NEFSC inshore surveys. The minimum along-shelf position, the furthest south where fish were found, has moved north in Jan.-Mar., Oct.-Dec., and yearly average NEFSC offshore and NEFSC inshore surveys, as well as, Apr.-Jul. NEFSC inshore and DEP surveys, and Jul.-Sep. NEFSC offshore surveys. An increase in the maximum distance (from the southernmost point sampled) at which winter flounder were found was only seen in the Jan.-Mar. NEFSC inshore survey.

While winter flounder have declined, not all surveys saw a decline in geometric mean catch-per-tow over the last few decades. The geometric mean catch-per-tow decreased for the Apr.-Jun., Oct.-Dec., and for the yearly average DEP surveys, as well as, for the Jul.-Sep. NEFSC inshore surveys. To the contrary, geometric mean catch-per-tow increased in the Oct.-Dec. NEFSC inshore surveys. Weight-per-fish increased in Jan.-Mar.,

Apr-Jun., Oct-Dec. and yearly average DEP surveys, as well as, in Jan.-Mar., Jul.-Sept. and the average NEFSC inshore surveys, and in Apr.-Jun. NEAMAP surveys.

Response to Temperature

The bottom water temperature for the area as well as the temperature in which winter flounder occurred increased over the study period. The temperature in which winter flounder were found increased in Oct.-Dec. DEP surveys, and in both Jul.-Sep. and average NFFSC offshore surveys. The mean temperature weighted by occurrence across surveys for all seasons ranged from 0-21 °C while the average temperature surveyed ranged from 2-23 °C. The average temperature of the surveyed area increased in Jul.-Sep. NEFSC inshore surveys and in Oct.-Dec. DEP surveys.

Average bottom water temperature did not have a relationship to mean depth weighted by occurrence, weighted mean across-shelf distance, weighted mean along-shelf distance, and geometric mean catch-per-tow for the majority of survey variables (Table 6). In the Jul.-Sep. NEFSC inshore surveys, geometric mean catch-per-tow had a negative relationship to bottom water temperature. The Jan.-Mar. DEP surveys and yearly average NEFSC inshore surveys revealed a positive relationship between weighted along-shelf distance and bottom water temperature while the Oct.-Dec. NEFSC surveys had a negative relationship. The Jan.-Mar. DEP surveys and the average NEFSC inshore surveys both revealed a negative relationship between weighted across-shelf distance and bottom water temperature.

Bottom water temperature was a significant descriptor variable of catch-per-tow in a general linear model (Table 7). The model that included bottom water temperature (AIC = 124760) explained catch-per-tow better than the model that did not include temperature (AIC = 140790). The other predictors in the model including along-shelf distance, across-

shelf distance, depth, survey, and year interacting with season also had significant effects on predicting catch-per-tow.

Survey Specific Responses

There were differences in how winter flounder adapted over time as seen by the DEP, NEFSC offshore, and NEFSC inshore surveys. When comparing winter flounder shifts across surveys, there were differences in the rate in which a shift would occur as well as the direction of the trend. Differences in how winter flounder adapted over time occurred for all seasons and for the annual average, and also occurred between significant and non-significant trends. Winter flounder subpopulations behaved differently in Jan.-Mar. surveys, in that the rate in which winter flounder for the NEFSC inshore surveys moved north at the southern edge was faster than winter flounder in the DEP surveys. They decreased in catch-per-tow in the DEP surveys but increased in the NEFSC offshore and inshore surveys. They also increased in weight at a faster rate in the DEP surveys compared to the NEFSC inshore surveys.

Looking at the minimum across-shelf distance in the Apr.-Jun. surveys, winter flounder moved offshore at a faster rate for the NEFSC inshore surveys than the DEP surveys. The rate in which winter flounder moved north at the southern minimum edge was faster in the NEFSC inshore surveys than the DEP surveys and the NEFSC offshore surveys. They also increased in weight in the Apr.-Jun. DEP surveys while in the NEFSC offshore surveys they decreased in weight.

In the Jul.-Sep. surveys, the winter flounder distribution moved inshore in NEFSC offshore surveys but offshore in DEP surveys. The distribution moved south in DEP surveys but north in NEFSC offshore surveys. The rate in which they were found further north at the minimum along shelf distance was faster in Jul.-Sep. NEFSC offshore surveys than DEP surveys. The temperature in which winter flounder occurred decreased for the DEP survey

but increased for the NEFSC inshore survey. The temperature for the study area decreased in the Jul.-Sep. DEP survey but increased in the NEFSC offshore and inshore surveys. Winter flounder also increased in weight at a faster rate for the NEFSC inshore survey than the NEFSC offshore survey.

In the Oct.-Dec. surveys the geometric mean catch-per-tow decreased in the DEP survey but increased in the NEFSC offshore and inshore surveys. For the SSB annual average of the seasonal surveys, the winter flounder distribution was found closer to shore in the NEFSC offshore survey and more offshore in the DEP survey. They were found further north at the minimum along shelf distance for the NEFSC offshore and inshore survey but further south for the DEP survey. The geometric mean catch-per-tow of winter flounder decreased at a faster rate for the SSB annual average DEP survey than the NEFSC inshore survey and decreased for the NEFSC offshore survey. The weight-per-fish also increased at a faster rate for the DEP survey than the NEFSC offshore survey (Table 8).

Winter flounder trends in subpopulations had the most differences between DEP and NEFSC inshore survey variables (n=11), then DEP and NEFSC offshore survey variables (n=9), and the least differences between NEFSC offshore and NEFSC inshore survey variables (n=4) (Table 9). Winter flounder in the NEAMAP did not appear to behave differently than winter flounder in any of the other surveys.

2.4 Discussion

Limitations of this Study

There were limitations in using these four defined surveys (DEP, NEAMAP, NEFSC offshore and inshore) to understand winter flounder distributional shifts over time. While differences did occur between surveys, these differences could also be attributed to the different spatial and temporal scales of the data. Another limitation to this study is that

winter flounder are inconsistently available to trawl gear due to seasonal migration as well as temperature dependent burial. Burial has a season component as well as an annual component due to temperature. If winter flounder are seasonally migrating into estuaries then they are unavailable in the trawl ranging from the fall to spring, depending on the time they enter and leave the estuary. Additionally, if there are resident bay fish, then they are never available to the trawl survey; therefore there is no index of change for bay fish.

Despite some degree of overlap, each survey is spatially and temporally unique. The NEAMAP surveys (most recent), as well as the Apr.-Jun. and Oct.-Dec. NEFSC surveys (discontinued) are short time series and therefore the power of the comparison tests for that survey may have been insufficient. The summer NEFSC offshore survey would have been ideal to study change over time since due to seasonal migration this would be the theoretical time when all of the fish would be on the shelf. The NEAMAP and NEFSC inshore areas surveyed overlap spatially and winter flounder in the NEAMAP survey are not found as far south as they were historically by the NEFSC inshore survey (Figure 3), yet I cannot combine these data to make a larger time series. While only consistently sampled strata across the time series were used, dividing the available data to focus only on the subdivision south of the Hudson Valley plays into the argument of only seeing certain trends at certain scales. However, I am confident that at the southernmost edge of the SNE/MAB stock, winter flounder are not being found as far south as they have been historically with further shifts in spatial distribution being altered on a local scale.

Directionality of the distributional shift for this subdivision of the region might not simply be explained by temperature due to the patchiness of preferred habitat caused by bathymetric, advection, upwelling, and seasonal effects on temperature. Poleward population shifts in a static temperature field would also signify a drop in mean occupied temperature, however at finer scales such as for the DEP survey which only encompassed

the coast of New Jersey, a poleward shift could signify being part of a large scale population shift but also could depend on local hydrology and ecosystem constraints. This issue of analytical scale (e.g., stock, regional) has become apparent in understanding winter flounder distributional shifts since when grouping two stocks (SNE/MAB and GB) as one unit showed a northern distributional shift for the southern portion of the population (Nye *et al.*, 2009), yet at the stock level (SNE/MA) there was no distributional shift for the species (Bell *et al.*, 2014b).

Changes in Distribution

Winter flounder have shifted in spatial distribution at the southern end of the SNE/MAB stock during the last several decades. This could be explained in two ways; one in which the adults are actively moving and the other in which recruitment is failing in one area but successful in another. Since winter flounder have shown to have a home range and strong site fidelity (Collette and Klein-MacPhee, 2002; Fairchild *et al.*, 2013), when observing distributional shifts on a larger scale (e.g., across the NEFSC survey) it is most likely recruitment success describing the distribution, yet on a finer scale (e.g., across the DEP survey) adult movement could also describe the distribution. This might be one reason why the NEFSC offshore and inshore surveys had a high percent of distribution shifts in the along shelf direction (50% and 47%, respectively) where estuarine conditions would play a strong role in defining distribution, but the DEP survey mainly had distributional changes in depth (63%).

Bottom water temperature can have negative impacts on survival (physiologically), but it is most likely not a direct relationship affecting adult abundance and distribution; especially, since the relationship between the geometric mean catch-per-tow trends and distributional trends (along-shelf, across-shelf, and depth) against temperature were mainly not similar. In the SNE/MAB stock, warm estuarine waters in spring (Able *et al.*,

2014) and winter (Bell *et al.*, 2014a) result in uniformly poor recruitment. It is more likely a complex feedback loop created by the increase in temperature that provides earlier overlaps with predator-prey habitat for young winter flounder (Manderson, 2006, 2008) that negatively impacts survival, than a direct physiological effect.

Ocean temperatures have increased significantly across the N.W. Atlantic shelf (Friedland and Hare 2007; Mills *et al.,* 2013) as seen in the Jul.-Sep. NEFSC inshore surveys and Oct.-Dec. DEP surveys, yet the temperature in which winter flounder were found has not significantly changed for the majority of these seasonal surveys. There was however a seasonal increase in mean temperature of occurrence in both NESFC offshore (Jul.-Sep. and average) and DEP (Oct.-Dec.) surveys. This increase in the temperature where winter flounder occurred happened in conjunction with a decrease in depth in the DEP (Oct.-Dec.) surveys and a shift north in the NEFSC offshore (Jul.-Sep. and average) surveys. To remain in preferred temperatures, winter flounder could have shifted their distribution in an attempt to find suitable habitat.

A decrease in depth was only seen for the DEP (across all seasons) and Jan.-Mar. NEFSC inshore surveys, which are both inshore. While seasonally migrating flounder move out of estuaries offshore or to deeper water in the spring, this would not be captured in this trend unless if there was a shift in the timing with more fish available in deeper water earlier. This decrease in depth however was not always seen in conjunction with a shift offshore; only the Apr.-Jun. DEP surveys demonstrated both trends. For this area, since the Hudson Valley shelf canyon is located off of northern New Jersey a northern shift as well as offshore shift could produce a decrease in occupied depth. A decrease in geometric mean catch-per-tow was only seen for the DEP and Jul.-Sep. NEFSC inshore surveys. This decrease could be due to mortality but also could be due to winter flounder becoming less

available inshore with a shift offshore in either weighted across-shelf distance (e.g. Apr.-Jun DEP) or minimum/maximum across shelf distance (e.g. Jan.-Mar. NEFSC inshore).

The weighted mean across-shelf distance shifted inshore in Jan.-Mar. NEFSC surveys, but the minimum distance from shore shifted offshore. This same trend was seen in the Jan.-Mar. and average NEFSC inshore surveys, as well as, Jul.-Sep. and yearly average NEFSC inshore surveys. This reveals a shifting across-shelf baseline with fish being found further offshore but the bulk of fish found closer to shore. The northern shift in both weighted mean along-shelf and minimum along-shelf distance was the trend most commonly seen across surveys and seasons in the SMAB.

The second most frequent pattern was the increase in weight-per-fish across surveys. Even though weight of fish was not spatially different across the study area, an increase in weight-per-fish was only seen in inshore surveys (DEP, NEAMAP, NEFSC inshore). An increase in weight or size of fish is contrary to what one might find in a temperate warming area where fish size can decrease with temperature increase (Perry *et al.,* 2005; Cheung and Sarmiento, 2013). While the temperature occupied by winter flounder did increase for the NEFSC offshore Jul.-Sep. and average surveys and the DEP Oct.-Dec. surveys, the bottom water temperature in which winter flounder occurred is still within a suitable range and thus would not decrease size. The increase in weight may be due to the relaxation of fishing pressure since the commercial fishery is currently closed, allowing larger fish to survive even though abundance has not yet rebounded from overfishing. This increase in weight-per-fish could also indicate recent recruitment failures, in which case few small fish would influence the mean and could explain why this trend was only seen inshore. Other authors have seen an increase in the average weight of winter flounder for this area but found that size effects were not a driving factor in describing winter flounder distribution (Bell *et al.*, 2014b). Lastly, weight per fish could be affected if

the timing of spawning has shifted and gonads were being developed and hydrated earlier than historically.

At the southern extent of the SNE/MAB stock there are differences between inshore and offshore populations as well as across the area managed. Test results lead to rejection of the null hypothesis that there is no difference in the results between surveys. A difference between the inshore and offshore age and size at maturity of the population was recently exposed off of New Jersey (Winton *et al.*, 2014), along with other evidence (Buckley *et al.*, 2008) supporting that the managed SNE/MAB stock unit really is comprised of local stocks. However, there are still authors that believe the current three stock model in the U.S. is genetically correctly defined (Wirgin *et al.*, 2014). Since I obtained different results when analyzing seasonal and survey specific data, caution is recommended when interpreting results where a further subdivision within a stock could explain adaptation differences (e.g., possibly seasonal migration) in a changing ocean.

Despite limitations, I was able to see clear trends of spatial movement over time for this region for several seasons as well as yearly averages. Understanding distributional shifts at this fine scale are important for identifying local impacts to the ecosystem and maritime community. Interpreting these distributional shifts is important for defining essential fish habitat that is no longer being used by winter flounder. While these results may not scale up to the stock level, there are changes in the distribution of winter flounder below the Hudson Valley shelf canyon, which is important for management to consider.

LIST OF TABLES

Table 1. Winter flounder collection methods for DEP, NEAMAP, and NEFSC bottom trawl surveys, including areas covered, and range of temperatures and depths sampled. See Figure 1 for sampling area.

Survey	**New Jersey Department of Environmental Protection (DEP)**	**Northeast Fisheries Science Center (NEFSC) offshore portion**	**Northeast Fisheries Science Center (NEFSC) inshore portion**	**Northeast Area Monitoring and Assessment Program (NEAMAP)**
Area	New Jersey Coastal Waters 15 strata off NJ, divided longitudinally by 30, 60 and 90 ft isobaths	Cape Hatteras to Nova Scotia subdivided to Offshore Cape Hatteras to the Hudson Canyon Strata: 1010-1040 1610-1760	Cape Hatteras to Nova Scotia subdivided Inshore Cape Hatteras to the Hudson Canyon Strata: 3130, 3160, 3190, 3220, 3250, 3280, 3310, 3340, 3370, 3400, 3430	Cape Hatteras to Massachusetts subdivided Inshore Cape Hatteras to the Hudson Canyon
Year	1988 to 2013 Missing Jan.-Mar. 1988; Apr.-Jun. 1988; Oct.-Dec. 2013	Started in 1963, using 1968 to 2013 Missing Jan.-Mar.: 1970, 1971; Apr.-Jun.: 1968, 1969, 1972, 1973, 1975, 1976, 1997-2013; Jul.-Sep.: 1968, 1975, 1976; and Oct.-Dec.: 1978, 2000-2002, 2004-2008, 2010-2013	Started in 1963, using 1972 to 2008 Missing Jan.-Mar.: 1972-74; Apr.-Jun.: 1972, 1975-76, 1983-86, 1988-2008; Jul.-Sep.: 1972-73, 1975-76, 1985; and Oct.-Dec.: 1987, 1984, 1987-1997, 2000-02, 2004-08	2007 to 2014
Seasons	Winter, Spring, Summer, and Fall	Winter, Spring, Summer, and Fall	Winter, Spring, Summer, and Fall	Spring and Fall
Depth	4.5 to 31.5 m	14 to 664 m	8 to 35 m	6.1 to 21.6 m
Effort	20 minute tows at 3 knots	30 minute tows at 3.5 knots	30 minute tows at 3.5 knots	20 minute tows at 3 knots
Gear	Otter Trawl	Otter Trawl	Otter Trawl	Otter Trawl

Vessel	*R/V* SeaWolf	*R/V* Albatrass IV, HB Bigelow (current)	*R/V* Albatrass IV, HB Bigelow (current)	*F/V* Darana R
Methods	(Byrne, 1989)	(Grosslein, 1969) (Despres-Patanjo, 1988)	(Grosslein, 1969) (Despres-Patanjo, 1988)	(NEFSC, 2006)

Table 2. Regression results of winter flounder spatial, size, and abundance metrics, as well as, an environmental variable to time, by season and for yearly average, as observed in the DEP survey. Significant (α = 0.05) results are in bold. See Figure 1 for sampling area.

	Jan.-Mar.	Apr.-Jun.	Jul.-Sept.	Oct.-Dec.	SSB Average
Weighted Depth	**R = 0.487** **P = 0.000** **S = -0.187** **N = 25**	**R = 0.276** **P = 0.007** **S = -0.163** **N = 25**	**R = 0.187** **P = 0.027** **S = -0.172** **N = 26**	**R = 0.487** **P = 0.000** **S = -0.356** **N = 25**	**R = 0.652** **P = 0.000** **S = -0.231** **N = 25**
Weighted Temperature	R = 0.042 P = 0.328 S = 0.039 N = 25	R = 0.033 P = 0.384 S = 0.031 N = 25	R = 0.139 P = 0.061 S = -0.145 N = 26	**R = 0.206** **P = 0.023** **S = 0.118** **N = 25**	R = 0.001 P = 0.870 S = 0.005 N = 25
Average Temperature	R = 0.004 P = 0.766 S = 0.012 N = 25	R = 0.093 P = 0.138 S = 0.062 N = 25	R = 0.068 P = 0.197 S = -0.086 N = 26	**R = 0.253** **P = 0.011** **S = 0.105** **N = 25**	R = 0.032 P = 0.395 S = 0.021 N = 25
Weighted Across Shelf	R = 0.001 P = 0.880 S = -0.023 N = 25	**R = 0.177** **P = 0.036** **S = 0.379** **N = 25**	R = 0.006 P = 0.713 S = 0.138 N = 26	R = 0.008 P = 0.670 S = 0.085 N = 25	R = 0.085 P = 0.158 S = 0.189 N = 25
Min. Across Shelf	R = 0.132 P = 0.74 S = 0.002 N = 25	R = 0.0196 P = 0.505 S = 0.001 N = 25	R = 0.014 P = 0.569 S = 0.004 N = 26	R = 0.145 P = 0.060 S = 0.016 N = 25	R = 0.135 P = 0.071 S = 0.005 N = 25
Max. Across Shelf	R = 0.113 P = 0.100 S = -0.001 N = 25	R = 0.104 P = 0.115 S = 0.001 N = 25	**R = 0.185** **P = 0.028** **S = -0.004** **N = 26**	R = 0.008 P = 0.670 S = 0.000 N = 25	R = 0.101 P = 0.122 S = -0.007 N = 25
Weighted Along Shelf	R = 0.030 P = 0.409 S = 0.215 N = 25	R = 0.074 P = 0.190 S = -0.311 N = 25	R = 0.024 P = 0.451 S = -0.282 N = 26	R = 0.014 P = 0.573 S = 0.108 N = 25	R = 0.027 P = 0.435 S = -0.101 N = 25
Min. Along Shelf	R = 0.068 P = 0.207 S = 0.002 N = 25	**R = 0.254** **P = 0.010** **S = 0.005** **N = 25**	R = 0.011 P = 0.605 S = 0.005 N = 26	R = 0.119 P = 0.091 S = 0.015 N = 25	R = 0.081 P = 0.169 S = 0.005 N = 25
Max. Along Shelf	R = 0.003 P = 0.779 S = 0.000 N = 25	R = 0.004 P = 0.760 S = -0.000 N = 25	R = 0.030 P = 0.399 S = -0.005 N = 26	R = 0.067 P = 0.212 S = 0.002 N = 25	R = 0.015 P = 0.559 S = -0.001 N = 25
Geometric mean Catch	R = 0.342 P = 0.37 S = -0.854 N = 25	**R = 0.274** **P = 0.007** **S = -0.935** **N = 25**	R = 0.044 P = 0.302 S = -0.382 N = 26	**R = 0.358** **P = 0.002** **S = -0.999** **N = 25**	**R = 0.432** **P = 0.000** **S = -0.786** **N = 25**
Weight-per-fish	**R = 0.619** **P = 0.000** **S = 0.014** **N = 25**	**R = 0.470** **P = 0.000** **S = 0.009** **N = 25**	R = 0.053 P = 0.257 S = 0.002 N = 26	**R = 0.247** **P = 0.012** **S = 0.007** **N = 25**	**R = 0.637** **P = 0.000** **S = 0.008** **N = 25**

Table 3. Regression results of winter flounder spatial, size, and abundance metrics, as well as, an environmental variable to time, by season and for yearly average, as observed in the NEFSC offshore survey. Significant ($\alpha = 0.05$) results are in bold. See Figure 1 for sampling area.

	Jan.-Mar.	Apr.-Jun.	Jul.-Sept.	Oct.-Dec.	SSB Average
Weighted Depth	R = 0.000 P = 0.963 S = -0.009 N = 40	R = 0.019 P = 0.686 S = 0.096 N = 11	R = 0.072 P = 0.103 S = -0.139 N = 38	R = 0.000 P = 0.968 S = 0.009 N = 19	R = 0.026 P = 0.307 S = -0.063 N = 42
Weighted Temperature	R = 0.034 P = 0.254 S = 0.031 N = 40	R = .092 P = 0.363 S = -0.080 N = 11	**R = 0.198** **P = 0.005** **S = 0.165** **N = 38**	R = 0.158 P = 0.092 S = 0.101 N = 19	**R = 0.100** **P = 0.041** **S = 0.052** **N = 42**
Average Temperature	R = 0.076 P = 0.071 S = 0.022 N = 44	R = 0.118 P = 0.330 S = -0.045 N = 10	R = 0.064 P = 0.106 S = 0.030 N = 42	R = 0.009 P = 0.687 S = -0.013 N = 21	R = 0.078 P = 0.074 S = 0.019 N = 42
Weighted Across Shelf	**R = 0.210** **P = 0.003** **S = -0.971** **N = 40**	R = 0.020 P = 0.677 S = -0.420 N = 11	**R = 0.311** **P = 0.000** **S = -1.285** **N = 38**	R = 0.070 P = 0.276 S = -0.626 N = 19	**R = 0.459** **P = 0.000** **S = -0.877** **N =42**
Min. Across Shelf	**R = 0.203** **P = 0.004** **S = 0.019** **N = 40**	R = 0.220 P = 0.146 S = 0.031 N = 11	**R = 0.320** **P = 0.000** **S = 0.021** **N = 38**	**R = 0.285** **P = 0.028** **S = 0.026** **N = 19**	**R = 0.425** **P = 0.000** **S = 0.016** **N = 42**
Max. Across Shelf	R = 0.067 P = 0.106 S = 0.012 N = 40	R = 0.007 P = 0.812 S = 0.002 N = 11	R = 0.037 P = 0.246 S = -0.004 N = 38	**R = 0.231** **P = 0.037** **S = -0.016** **N = 19**	R = 0.000 P = 0.954 S = 0.000 N = 42
Weighted Along Shelf	**R = 0.220** **P = 0.002** **S = 2.949** **N = 40**	R = 0.215 P = 0.151 S = 1.456 N = 11	**R = 0.266** **P = 0.001** **S = 1.785** **N = 38**	R = 0.011 P = 0.672 S = 0.386 N = 19	**R = 0.287** **P = 0.000** **S = 1.480** **N = 42**
Min. Along Shelf	**R = 0.277** **P = 0.001** **S = 0.032** **N = 40**	R = 0.177 P = 0.198 S = 0.041 N = 11	**R = 0.454** **P = 0.000** **S = 0.042** **N = 38**	**R = 0.322** **P = 0.011** **S = 0.044** **N = 19**	**R = 0.541** **P = 0.000** **S = 0.030** **N = 42**
Max. Along Shelf	R = 0.090 P = 0.059 S = 0.019 N = 40	R = 0.005 P = 0.838 S = 0.002 N = 11	R = 0.038 P = 0.240 S = 0.005 N = 38	R = 0.033 P = 0.460 S = -0.008 N = 19	R = 0.065 P = 0.105 S = 0.006 N = 42
Geometric mean Catch	R = 0.015 P = 0.456 S = 0.023 N = 40	R = 0.007 P = 0.812 S = -0.029 N = 11	R = 0.068 P = 0.113 S = 0.170 N = 38	R = 0.051 P = 0.354 S = 0.114 N = 19	R = 0.083 P = 0.065 S = 0.088 N = 42
Weight-per-fish	R = 0.004 P = 0.703 S = 0.001 N = 40	R = 0.055 P = 0.486 S = -0.004 N = 11	R = 0.038 P = 0.241 S = 0.002 N = 38	R = 0.001 P = 0.883 S = 0.000 N = 19	R = 0.034 P = 0.240 S = 0.001 N = 42

Table 4. Regression results of winter flounder spatial, size, and abundance metrics, as well as, an environmental variable to time, by season and for yearly average, as observed in the NEFSC inshore survey. Significant ($\alpha = 0.05$) results are in bold. See Figure 1 for sampling area.

	Jan.-Mar.	Apr.-Jun.	Jul.-Sept.	Oct.-Dec.	SSB Average
Weighted Depth	**R = 0.116** **P = 0.049** **S = -0.054** **N =** 34	R = 0.067 P = 0.502 S = 0.076 N = 9	R = 0.009 P = 0.766 S = -0.028 N = 12	R = 0.318 P = 0.071 S = 0.104 N = 11	R = 0.086 P = 0.210 S = 0.032 N = 20
Weighted Temperature	R = 0.055 P = 0.181 S = 0.045 N =34	R = 0.277 P = 0.146 S = -0.323 N =9	R = 0.188 P = 0.159 S = 0.475 N =12	R = 0.023 P = 0.659 S = 0.088 N =11	R = 0.023 P = 0.527 S = 0.077 N =20
Average Temperature	R = 0.001 P = 0.864 S = 0.004 N =34	R = 0.206 P = 0.258 S = -0.285 N =8	**R = 0.447** **P = 0.000** **S = 0.129** **N =32**	R = 0.034 P = 0.510 S = 0.038 N =15	R = 0.145 P = 0.097 S = 0.078 N =20
Weighted Across Shelf	**R = 0.329** **P = 0.000** **S = -1.093** **N =34**	R = 0.110 P = 0.384 S = -1.155 N =9	R = 0.002 P = 0.890 S = -0.089 N =12	R = 0.463 P = 0.021 S = -0.841 N =11	**R = 0.292** **P = 0.014** **S = -0.610** **N =**20
Min. Across Shelf	**R = 0.386** **P = 0.000** **S = 0.029** **N =34**	R = 0.548 P = 0.023 S = 0.086 N =9	R = 0.203 P = 0.142 S = 0.012 N =12	R = 0.198 P = 0.170 S = 0.013 N =11	**R = 0.569** **P = 0.000** **S = 0.018** **N =**20
Max. Across Shelf	**R = 0.166** **P = 0.017** **S = 0.016** **N =34**	R = 0.174 P = 0.264 S = 0.007 N =9	R = 0.002 P = 0.904 S = 0.000 N =12	R = 0.248 P = 0.119 S = 0.001 N =11	R = 0.101 P = 0.172 S = 0.005 N =20
Weighted Along Shelf	**R = 0.293** **P = 0.001** **S = 3.652** **N =34**	R = 0.122 P = 0.356 S = 3.433 N =9	R = 0.019 P = 0.667 S = 0.334 N =12	**R = 0.406** **P = 0.035** **S = 0.881** **N =11**	**R = 0.237** **P = 0.030** **S = 1.603** **N =**20
Min. Along Shelf	**R = 0.428** **P = 0.000** **S = 0.057** **N =34**	**R = 0.666** **P = 0.007** **S = 0.149** **N =9**	R = 0.311 P = 0.060 S = 0.029 N =12	**R = 0.395** **P = 0.038** **S = 0.030** **N =11**	**R = 0.647** **P = 0.000** **S = 0.038** **N =**20
Max. Along Shelf	**R = 0.175** **P = 0.014** **S = 0.030** **N =34**	R = 0.044 P = 0.587 S = 0.014 N =9	R = 0.002 P = 0.899 S = -0.001 N =12	R = 0.097 P = 0.353 S = 0.003 N =11	R = 0.091 P = 0.196 S = 0.009 N =
Geometric mean Catch	R = 0.001 P = 0.865 S = 0.010 N =34	R = 0.192 P = 0.238 S = -1.465 N =9	**R = 0.355** **P = 0.041** **S = -0.299** **N =12**	**R = 0.435** **P = 0.030** **S = 1.750** **N =11**	R = 0.002 P = 0.836 S = -0.041 N =20
Weight-per-fish	**R = 0.461** **P = 0.000** **S = 0.007** **N =34**	R = 0.097 P = 0.414 S = 0.005 N =9	**R = 0.568** **P = 0.005** **S = 0.013** **N =12**	R = 0.303 P = 0.080 S = 0.007 N =11	**R = 0.440** **P = 0.001** **S = 0.006** **N =**20

Table 5. Regression results of winter flounder spatial, size, and abundance metrics, as well as, an environmental variable to time, by season and for yearly average, as observed in the NEAMAP survey. Significant ($\alpha = 0.05$) results are in bold. See Figure 1 for sampling area.

	Jan.-Mar.	Apr.-Jun.	Jul.-Sept.	Oct.-Dec.	SSB Average
Weighted Depth		R = 0.075 P = 0.553 S = -0.225 N = 7		R = 0.416 P = 0.167 S = 0.514 N = 6	R = 0.092 P = 0.560 S = 0.156 N = 6
Weighted Temperature		R = 0.066 P = 0.577 S = -0.195 N =7		R = 0.575 P = 0.081 S = -0.205 N =6	R = 0.004 P = 0.909 S = -0.026 N =6
Average Temperature		R = 0.027 P = 0.724 S = -0.093 N =7		R = 0.489 P = 0.080 S = -0.435 N =7	R = 0.009 P = 0.856 S = -0.042 N =
Weighted Across Shelf		R = 0.362 P = 0.153 S = -2.343 N =7		R = 0.000 P = 0.997 S = 0.021 N =6	R = 0.004 P = 0.908 S = -0.346 N =6
Min. Across Shelf		R = 0.042 P = 0.661 S = 0.071 N =7		R = 0.025 P = 0.765 S = -1.543 N =6	R = 0.022 P = 0.781 S = -0.743 N =6
Max. Across Shelf		R = 0.318 P = 0.187 S = -3.286 N =7		R = 0.009 P = 0.857 S = -1.143 N =6	R = 0.225 P = 0.341 S = -3.486 N =6
Weighted Along Shelf		R = 0.284 P = 0.219 S = 2.991 N =7		R = 0.007 P = 0.871 S = -0.819 N =6	R = 0.001 P = 0.949 S = -0.211 N =6
Min. Along Shelf		R = 0.460 P = 0.094 S = 9.843 N =7		R = 0.078 P = 0.593 S = -5.816 N =6	R = 0.057 P = 0.650 S = 3.378 N =6
Max. Along Shelf		R = 0.071 P = 0.562 S = 0.163 N =7		R = 0.021 P = 0.785 S = 1.304 N =6	R = 0.030 P = 0.743 S = 0.782 N =6
Geometric mean Catch		R = 0.199 P = 0.316 S = -0.694 N =7		R = 0.214 P = 0.355 S = -0.279 N =6	R = 0.477 P = 0.129 S = -0.837 N =6
Weight-per-fish		**R = 0.858** **P = 0.003** **S = 0.034** **N =7**		R = 0.279 P = 0.282 S = 0.033 N =6	R = 0.534 P = 0.099 S = 0.031 N =6

Table 6. Cross correlation coefficient (C), at zero-lag, of the geometric mean catch of winter flounder and average bottom water temperature observed by each survey for each year, by season and for yearly average, after the respective means have been subtracted. Significant ($\alpha = 0.05$) results are in bold (P). Number of years used is defined by N.

Cross	Survey	Jan.-Mar.	Apr.-Jun.	Jul.-Sept.	Oct.-Dec.	SSB Average
Geometric mean catch and average bottom water temperature	DEP	C = 0.377 P = 0.063 N = 25	C = 0.052 P = 0.806 N = 25	C = -0.211 P = 0.301 N = 26	C = -0.318 P = 0.121 N = 25	C = -0.301 P = 0.145 N = 25
	NEFSC	C = -0.0323 P = 0.841 N = 40	C = 0.558 P = 0.094 N = 10	C = 0.081 P = 0.630 N = 38	C = -0.108 P = 0.661 N = 19	C = 0.229 P = 0.144 N = 42
	NEFSC inshore	C = 0.006 P = 0.972 N = 34	C = 0.492 P = 0.216 N = 8	**C = -0.660** **P = 0.020** **N = 12**	C = -0.215 P = 0.526 N = 11	C = 0.187 P = 0.430 N = 20
	NEAMAP		C = -0.406 P = 0.366 N = 7		C = -0.500 P = 0.312 N = 6	C = -0.311 P = 0.549 N = 6
Weighted along shelf distance and average bottom water temperature	DEP	**C = 0.485** **P = 0.014** **N = 25**	C = -0.451 P = 0.745 N = 25	C = 0.234 P = 0.811 N = 26	C = 0.237 P = 0.253 N = 25	C = 0.042 P = 0.843 N = 25
	NEFSC	C = 0.264 P = 0.100 N = 40	C = -0.438 P = 0.205 N = 10	C = 0.058 P = 0.728 N = 38	**C = -0.607** **P = 0.006** **N = 19**	C = 0.143 P = 0.368 N = 42
	NEFSC inshore	C = -0.068 P = 0.704 N = 34	C = 0.100 P = 0.815 N = 8	C = -0.168 P = 0.602 N = 12	C = 0.108 P = 0.753 N = 11	**C = 0.544** **P = 0.013** **N = 20**
	NEAMAP		C = -0.043 P = 0.926 N = 7		C = -0.199 P = 0.706 N = 6	C = -0.067 P = 0.899 N = 6
Weighted across shelf distance and average bottom water temperature	DEP	**C = -0.451** **P = 0.024** **N = 25**	C = 0.014 P = 0.949 N = 25	C = -0.022 P = 0.914 N = 26	C = -0.098 P = 0.640 N = 25	C = 0.024 P = 0.908 N = 25
	NEFSC	C = -0.254 P = 0.114 N = 40	C = -0.332 P = 0.350 N = 10	C = -0.051 P = 0.762 N = 38	C = 0.206 P = 0.398 N = 19	C = -0.126 P = 0.428 N = 42
	NEFSC inshore	C = -0.044 P = 0.806 N = 34	C = 0.006 P = 0.989 N = 8	C = 0.181 P = 0.574 N = 12	C = -0.040 P = 0.908 N = 11	**C = -0.583** **P = 0.007** **N = 20**
	NEAMAP		C = -0.017 P = 0.971 N = 7		C = 0.176 P = 0.738 N = 6	C = 0.128 P = 0.809 N = 6
Weighted depth and average bottom water temperature	DEP	C = 0.234 P = 0.260 N = 25	C = -0.071 P = 0.737 N = 25	C = -0.082 P = 0.692 N = 26	C = 0.375 P = 0.065 N = 25	C = 0.147 P = 0.485 N = 25
	NEFSC	C = 0.112 P = 0.493 N = 40	C = 0.519 P = 0.124 N = 10	C = -0.071 P = 0.672 N = 38	C = 0.014 P = 0.954 N = 19	C = -0.067 P = 0.675 N = 42
	NEFSC inshore	C = 0.061 P = 0.734 N = 34	C = -0.413 P = 0.309 N = 8	C = 0.364 P = 0.244 N = 12	C = -0.102 P = 0.767 N = 11	C = -0.080 P = 0.737 N = 20
	NEAMAP		C = 0.157 P = 0.744 N = 7		C = -0.285 P = 0.584 N = 6	C = -0.203 P = 0.700 N = 6

Table 7. Results of two general linear models modeling winter flounder catch-per-tow, each with a Poisson distribution link function. All variables are significant at $\alpha = 0.001$ level. The Akaike information criterion (AIC) is listed. Model 1 does not include temperature as an explanatory variable but Model 2 does.

Model 1: log(catch-per-tow) ~ 1 + along shelf distance + across shelf distance + depth + survey + year * season				
AIC	140790			
Estimated Coefficients	Estimate	SE	tStat	pValue
(Intercept)	63.194	2.146	29.448	<0.001
Along shelf	-0.035	<0.001	-127.990	<0.001
Across shelf	0.011	<0.001	60.840	<0.001
Depth	0.027	<0.001	58.771	<0.001
Year	-0.035	0.001	-32.723	<0.001
Survey	-0.209	0.009	-23.110	<0.001
Season	11.797	0.886	13.308	<0.001
Year * Season	-0.006	<0.001	-13.747	<0.001
Model 2: log(catch-per-tow) ~ 1 + along shelf distance + across shelf distance+ depth + survey + temperature + year * season				
AIC	124760			
Estimated Coefficients	Estimate	SE	tStat	pValue
(Intercept)	58.800	2.121	27.729	<0.001
Along shelf	-0.038	<0.001	-139.000	<0.001
Across shelf	0.009	<0.001	48.222	<0.001
Depth	0.021	<0.001	46.486	<0.001
Temperature	-0.134	0.001	-110.930	<0.001
Year	-0.033	0.001	-30.634	<0.001
Survey	-0.263	0.009	-28.458	<0.001
Season	5.925	0.874	6.778	<0.001
Year * Season	-0.003	<0.001	-6.653	<0.001

Table 8. Results of ANOCOVA comparing winter flounder spatial, size, and abundance metrics, as well as, an environmental variable across surveys (DEP, NEFSC offshore, NEFSC inshore, and NEAMAP) for all seasons sampled and the yearly average. Significant ($\alpha = 0.05$) results are in bold.

Variable tested	Degree's of Freedom	Sum of Squares	Mean Square	F statistic	P-value
Jan.-Mar. weighted across shelf	2	1153.7	576.87	1.7	0.189
Jan.-Mar. weight along shelf	2	11192.9	5596.4	1.71	0.187
Jan.-Mar. minimum across shelf	2	0.701	0.351	2.38	0.098
Jan.-Mar. minimum along shelf	**2**	**3.065**	**1.533**	**4.52**	**0.013**
Jan.-Mar. maximum across shelf	2	0.266	0.133	0.69	0.506
Jan.-Mar. maximum along shelf	2	0.811	0.405	1	0.371
Jan.-Mar. weighted depth	2	55.54	27.77	0.29	0.748
Jan.-Mar. weighted temperature	2	0.432	0.216	0.06	0.941
Jan.-Mar. average temperature	2	0.764	0.382	0.27	0.761
Jan.-Mar. geometric mean catch	**2**	**874.11**	**437.05**	**16.76**	**<0.001**
Jan.-Mar. weight-per-fish	**2**	**0.224**	**0.112**	**6.92**	**0.002**
Apr.-Jun. weighted across shelf	3	626.56	208.85	1.26	0.300
Apr.-Jun. weight along shelf	3	2757.6	919.2	2.18	0.104
Apr.-Jun. minimum across shelf	**3**	**1.171**	**0.390**	**5.86**	**0.002**
Apr.-Jun. minimum along shelf	**3**	**3.084**	**1.028**	**7.23**	**0.001**
Apr.-Jun. maximum across shelf	3	0.004	0.001	0.14	0.933
Apr.-Jun. maximum along shelf	3	0.025	0.009	0.31	0.816
Apr.-Jun. weighted depth	3	5.96	1.99	0.23	0.873
Apr.-Jun. weighted temperature	3	19.314	6.438	2.26	0.094
Apr.-Jun. average temperature	3	17.054	5.685	2.23	0.099
Apr.-Jun. geometric mean catch	3	397.17	132.39	1.31	0.282
Apr.-Jun. weight-per-fish	**3**	**0.087**	**0.029**	**4.18**	**0.011**
Jul.-Sep. weighted across shelf	**2**	**2886.9**	**1443.4**	**3.65**	**0.031**
Jul.-Sep. weighted along shelf	**2**	**5627.6**	**2813.82**	**3.47**	**0.037**
Jul.-Sep. minimum across shelf	2	0.372	0.186	1.87	0.161
Jul.-Sep. minimum along shelf	**2**	**1.576**	**0.788**	**3.28**	**0.044**
Jul.-Sep. maximum across shelf	2	0.012	0.006	0.2	0.822
Jul.-Sep. maximum along shelf	2	0.128	0.064	0.77	0.468
Jul.-Sep. weighted depth	2	112.5	56.23	2.48	0.091
Jul.-Sep. weighted temperature	**2**	**208.74**	**104.369**	**4.76**	**0.012**
Jul.-Sep. average temperature	**2**	**47.89**	**23.943**	**7.64**	**0.001**
Jul.-Sep. geometric mean catch	2	436.78	218.39	2.23	0.115
Jul.-Sep. weight-per-fish	**2**	**0.083**	**0.042**	**3.91**	**0.025**
Oct.-Dec. weighted across shelf	3	578	192.7	0.63	0.596
Oct.-Dec. weight along shelf	3	332.6	110.87	0.16	0.921
Oct.-Dec. minimum across shelf	3	0.221	0.074	0.59	0.626
Oct.-Dec. minimum along shelf	3	0.738	0.246	0.92	0.440
Oct.-Dec. maximum across shelf	3	0.327	0.109	2.69	0.056
Oct.-Dec. maximum along shelf	3	0.128	0.043	0.46	0.709
Oct.-Dec. weighted depth	3	104.7	34.88	0.86	0.466
Oct.-Dec. weighted temperature	3	2.167	0.722	0.08	0.971
Oct.-Dec. average temperature	3	18.495	6.165	2.31	0.085
Oct.-Dec. geometric mean catch	**3**	**3870.14**	**1290.05**	**10.64**	**<0.001**
Oct.-Dec. average weight-per-fish	3	0.066	0.022	2.18	0.101
SSB ann. weighted across shelf	**3**	**1257.74**	**419.2**	**4.08**	**0.009**
SSB annual weight along shelf	3	2956.5	985.5	1.62	0.190
SSB annual minimum across shelf	3	0.146	0.049	1.38	0.256
SSB annual min. along shelf	**3**	**0.897**	**0.299**	**3.48**	**0.020**
SSB annual maximum across shelf	3	0.039	0.013	0.34	0.795
SSB annual maximum along shelf	3	0.082	0.027	0.41	0.747
SSB annual weighted depth	3	97.7	32.55	2.57	0.060
SSB annual weighted temp.	3	3.933	1.311	0.19	0.904
SSB annual average temperature	3	4.586	1.529	1.24	0.302

SSB annual geo. mean catch	**3**	**846.24**	**282.08**	**8.71**	**<0.001**
SSB annual weight-per-fish	**3**	**0.086**	**0.029**	**5.03**	**0.003**

Table 9. Results of Tukey's honest significant difference test on pairwise comparisons testing which surveys (DEP, NEFSC offshore, NEFSC inshore, and NEAMAP) had significantly different results for winter flounder and environmental metrics tested. Only variables that were significant in the ANOCOVA are included in this table. Significant ($\alpha = 0.05$) results are in bold.

Variable tested	Group 1	Group 2	Lower conf. interval for the difference	Est. difference between the intercepts of groups 1 & 2	Upper conf. interval for the difference	P-value
Jan.-Mar. minimum along shelf	DEP	NEFSC	-0.072	-0.030	0.013	0.223
	DEP	**NEFSC inshore**	**-0.100**	**-0.055**	**-0.009**	**0.014**
	NEFSC	NEFSC inshore	-0.055	-0.025	0.004	0.120
Jan.-Mar. geometric mean catch	**DEP**	**NEFSC**	**-1.247**	**-0.877**	**-0.507**	**<0.001**
	DEP	**NEFSC inshore**	**-1.263**	**-0.864**	**-0.466**	**<0.001**
	NEFSC	NEFSC inshore	-0.248	0.013	0.274	0.992
Jan.-Mar. weight-per-fish	**DEP**	**NEFSC**	**0.004**	**0.013**	**0.022**	**0.003**
	DEP	NEFSC inshore	-0.003	0.007	0.017	0.240
	NEFSC	NEFSC inshore	-0.013	-0.006	<0.001	0.060
Apr.-Jun. minimum across shelf	DEP	NEFSC	-0.066	-0.030	0.005	0.117
	DEP	**NEFSC inshore**	**-0.147**	**-0.085**	**-0.025**	**0.003**
	DEP	NEAMAP	-0.183	-0.052	0.080	0.721
	NEFSC	NEFSC inshore	-0.120	-0.055	0.009	0.118
	NEFSC	NEAMAP	-0.155	-0.022	0.112	0.973
	NEFSC inshore	NEAMAP	-0.109	0.034	0.176	0.921
Apr.-Jun. minimum along shelf	DEP	NEFSC	-0.088	-0.036	0.016	0.258
	DEP	**NEFSC inshore**	**-0.233**	**-0.145**	**-0.056**	**<0.001**
	DEP	NEAMAP	-0.295	-0.103	0.089	0.488
	NEFSC	**NEFSC inshore**	**-0.203**	**-0.109**	**-0.014**	**0.018**
	NEFSC	NEAMAP	-0.262	-0.067	0.128	0.797
	NEFSC inshore	NEAMAP	-0.166	0.042	0.250	0.950
Apr.-Jun. weight-per-fish	**DEP**	**NEFSC**	**0.002**	**0.013**	**0.024**	**0.020**
	DEP	NEFSC inshore	-0.016	0.004	0.024	0.947
	DEP	NEAMAP	-0.068	-0.025	0.017	0.405
	NEFSC	NEFSC inshore	-0.030	-0.009	0.012	0.662
	NEFSC	NEAMAP	-0.081	-0.038	0.005	0.102
	NEFSC inshore	NEAMAP	-0.075	-0.029	0.017	0.343
Jul.-Sep. weighted across shelf	**DEP**	**NEFSC**	**0.021**	**1.423**	**2.826**	**0.046**
	DEP	NEFSC inshore	-1.887	0.228	2.343	0.964
	NEFSC	NEFSC inshore	-3.024	-1.196	0.633	0.267
Jul.-Sep. weighted along shelf	**DEP**	**NEFSC**	**-4.076**	**-2.067**	**-0.057**	**0.042**
	DEP	NEFSC inshore	-3.646	-0.616	2.414	0.878
	NEFSC	NEFSC inshore	-1.168	1.451	4.070	0.385
Jul.-Sep. minimum along shelf	**DEP**	**NEFSC**	**-0.071**	**-0.037**	**-0.002**	**0.035**
	DEP	NEFSC inshore	-0.075	-0.023	0.029	0.535
	NEFSC	NEFSC inshore	-0.032	0.013	0.058	0.757
Jul.-Sep. weighted temperature	DEP	NEFSC	-0.640	-0.309	0.021	0.071
	DEP	**NEFSC inshore**	**-1.118**	**-0.620**	**-0.121**	**0.011**
	NEFSC	NEFSC inshore	-0.741	-0.310	0.120	0.203
Jul.-Sep. average temperature	DEP	NEFSC	-0.237	-0.116	0.006	0.067
	DEP	**NEFSC inshore**	**-0.350**	**-0.215**	**-0.081**	**0.001**
	NEFSC	**NEFSC inshore**	**-0.192**	**-0.100**	**-0.007**	**0.032**
Jul.-Sep. weight-per-fish	DEP	NEFSC	-0.007	<0.001	0.008	0.986
	DEP	NEFSC inshore	-0.021	-0.011	<0.001	0.063
	NEFSC	**NEFSC inshore**	**-0.020**	**-0.011**	**-0.002**	**0.019**
Oct.-Dec. geometric	**DEP**	**NEFSC**	**-2.119**	**-1.113**	**-0.107**	**0.025**
	DEP	**NEFSC inshore**	**-4.040**	**-2.749**	**-1.458**	**<0.001**

mean catch	DEP	NEAMAP	-7.749	-0.720	6.309	0.993
	NEFSC	**NEFSC inshore**	**-2.804**	**-1.636**	**-0.467**	**0.003**
	NEFSC	NEAMAP	-6.614	0.393	7.400	0.999
	NEFSC inshore	NEAMAP	-5.025	2.028	9.082	0.871
SSB annual weighted across shelf	**DEP**	**NEFSC**	**0.263**	**1.066**	**1.869**	**0.004**
	DEP	NEFSC inshore	-0.196	0.800	1.796	0.160
	DEP	NEAMAP	-5.854	0.535	6.925	0.996
	NEFSC	NEFSC inshore	-1.010	-0.267	0.477	0.783
	NEFSC	NEAMAP	-6.886	-0.531	5.824	0.996
	NEFSC inshore	NEAMAP	-6.646	-0.264	6.118	1.000
SSB annual minimum along shelf	**DEP**	**NEFSC**	**-0.048**	**-0.025**	**-0.002**	**0.028**
	DEP	**NEFSC inshore**	**-0.062**	**-0.033**	**-0.004**	**0.018**
	DEP	NEAMAP	-0.239	-0.054	0.131	0.867
	NEFSC	NEFSC inshore	-0.029	-0.008	0.014	0.776
	NEFSC	NEAMAP	-0.213	-0.029	0.155	0.976
	NEFSC inshore	NEAMAP	-0.206	-0.021	0.163	0.990
SSB geometric mean catch	**DEP**	**NEFSC**	**-1.325**	**-0.874**	**-0.423**	**<0.001**
	DEP	**NEFSC inshore**	**-1.304**	**-0.744**	**-0.185**	**0.004**
	DEP	NEAMAP	-3.538	0.051	3.640	1.000
	NEFSC	NEFSC inshore	-0.288	0.129	0.547	0.848
	NEFSC	NEAMAP	-2.645	0.925	4.495	0.905
	NEFSC inshore	NEAMAP	-2.790	0.796	4.381	0.937
SSB weight-per-fish	**DEP**	**NEFSC**	**0.001**	**0.007**	**0.013**	**0.015**
	DEP	NEFSC inshore	-0.005	0.002	0.010	0.869
	DEP	NEAMAP	-0.071	-0.023	0.025	0.584
	NEFSC	NEFSC inshore	-0.010	-0.005	0.001	0.109
	NEFSC	NEAMAP	-0.077	-0.030	0.017	0.348
	NEFSC inshore	NEAMAP	-0.073	-0.025	0.022	0.508

FIGURE CAPTIONS

Figure 1. Areas sampled for winter flounder in each survey with the Northeastern Fisheries Science Center (NEFSC) in blue, Northeastern Fisheries Science Center inshore (NEFSC inshore) portion in green, the Northeastern Area Monitoring and Assessment Program (NEAMAP) in yellow, and the Department of environmental Protection (DEP) in red. The coastline is denoted in black. Inshore surveys (DEP, NEFSC inshore, and NEAMAP) all overlap off of NJ. The NEFSC inshore and NEAMAP surveys overlap spatially for the whole costal study area. The NEFSC offshore survey has minor overlap off of southern NJ with other surveys but is mainly focused offshore.

Figure 2. Fall centers of biomass for winter flounder in each survey with the Northeastern Fisheries Science Center (NEFSC) in blue, Northeastern Fisheries Science Center inshore (NEFSC inshore) portion in green, and the Department of environmental Protection (DEP) in red.

Figure 3. The spawning stock biomass yearly average centers of biomass for winter flounder in each survey with the Northeastern Fisheries Science Center (NEFSC) in blue, Northeastern Fisheries Science Center inshore (NEFSC inshore) portion in green, the Northeastern Area Monitoring and Assessment Program (NEAMAP) in yellow, and the Department of environmental Protection (DEP) in red.

Figure 1.

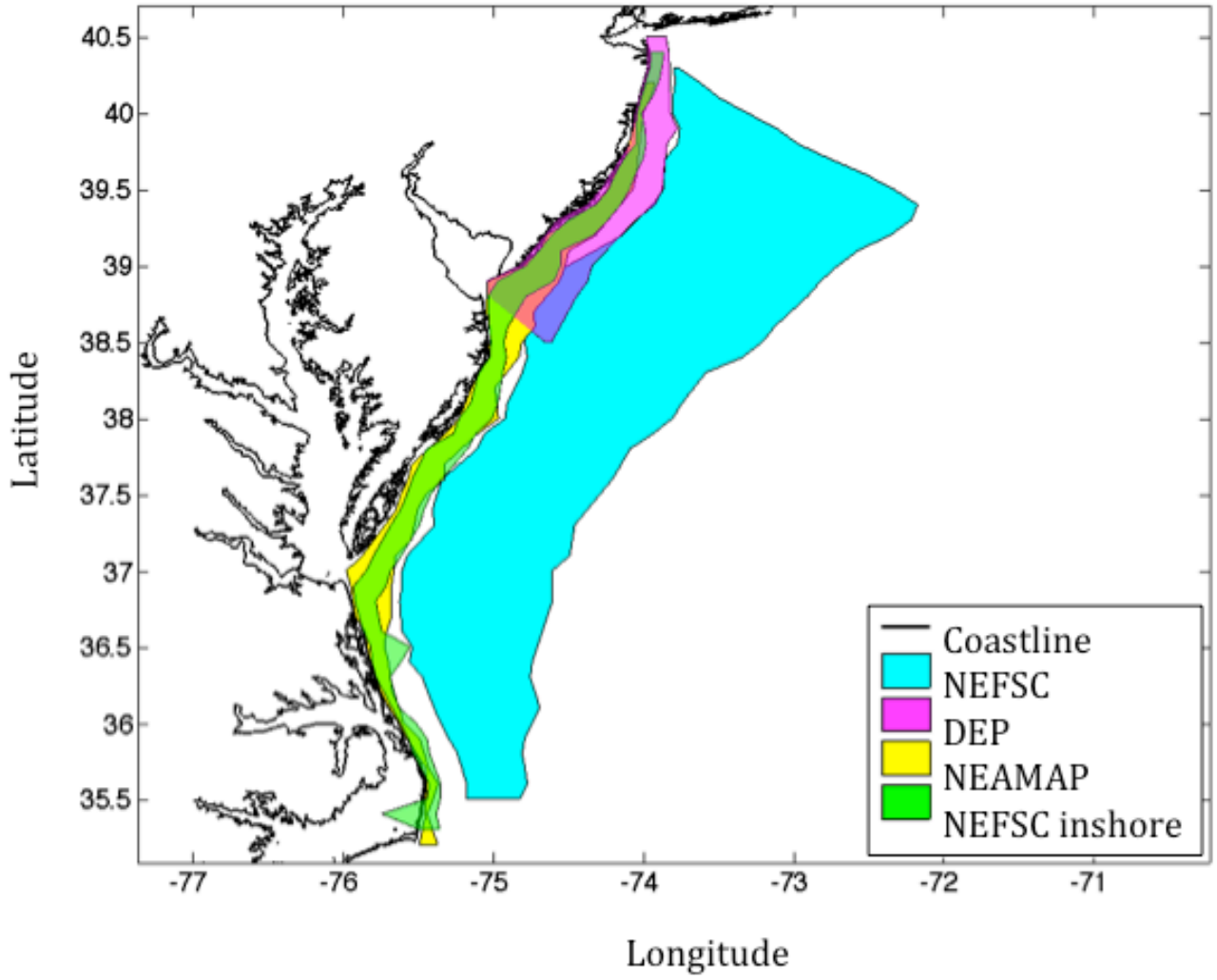
40.5
40
39.5
39
38.5
38
37.5
37
36.5
36
35.5
Latitude
-77
-76
-75
-74
-73
-72
-71
Longitude
Coastline
NEFSC
DEP
NEAMAP
NEFSC inshore

Figure 2.

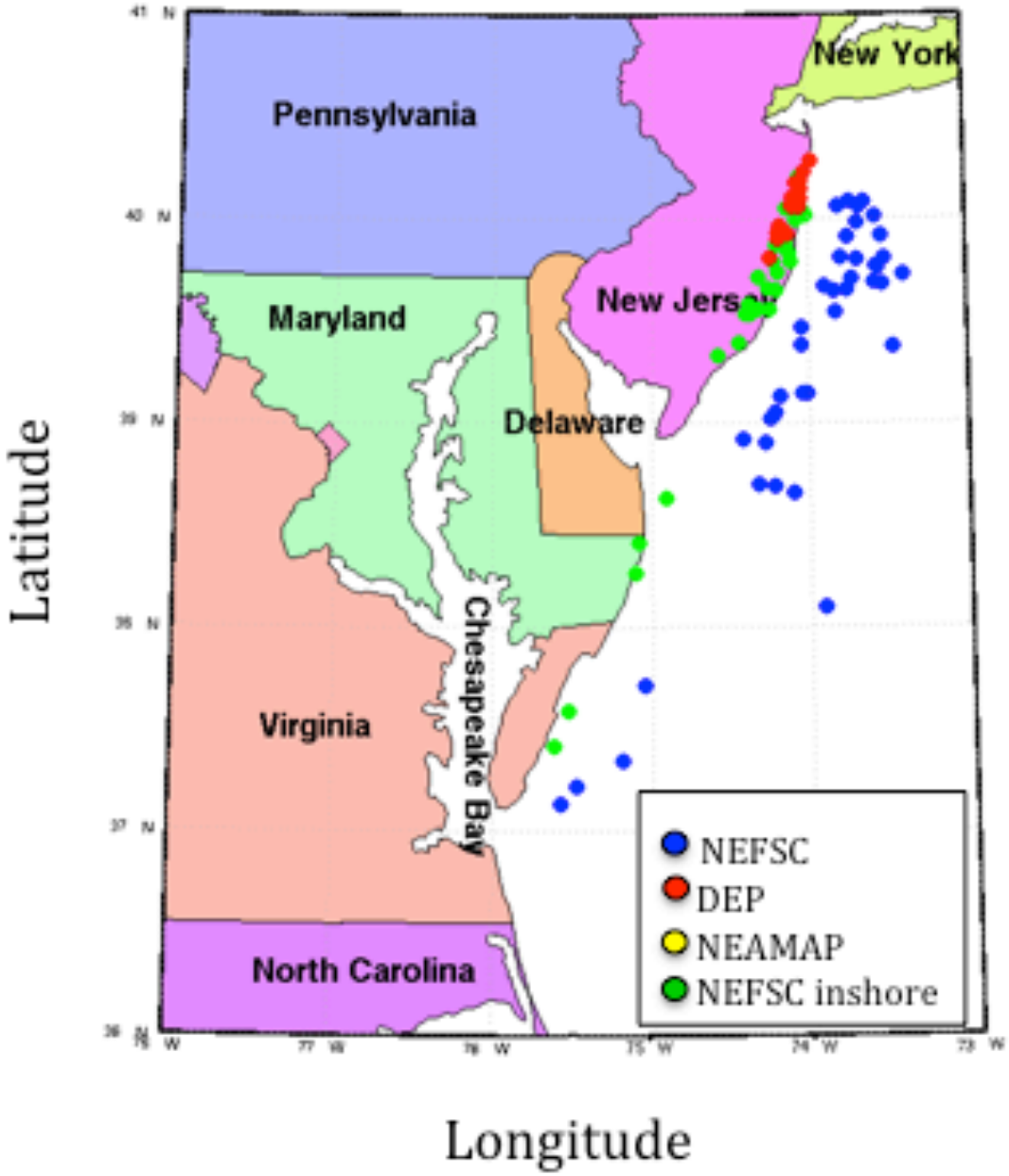
Pennsylvania
New York
Maryland
New Jersey
Delaware
Chesapeake Bay
Virginia
North Carolina
NEFSC
DEP
NEAMAP
NEFSC inshore
Latitude
Longitude

Figure 3.

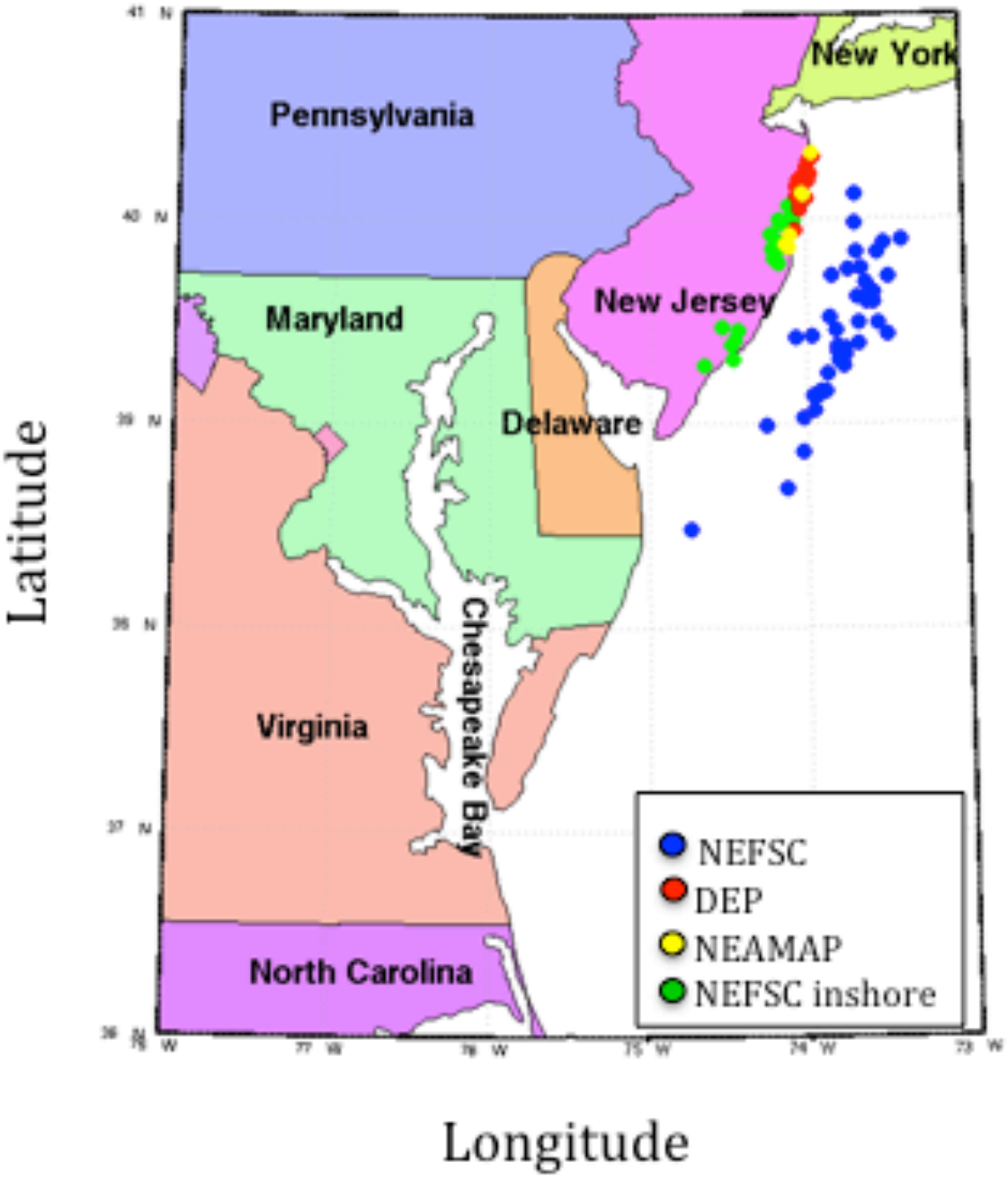
Pennsylvania
New York
New Jersey
Maryland
Delaware
Chesapeake Bay
Virginia
North Carolina
NEFSC
DEP
NEAMAP
NEFSC inshore
Latitude
Longitude

– Chapter 3 –

TAGGING AND TRACKING WINTER FLOUNDER: MULTIPLE APPROACHES USED IN THE MID-ATLANTIC

Abstract

The goal of this study was to better understand where adult winter flounder are while seasonally spawning in the central to southern Mid-Atlantic Bight as well as their range of motion on the shelf. We accomplished this through the use of cutting edge tagging and tracking methods as well as historic tagging records. Through the use of American Littoral Society historic release and recapture locations I observed residency and site fidelity of winter flounder along the Northeastern U.S. coast. While the release of tagged winter flounder was successful, I experienced a very low recapture rate and was unable to work out seasonal spawning connectivity between the ocean and estuary. I found that the majority of fish tagged during this study were female and within the defined size limits for mature winter flounder for our area. I was able to observe some behavioral characteristics and habitat preferences for the minor subset of the population sampled (n=4) in the fall of 2012. Two winter flounder fitted with acoustic tags moved inshore and north from the release site while one tagged winter flounder moved offshore. Additionally one winter flounder fitted with an archival tag was recovered in deeper waters. This flounder had a strong preference to water temperatures of 9.48 °C ± 0.18 °C (range 9.08 °C to 9.91 °C) and mean salinity of 32.55 ± 1.21 (range 28.64 to 33.92).

3.1 Introduction

Since marine animals depend on multiple habitats throughout their life cycle, connectivity has become a central theme in ecology, conservation, and population dynamics

(e.g. Ray, 2005; Sheaves, 2009; Kämpf *et al.,* 2010). This is especially evident for many estuarine fish species (Able, 2005; Able and Fahay, 2010). Here I accept the definition of Secor and Rooker (2005) in which connectivity "refers to the dependence of fish production and population dynamics on dispersal and migration among multiple habitats". This definition is appropriate to consider in mitigating the decline of winter flounder, such as protecting spawning habitat from dredging.

Juveniles of many fish species benefit from being in estuaries in the spring (e.g. Rice *et al.,* 1999). In order to arrive there, most species spawn pelagic eggs on the continental shelf, and the drift of these eggs to estuaries is a risky phase. It is likely that the secondarily derived trait of laying demersal adhesive eggs (Pearcy, 1962; Scarlett and Allen, 1992) allows winter flounder to circumvent this risk. A long-term study in a New Jersey estuary found that larvae were most abundant in the system in April and May, while juveniles were commonly found in June but could be present as early as April and as late as November (Able *et al.*, 2014). Estuaries are dynamic and potentially hostile to adults and eggs in winter, and as seen for other fish species, this can result in the evolutionary adoption of a wider spawning habitat to "buffer" detrimental episodic environmental fluctuations (Warner and Chesson, 1985; Kraus and Secor, 2004; Secor, 2007). This occurs for other pleuronectid flatfishes such as flounder (*Pleuronectes flesus*) in the Baltic Sea (Nissling *et al.,* 2002; Nissling and Dahlman, 2010).

Numerous authors report that winter flounder adults move into estuaries in fall in anticipation of spawning there in the winter (Bigelow and Schroeder, 1953; Perlmutter, 1947; McCracken, 1963; Jeffries and Johnson, 1974; Phelan, 1992; Scarlett and Allen, 1992; Stoner *et al.,* 1999; Collette and Klein-MacPhee, 2002). Regardless of timing, the above authors believed spawning south of Cape Cod occurs solely in estuaries, as do others (Saila, 196; Crawford and Carey, 1985) including in New Jersey (Scarlett, 1991 a, b, 1992).

Estuarine spawning of acoustically tagged adults has been observed in the Navesink River, New Jersey (Grothues *et al.,* 2012). Up-estuary movement of telemetered fish occurred in early February and again in late March or early April, apparently triggered by local warming events in a narrow range (7-12 °C) of the total temperature range (0-20 °C), although not all tagged fish participated in within-estuary migration (Grothues *et al.*, 2012). However, some fish were already available to trawl and capture fyke nets in the upper estuary by February, and may have moved up much earlier (Grothues *et al.*, 2012). Sexual differences of timing also occurred, with males demonstrating more activity than females, leaving the ocean to move into the estuary several weeks prior to females (Pravatiner, 2010). Others report that adult winter flounder do not move into estuaries until the winter (Pearcy, 1962; *Stoner et al*., 1999).

At the same time, there is some evidence of year-round residence in estuaries by individuals in the SNE/MAB (Phelan, 1992; Sagarese and Frisk, 2011). This interpretation may be confirmed or confounded by the high degree of estuarine fidelity (Phelan, 1992; Crivello *et al.,* 2004), which may reflect local population differences. Winter flounder spawn and use estuaries as young-of-the-year (YOY) in New Jersey based on the abundance of larvae (Witting *et al.,* 1999; Curran and Able, 2002), the frequent collection of YOY (Able *et al.,* 1996), and their fast growth in a variety of estuarine habitats (Sogard and Able, 1992, 1994; Able and Fahay, 1998; Phelan *et al,*. 2000; Sogard *et al.,* 2001). The distribution of larvae supports that hatching and rapid growth occurs near or in the general spawning grounds (Frank and Leggett, 1983; Crawford and Carey, 1985; Stoner *et al.,* 1999, 2001).

There appear to be differences in movement patterns and residency between the winter flounder stocks north and south of Cape Cod (McCracken, 1963; Howe and Coates, 1975). North of Cape Cod in the Gulf of Maine (GOM) stock, a telemetry study indicated that winter flounder consisted of two different contingents (an example of divergent migration

as defined by Secor, 1999), with one spawning in the estuary and the other along the coast (DeCelles and Cadrin, 2010). Further, reported patterns of adult winter flounder movements and the location of spawning in the GOM is varied and includes residency in the ocean, residency in estuaries, but also seasonal movements between ocean to estuary (DeCelles and Cadrin, 2010; Able and Fahay, 2010).

In the Southern New England/Mid-Atlantic Bight (SNE/MAB) stock, two migratory groups were defined in Long Island as 'bay' fish that are resident in estuaries and 'offshore' fish that migrate between the two habitats (Perlmutter, 1947; Sagarese and Frisk, 2011). Frisk *et al.,* (2014) has defined three possibilities for these strategies: (1) 'bay' fish and 'offshore' fish are genetically controlled traits and heritable, (2) 'bay' fish and 'offshore' fish are the same population but behavior was selected in early life history (re Secor, 1999), or (3) they are the same population but 'bay' or 'offshore' behavior is decided upon annually and could be linked to energetic requirements. Understanding the difference between behavior and genetic heritability on migration would be important for management and assessment since these strategies seasonally overlap essential fish habitat (Frisk *et al.*, 2014).

Several authors believe that spawning may also occur in the ocean for inshore stocks (Howe and Coates, 1975; Wuenschel *et al.,* 2009; DeCelles and Cadrin, 2010; Sagarese and Frisk, 2011; Fairchild *et al.,* 2013; Frisk *et al*., 2014). This seems possible given that spawning is well documented to occur in the ocean on Georges Bank (GB) for the offshore GB stock (Collette and Klein-McPhee, 2002; Bigelow and Schroeder, 1953). This third possibility for the SNE/MAB stock would be a behavioral or genetic group that is resident and spawns offshore (called 'ocean spawning' fish here). However there are regional differences between the stocks that affect spawning seasonality and strategies that would make timing and ocean spawning in the SNE/MAB stock different than the GOM and

GB stock (O'Brien *et al.,* 1993; DeCelles and Cadrin, 2011). This ocean spawning strategy could be supported south of Cape Cod inclusive of New Jersey due to reports of the continuous presence of adults (> 18 cm) in the ocean (Phelan, 1992; Able and Hagan, 1995; Wuenschel *et al.,* 2009). Evidence for ocean spawning outside of estuaries in coastal waters has been observed in the SNE/MAB stock but to a minimal degree; Press *et al.,* (2014) found 1% of mature females had ovulated eggs in March in coastal waters; Wuenschel *et al.,* (2009) also found fish with mature gonads off of New Jersey in winter, and actively spawning fish have been collected offshore (NEFSC bottom trawl surveys, unpubl. data; M. Wuenschel, pers. obs from Press *et al*., 2014).

This ocean spawning interpretation could be confounded since winter flounder have the ability to skip spawning instead of spawning annually (Tyler and Dunn, 1976; Burton and Idler, 1984, 1987a, 1987b; Burton, 1991; Maddock and Burton, 1994, Rideout *et al.,* 2005; Rideout and Tomkiewicz, 2011). An individual's fecundity is determined prior to spawning in the time period after the individual has spawned from the previous year (McBride *et al.*, 2013). If conditions are poor after spawning (i.e. low nutrition) this could cause the next cohort of oocytes not to advance causing the individual to skip spawning the subsequent year, denoted as a 'resting type' female (Tyler and Dunn, 1976; Burton and Idler, 1984, 1987a, 1987b; Rideout *et al*., 2005). Press *et al.,* (2014) observed that resting type fish were rare and only occurred in the inshore stocks of SNE and GOM, but not for the GB stock (McElroy *et al.*, 2013). Additionally, skipped spawning was less likely to occur in the stocks in the United States than in the higher latitude Canadian stocks (McBride *et al.,* 2013; Press *et al.,* 2014). Wuenschel *et al.,* (2009) suggests that the value for skipped spawning fish in the SNE/MAB stock may be approximately 5%, and thus does not account for all the variation observed in seasonal spawning patterns.

The confusion about winter flounder spawning habitat compromises effective management of the fisheries for winter flounder and its usefulness as an indicator species, especially relative to the permitting for estuarine dredging for improved navigation and ocean dredging for sand for beach nourishment. The seeming contradictions reported in spawning habitat (estuary vs. ocean) or some combination may be the result of much greater mobility by the adults than is often understood. Given these considerations and the growing evidence for the importance of adult movements rather than larvae in genetic diversification (Sagarese and Frisk, 2011; Press *et al.,* 2014; Frisk *et al.,* 2014), we reevaluated the seasonal movements of adults and thus, a determination of the spawning sites for winter flounder (estuary and/or ocean) in New Jersey with archival tags (an approach unique to this species), acoustic tags, and American Littoral Society (ALS) marker tags. This is especially warranted given the increasing influence of climate change (e.g. Nye *et al.,* 2009; Lucey and Nye, 2010) on spawning patterns of coastal fish in the region as for Atlantic croaker (Hare and Able, 2007) and winter flounder (Keller and Klein MacPhee, 2000; Oviatt, 2004).

A further potentially confounding factor is that burial of tagged winter flounder may interfere with acoustic tag detection (Sagarese and Frisk, 2011; Grothues *et al.,* 2012) and thus compromise our understanding of habitat use and connectivity. This problem is avoided by the use of long duration archival tags in this study, because these tags constantly record data. Telemetry can provide high resolution (to meter scale) movements, but is limited by the placement of hydrophone equipment to detect tagged fish and thus presents logistical constraints of tracking fish over long distances. While there are extensive hydrophone arrays in bays, rivers, and inshore (such as in Delaware Bay), telemetry may not be easily applied to questions of large seasonal migrations offshore where depth

becomes a factor as well as spatial overlap. This is one of the difficulties identified in telemetered studies with winter flounder (Grothues *et al.*, 2012).

3.2 Methods

Study Area

This study focused on the southern portion of winter flounder range in the Mid-Atlantic, mainly off of northern New Jersey. The study area extended from northern New Jersey estuaries to coastal shelf habitat. I collected winter flounder inshore between Belmar and Sandy Hook (Table 1, 2, 3) with a focus on the False Hook ocean-side off of Sandy Hook and offshore at the Mud Hole (40.1588, -73.6842), a depositional feature that is part of the Hudson Valley submarine canyon (Figure 1). Fish were captured on the southwest edge of the valley in an approximate 3000-meter stretch, with a drop in abundance directly outside of this zone (approximately 38 fathoms, Captain Jim Lovgren, *Viking II*, per. communication). As the name Mud Hole implies, the bottom habitat is made up of medium, fine, and very fine sand, clay, silt, and mud (USGS, 2013), which is conducive to burial of young winter flounder (Phelan *et al.*, 2001).

Capture and Tagging Techniques

We used three different tags (archival, acoustic, and marker) each with their respective advantages for investigating winter flounder connectivity. Archival tags (Star-Oddi Inc. Reykjavik, Iceland, 15 mm X 46 mm, 19 g in air) record conductivity (converted to salinity in post-processing using temperature), temperature, and pressure (depth), (comprehensively abbreviated as CTD) with a time stamp. The temperature sensing range of these tags is -1°C to +40°C (accuracy of ±0.1°C); the depth range (user selected at 1 m to 100 m, at an accuracy of ±0.4 m) and conductivity range of 3 to 37 mS/cm (accurate to ±1 PSU). Non-volatile memory allowed storage of up to 87,217 measurements per sensor for

up to four years (determined by battery). We set sensors to record every 24 minutes so that memory capacity matched battery life span. Acoustic tags (Lotek Wireless, Inc., St. Johns, Canada) emit a coded signal that can be detected up to 500-meters away (condition dependent) with specialized hydrophones. The acoustic tags had a battery life of approximately three months. Lastly, we used marker tags (The American Littoral Society, ALS, a citizen science based organization) printed with unique identification numbers.

In the ocean, capture took place during annual groundfish surveys by the New Jersey Department of Environmental Protection (NJDEP) and on a chartered commercial trawler, the *F/V Viking II*, for directed capture of a large number of individuals. This trawl effort consisted of on average 20-minute tows with a net and mesh conforming to commercial trawling regulations. Tagging was also done on the *R/V SeaWolf* in conjunction with the NJDEP groundfish trawl survey on October 11, August 15, and June 29, 2012 and October 16, January 23, 2013 and on the *F/V Viking II,* on September 6 and 7, 2012. We also attempted to tag fish on June 26 and 28, and August 14 and 24, 2012, on the *R/V SeaWolf* but captured no suitable winter flounder. Acoustic tags were only deployed on the *F/V Viking II* on September 7, 2012 and released in conjunction with the archival tags as a way to monitor dispersal of this subpopulation from the release position.

We tagged large (> 25 cm for ALS tags, > 35 cm for acoustic and archival tags) adult winter flounder (Figure 2) with multiple techniques. Adults were defined on the basis of size at maturity, which is a median length of 27 cm in southern New Jersey and 28 ± 8.1 cm (age 2.4 ± 0.1) for the Mid-Atlantic Bight (McBride *et al.,* 2012). Once captured, before tagging, all fish were sexed (if able), length was measured, and then we tagged the fish with archival tags (n = 60), acoustic (n = 12), and ALS tags (n=159) primarily in the fall and winter of 2012.

For acoustic and archival tags, in every instance, tag attachment used two small punctures made with a slotted hypodermic needle through the pterygiophores of the dorsal fin at the level of the pectoral fin. Archival tags were externally attached with plastic-coated stainless steel surgical wires. These wires, at the end of the tag, were run through the needles punctures and secured on the blind side of the fish after needle withdrawal. A nylon shield on the blind side was not used because it was not found to reduce chafing (Fairchild *et al.*, 2008). To reduce stress, a cool, damp, cloth was placed over the eyes during this process. Prior to release, fish were retained for 10 to 25 minutes to allow for recovery and a post-surgical health assessment, as was previously done in Pravatiner (2010) and Grothues *et al.,* (2012). Ice was used to maintain preferred temperatures in the holding tanks prior to and after tagging and excess mucous was scooped out of the tank to help keep the mouth and gills free. All fish to be tagged were judged on their condition while in the holding tank based on their energy, if they were bleeding, and how they were breathing. The fitness of the fish was judged on a 1 to 3 scale with 1 being the most hearty. Only hearty fish were released after being tagged.

Environmental conditions were monitored within the holding tank as well as at the capture locations (at the Mud Hole and along the coast) to verify accuracy of the archival tag recordings. This was done with a hand held CTD (YSI). Environmental conditions in the holding tank on Sept. 6 were as follows: dissolved oxygen of 65.4% or 5.04 mg/L, temperature of 18.66°C, salinity of 30.53, and pH of 7.86. Average bottom water environmental conditions on Sept. 6 were as follows: dissolved oxygen of 42% or 3.59 mg/L, temperature of 12.36°C, salinity of 32.31, and pH of 7.38. Environmental conditions in the holding tank on Sept. 7 were as follows: dissolved oxygen of 82.5% or 6.26 mg/L, temperature of 19.6°C, salinity of 31.61, and pH of 8.1.

Other individuals captured in the trawls were fitted with American Littoral Society (ALS) code-specific marker tags inserted at the base of the dorsal fin towards the caudal peduncle with a hollow sterilized needle. Marker tags were not tied in simple over hand knots as recommended by the ALS because these knots failed after days to weeks for flounders kept in our test tank (n = 3). Marker tags were fastened with small zip ties leaving enough room between the tag and the fish for growth but not enough to cause entanglement on ocean debris. We recorded length (total length in mm), capture location, and date on an ALS supplied tagging card and mailed the cards to the ALS. The ALS sends raw data to the National Marine Fisheries Service, Woods Hole, MA for processing and entry into a long-term database (J. Dement, ALS, pers. comm.). For all tagged fish, I attempted to determine the sex based on the presence of a visible bulge from a mature ovary or gamete expression, as has been done previously in the study area (Pravatiner, 2010). We sacrificed 39 individuals collected at the Mud Hole on September 6 to surgically examine gonads since it was too early in the year to determine sex and maturity by visual inspection.

Recapture/Detection Techniques

Acoustic tracking was done on the *Viking II*, immediately after deployment (September 7) as well as on charter boats, *M/V Venture III* and *M/V Fin-Ominal* (September 13, 20, 27, and October 4 and 5, 2012). I towed mobile hydrophones (LPH_1 attached to MAP 600 RT receiver/processor) at 0.8 knots off of both sides aft of the vessel while recording time-stamped boat position from a hand-held global positioning system (GPS). In addition, we deployed an autonomous underwater vehicle (AUV, REMUS-100, Hydroid Inc., MA) with a coaxial-mounted hydrophone (Grothues *et al.*, 2010) to detect acoustically tagged fish. The AUV was used for two missions on September 13, 2012. Search efforts on the charter vessels were focused within a 1600-3200 meter radius around the release point

and consisted of long transects, boustrophedon sections, and circles (Figure 3). Both mobile loggers recorded the tag identity along with the tag signal strength (dB), and time stamp.

In order to detect winter flounder with acoustic tags moving between the estuaries and ocean, we mounted three submerged hydrophones (MAP 3050 SDL, Lotek Wireless, Inc.) at the mouths of the Navesink River, Shark River, and Manasquan River attached to a base and tethered to boat docks (Figure 1). They were active from September 7, 2012 to January 2, 2013 in conjunction with when the acoustic tag batteries were active. These were sufficiently sensitive to detect the deployed tags from across the entire river to monitor passage under most conditions. The greatest distance across the rivers was 400 meters, while tags are typically detectable to 500 meters (Grothues, 2009).

Since recovery of the archival and ALS tags was crucial, an outreach effort was extended to the commercial (through National Fisheries Institute, fishing co-ops, and others) and recreational (American Littoral Society) fishing sectors in collaboration with New Jersey SeaGrant Extension Services (especially M. Danko) to promote recovery of tags. Reward flyers in local bait and tackle shops (mainly in New Jersey) advertised a $200 reward for the return of each archival tag.

Data Analysis

Data analysis varied for each tag type. To calculate acoustics tag positions, we used a Sound Pressure Level Weighted Center of Activity (SPLCoA) method (outlined in Grothues and Davis, 2013). From a sequence of such position estimates, I then calculated distance and direction traveled until the last detection.

Habitat visitation/ residence over time, and thus movements for each individual fish, can, in theory, be determined based on the archival tag's ability to sense and record the habitat where it was present. This methodology is explored and tested rigorously in simulation in Chapter 4. It is not elaborated on further here, because only a single archival

tag was recovered and path was not an important consideration for that case. Instead, the data was analyzed for the fish's response to environmental dynamics.

In order to get a more accurate position, tidal signal was removed from the archival tag depth record. Removing the tide from the data is useful when trying to resolve the depth of the fish as a function of bathymetry, which is itself important as a constraint of locality. Additionally, the tidal signal can be extracted and used as a variable to help resolve location of the tag during the path reconstruction because different locations experience slightly different tides. The dominant tide was first identified using a spectral analysis. Since the tagged fish is not necessarily stationary, I segmented the data into smaller manageable sections. A large depth change was sampled in the archival tag (ID no. 6663) data and thus depth was subsampled before and after that large change to better resolve de-tided depth. A Lanczos lowpass filter (MATLAB function written by R. Chant, Rutgers University) was then used to remove the tidal signature from the depth data segments. A Nyquist frequency is used in this process and is the folding frequency or half window-length of a sample system. The Nyquist frequency should be larger than the cut-off frequency (decided by the period), so at the sampling frequency of 24 minutes (for the archival tag) the period would be 80 (samples per 32 hours) and thus the Nyquist frequency should be 160. However, when used, a higher Nyquist frequency removed the edges of the time series. Since we need information at the edges of the time record, a lower Nyquist frequency was used but filtered tidal signal out of the record less efficiently.

I also looked for abnormalities in winter flounder behavior by plotting temperature and salinity against depth and to get an estimate of the range of temperature or salinity experiences by the individual.

We analyzed ALS historic tag data from 1980-2012 for direction of movement, distance over time, and movements across stock boundaries. These data encompassed the

inshore SNE/MAB and the Gulf of Maine stocks but not the offshore Georges Bank stock. The regions or "states" where winter flounder were released and recaptured were predefined (based on ALS reporting procedure) as Connecticut (CT), Delaware Bay (DE Bay), Massachusetts north (MA-north), Massachusetts (MA), North Carolina (NC), New Jersey (NJ), New York (NY), and Rhode Island (RI). Additional regions where tagged fish were released, but for which no tags were recovered, were Virginia (VA), Maryland (MD), Connecticut Bay (C Bay), Hudson Bay, Delaware (DE), and North Carolina Inlet (NC-in).

Analyses applied MATLAB version R2014a.

3.3 Results

Sex, Size, and the Environment

The subset of the population sampled from the Mud Hole was composed mostly of females (74.36%), (Table 4), which appeared to be within the size limits of a mature individual. The majority of attempts to sex fish in the field through visual and tactile inspection were inconclusive. The gonadosomatic index (GSI) of the ovary weight ratio to ovary-free body weight for sacrificed females was 3.65. Females averaged 367 ± 37 mm in length and males averaged 321 ± 16 mm in length, with the larger fish outfitted with heavier tags (Figure 2).

I was able to recover one winter flounder fitted with an archival tag, and from these data discern the environmental conditions that the individual experienced. A commercial trawler (Captain Lovgren) recovered a single archival tag (ID no. 6663) downslope of its original release site, 11 days later (Figure 4). Spectral analysis of the recovered data (number of data points) found the predominant tidal signal to be a lunar semidiurnal, M2, tide (Figure 5). This winter flounder demonstrated what appears to be a strong reaction to a warm water intrusion on Sept. 12 (Figure 7) that was slightly less saline (Figure 8) than

water occupied until then. The fish moved to a location that was 13.5 meters deeper from Sept. 12 to Sept. 13, then maintained the new depth with variance similar to that prior to the intrusion (Figure 6). During these 11 days it stayed in water of mean temperature 9.48 °C ± 0.18 °C (range 9.08 °C to 9.91 °C, Figure 9) and mean salinity 32.55 ± 1.21 (range 28.64 to 33.92, Figure 10). This one recaptured archival tag (ID No. 6663, recovered September 20) was reprogrammed and deployed again on October 11, 2012 during a NJDEP cruise.

Residency and Movement

I was able to monitor some movements through the use of the acoustic and archival techniques as well as residency through the use of ALS (marker) techniques. All fish tagged with acoustic tags (n=12) were calculated to still be within the Mud Hole and within 102.81 ± 35.7meters (ranging 32.04 m to 147.42 m) from the release point on September 7, 2012, on the same day as tagging shortly after release (Figure 3). We assumed no fish died due to tagging mortality, since all fish moved from the release point and were not consistently found in the same location in the weeks following release. Six days after release, the AUV detected tag ID no. 12404 at 2304 meters northwest from the release point. On the same date, tag ID no. 9291 was found northwest, 2315 m from the release point. Tag ID no. 12316 was found on September 27 from the *M/V Finominal* approximately 1600 m east of the release point. No tags were recorded entering estuaries through the passive submerged hydrophone gates, during the period of September (2012) to January (2013).

The recapture/ detection rate varied with tag type. Out of 3117 ALS marker tags deployed from 1980-2011, 98 (3.14%) were recaptured from 1983-2012 with a yearly average recovery rate of 0.39%. Rate of recovery diminished with time-at-liberty (2% to 0.03%). Average time-at-liberty was 220 ± 256 days, ranging from 3 to 1688 days (4.6 years). Five tags had a recovery date with no other information about recovery site, so the following comparison on recovery site uses 93 tags. The majority of tags were recovered in

the state or bay from which they were released (94.62%), but 5 of the tags were recovered outside of the release area. Distances between extra-regional release and recovery (with precision constrained by reporting convention) ranged from small distances such as DE Bay to NJ (n = 1, 51 km, 32 d) to distances like MA-north to MA (n = 1, 103 km, 64.5 d), NY to MA (n = 1, 267 km, 167 d), and NY to RI (n = 1, 200 km, 125 d), with the largest distance from NJ to NC (n = 1, 536 km, 335 d). This last record could be skewed if the tagged fish was not in fact captured in NC since large ground fish (65 feet plus) vessels are very mobile and are known to fish off of NJ, thus it could have been reported where it was landed rather than where it was captured. On average, ALS tags that were recaptured moved 165.34 ± 387.42 meters a day, however this is an underestimation since it assumes linear movement. No ALS tags from our new tagging effort were recovered during this study period.

3.4 Discussion

Size, Sex, and the Environment

Gonad condition of captured winter flounder implies that they were not mature or were maturing but compared to the median length of adults for the area most winter flounder were within the mature size range. The gonad weight ratio to ovary-free body weight for sacrificed females was much lower than the published ratio of 34-41% for later oocyte maturation stages (Press *et al.*, 2014). Females sampled averaged 366.97 ± 37.09 mm in length, which is larger than the median length of adult maturation (280 ± 81 mm) but still within the range (140-450 mm) of median length at annual maturation in the Mid-Atlantic (McBride *et al.*, 2013). Compared to females in the SNE portion of the SNE/MAB stock in September which were immature at 174-358 mm and mature at 281-457 mm (Press *et al.*, 2014), the females sampled here could be either immature or mature.

Therefore we cannot assume that all females tagged were spawning, but the majority of fish tagged with larger tags (archival and acoustic) were within the mature size range.

The single archival tag supported a temperature preference of winter flounder for 9.5 °C in this region as defined by Winton *et al*., (2014). My interpretation of the recovered archival data time series is that this fish remained near its tagging site in the Mud Hole South until water warmed abruptly by 0.5 °C due to an advection event, upon which it moved over the lip of the Mud Hole depression and downslope into the canyon until encountering the previously occupied water temperature. Despite the filtering method leaving some tidal information in the depth profile, a semidiurnal tidal motion is common in the study area (Chant *et al.*, 2000) and was correctly identified as the dominant signature to remove.

Residency and Movement

There were limitations to this study and respectively for each tag type. Winter flounder are known to bury in times of extreme heat or cold (He, 2003). This burial response has been proven to hinder hydrophone detection (Grothues *et al.*, 2012) and might be a reason why we were only able to detect three acoustic tags after the deployment date. In addition, we only had the capacity to search the release site (and the surrounding area up to approximately 5 km away) even though the search radius would have grown exponentially over time. The capability of using the REMUS as well as towed hydrophones from a vessel addressed this issue, however there was still a large area unsearched. Winter flounder are well known to have a home range and site fidelity so this area could range as far as approximately 60 km (Collette and Klein-MacPhee, 2002; Fairchild *et al.*, 2013) from the release site.

While there were no entries of acoustically tagged winter flounder into the estuary, the hydrophones may have been periodically ineffectual and could have missed tags.

Superstorm Sandy occurred during this period and stirred sediment into the water column (observed on the shelf by Miles *et al.,* 2013) and debris could have hindered detection (pers. comm. J. Warren). The hydrophone in the Manasquan River was moved from its base and deposited behind a nearby pier at an unknown time (most likely during the storm), which would have hindered tag detection. In addition, there may have been mortality of the tagged fish due to Sandy, the tagging process, natural mortality due to age (since these were larger and thus assumed to be older fish), or predator mortality especially since marine mammals have recently been reported to target acoustically tagged fish (Stansbury *et al.*, 2015). The addition of more passive hydrophones both in the estuary and in the ocean would have enhanced our resolution as well as the deployment of additional tags would have enhanced detection probability. However, the primary reason for the use of acoustic tags was to observe dispersal of the tagged fish from the release site as a proxy for other fish tagged without telemetered tags, which we were able to see dispersal. Further, it was clear that winter flounder could remain at the offshore site as late as December (when the tag batteries failed), which contrasts with a model of earlier migration to the estuary for spawning. Skipped spawning (Rideout *et al.*, 2005; Rideout and Tomkiewicz, 2011; Wuenschel *et al.*, 2009) could be another reason why winter flounder would be on the shelf in late December instead of migrating inshore.

While we did not recover any ALS tagged winter flounder from our study, but I was able to discern winter flounder residency using historic ALS tag release and recapture data. The ALS marker tags only provide data for two points in time, so while the historic data was helpful in describing the range of winter flounder movement and exchange of individuals between states and stocks these data were unhelpful in describing connectivity between the ocean and estuary. Like the archival tags, both rely heavily on retrieval for the data to be pertinent. Closure of the commercial fishery (except for a minor by-catch limit of 50 fish),

severely limited the possible recapture rate, especially since the tagged fish may remain offshore and unreachable by the majority of recreational fishers. Fairchild *et al.,* (2013) reported a 5% acoustic tag return rate in the GOM for a fixed (but repositioned) hydrophone array, so comparatively the return rate for our area is far less (3.14% for all historic ALS tags across all years and 0.44% for the first year of our tagging study). The external attachment of tags, contrary to internal, did increase the probability of recapture due to the entanglement in nets (Rikardsen and Thorstad, 2006). For our study, this did appear to assist in the recapture of one of our archival tags; the holes through the fish where the tag was attached were torn suggesting that the trawl net snagged and pulled the tag. This could be problematic if the tag was detached by the net and lost on the deck of a trawler or in the water while the net was being towed. Other groundfish (e.g. cod) have demonstrated high shedding rates with external archival tags (pers. comm. D. Zemeckis), yet this has not been observed for flatfish and is a common form of attachment owing to the limited ventral access (due to compressed body shape) for surgical implantation (Yergey *et al.*, 2012; Grothues *et al.,* 2012).

I was able to discern two patterns of across shelf movement through acoustic and archival tagging techniques. Two acoustic tagged fish appeared to be heading inshore moving northwest from the release point, while the third acoustic tagged fish was heading East and the archival tagged fish moved deeper, which must be southeast. Even though this is a short time series, it does break out two forms of behavior during the early migration season, with half of the fish detected or recaptured moving towards the coast and the others away from it.

It was not possible to resolve estuary ocean connectivity through any of the methods employed during the particular period and location of this study; however, since the archival tags are capable of logging data for up to four years, it remains possible that

valuable data will still be recovered. In the event that winter flounder stock recovery is strong enough to increase the odds of archival tag recovery again, it is clear that development of algorithms to ascertain connectivity from such tags will be very valuable, and this is presented in a following chapter. Prior to stock recovery (and particularly when this research is needed) an increased effort at acoustic tagging, with moored hydrophones at the Mud Hole, increased tag deployment, and increased mobile tracking efforts, will benefit from the lessons learned in this pilot acoustic study. From these results there appear to be two different behaviors present at least for the fall.

LIST OF TABLES

Table 1. All acoustically tagged winter flounder were caught by trawl 8 on 9/7/12 and released at the Mud Hole (40.1588, -73.6842). Released fish were selected based on a condition rating high enough to likely survive after being tagged. See Figure 1 for location.

Date Released and First Detected	Tow No.	Tag No.	Length (mm)	Time of Tagging	Time of Release	Release Latitude	Release Longitude	Comments	Detected	Detection Latitude	Detection Longitude
9/7/12	8	11885	410	11:53	12:49	40.1588	-73.6842	Punctured twice			
9/7/12	8	12360	440	11:56	12:49	40.1588	-73.6842	Tail slightly bloody			
9/7/12	8	11841	474	11:59	12:49	40.1588	-73.6842				
9/7/12	8	8055	437	12:00	12:49	40.1588	-73.6842	Punctured twice			
9/7/12	8	12316	392	12:06	12:49	40.1588	-73.6842	Ripped tail	9/27/12	N/A	N/A
9/7/12	8	9291	409	12:07	12:49	40.1588	-73.6842		9/13/12	40.167028	-73.709188
9/7/12	8	12404	385	12:10	12:49	40.1588	-73.6842		9/13/12	40.159051	-73.684475
9/7/12	8	9419	445	12:18	12:49	40.1588	-73.6842				
9/7/12	8	8099	400	12:21	12:49	40.1588	-73.6842				
9/7/12	8	12448	401	12:24	12:49	40.1588	-73.6842				
9/7/12	8	9332	378	12:24	12:49	40.1588	-73.6842				
9/7/12	8	9501	373	12:30	12:49	40.1588	-73.6842	Tail slightly bloody			

Table 2. Winter flounder with archival tags were caught on Sept. 6 and 7, 2012 at the Mud Hole (by trawls 1-7), as well as, in October 2012 and January 2013 off of northern New Jersey with the New Jersey Department of Environmental Protection (DEP). Tag 6663 occurs twice because the tag was reused after recapture and the data record was removed. Released fish were selected based on a condition rating high enough to likely survive after being tagged. See Figure 1 for location.

Date	Tow No.	Tag No.	Length (mm)	Time of Tagging	Time of Release	Release Latitude	Release Longitude	Condi-tion	Comment	Recap. date
9/6/12	1	6653	431			40.1324	-73.6086	2		
9/6/12	1	6592	395			40.1324	-73.6086	2		
9/6/12	1	6610	400			40.1324	-73.6086	1		
9/6/12	1	6622	410			40.1324	-73.6086	2	Minor scales missing on tail fin	
9/6/12	1	6639	467	10:15		40.1324	-73.6086	1	Some scales missing on tail, switched to long needles, initial tag attempt failed, poked the abdominal area	
9/6/12	1	6630	362	10:21		40.1324	-73.6086	2	bleeding from puncture hole	
9/6/12	2	6629	372	11:00		40.1324	-73.6086	2		
9/6/12	2	6654	427	11:03		40.1324	-73.6086	2		
9/6/12	2	6584	402	11:06		40.1324	-73.6086	2		
9/6/12	3	6607	440	12:15		40.1324	-73.6086	2		
9/6/12	3	6595	434	12:17		40.1324	-73.6086	2	Blood during tagging operation	
9/6/12	3	6637	395	12:19		40.1324	-73.6086	2		
9/6/12	3	6604	380	12:21		40.1324	-73.6086	2		
9/6/12	3	6652	380	12:23		40.1324	-73.6086	2		
9/6/12	4	6611	410	13:55	13:57	40.1649	-73.6887	2		
9/6/12	4	6619	405	13:58	13:59	40.1649	-73.6889	2		
9/6/12	4	6618	411	14:01	14:02	40.1649	-73.6893	2		
9/6/12	4	6635	393	14:03	14:04	40.1649	-73.6894	2		
9/6/12	4	6636	397	14:06	14:07	40.1647	-73.6897	2	Blood during tagging operation	
9/6/12	4	6620	396	14:08	14:09	40.1647	-73.6900	2	Punctured twice during tag insert	
9/6/12	4	6641	410	14:10	14:21	40.1644	-73.6912	2		
9/6/12	4	6654	399	14:14	14:16	40.1466	-73.6909	2		
9/6/12	4	6651	387	14:16	14:17	40.1645	-73.6907	2		
9/6/12	4	6638	411	14:17	14:19	40.1645	-73.6909	1	Belly up still 30ft down	
9/6/12	5	6634	426	15:38	15:39	40.1507	-73.6730	1	Pigmented caudal peduncle	

9/6/12	5	6593	473	15:39	15:40	40.1507	-73.6729	1		
9/6/12	5	6624	500	15:41	15:42	40.1508	-73.6728	1		
9/6/12	5	6628	402	15:44	15:45	40.1508	-73.6727	1		
9/6/12	5	6656	411	15:46	15:47	40.1508	-73.6726	1		
9/6/12	5	6645	400	15:47	15:48	40.1508	-73.6725	2	Bleeding from puncture hole	
9/6/12	5	6643	380	15:48	15:49	40.1509	-73.6725	2		
9/6/12	5	6615	390	15:50	15:51	40.1509	-73.6725	2		
9/6/12	5	6644	380	15:51	15:52	40.1511	-73.6724	2	Bleeding from puncture hole	
9/6/12	5	6598	409	15:52		40.1512	-73.6724	2	Abrasion on abdomen	
9/6/12	5	6640	380	15:54	15:55	40.1513	-73.6724	2		
9/7/12	6	6676	410	8:35	8:36	40.1636	-73.6864	1		
9/7/12	6	6669	430	8:37	8:39	40.1637	-73.6862	2		
9/7/12	6	6670	390	8:40	8:41	40.1639	-73.6861	2		
9/7/12	6	6667	405	8:42	8:43	40.1640	-73.6861	2		
9/7/12	6	6672	391	8:43	8:45	40.1641	-73.6861	2	Bloody tail	
9/7/12	6	6609	401	8:46	8:47	40.1643	-73.6860	2	Minimal bloody scales	
9/7/12	6	6665	439	8:48	8:50	40.1645	-73.6859	2	Minimal bloody scales	
9/7/12	6	6664	385	8:50	8:51	40.1646	-73.6859	2	Broad body	
9/7/12	7	6621	428	10:12	10:13	40.1427	-73.6746	2		
9/7/12	7	6658	397	10:14	10:15	40.1429	-73.6747	2		
9/7/12	7	6627	394	10:16	10:18	40.1432	-73.6746	1	Bleeding from puncture hole	
9/7/12	7	6616	410	10:19	10:20	40.1437	-73.6741	1	Bleeding from puncture hole, belly up	
9/7/12	7	6663	388	10:21	10:23	40.1438	-73.6739	2		9/20/12
9/7/12	7	6657	398	10:24	10:25	40.1441	-73.6738	2		
9/7/12	7	6649	404	10:26	10:27	40.1443	-73.6738	2		
10/11/12	156	6663	420	11:56	12:20	40.4006	-73.9597	1	DEP trawl, 2nd release of this tag	
1/23/13	1	6711	385	9:00	10:00	40.2356	-73.9340	1	DEP	
1/23/13	1	6714	420	9:00	10:00	40.2356	-73.9340	2	DEP, Bleeding a lot but active	
1/23/13	1	6715	430	9:00	10:00	40.2356	-73.9340	1	DEP	
1/23/13	1	6716	380	9:00	10:00	40.2356	-73.9340	1	DEP	

Table 3. Winter flounder with American Littoral Society (ALS) marker tags were released across the whole study period (at the Mud Hole and ranging the coast of New Jersey, from June 2012 - May 2014). One tag (ID no. 825083) remained unused since it was used in a tank study on tag retention.

Date Caught	Tag No.	Length (mm)	Location Released Latitude	Location Released Longitude
6/29/12	825040	245	40.42571668	-73.91641991
6/29/12	825041	300	40.43246804	-73.91874018
6/29/12	825042	262	40.43883993	-73.92094905
6/29/12	825043	294	40.43860903	-73.92130646
6/29/12	825044	355	40.41209905	-73.95002801
6/29/12	825045	298	40.41812993	-73.9544369
8/15/12	825046	264	40.45342174	-73.98009451
8/15/12	825047	273	40.45335729	-73.97891617
9/6/12	825048	383	40.13233117	-73.60986641
9/6/12	825049	400	40.1322608	-73.6100087
9/6/12	825050	329	40.13219916	-73.61012732
9/6/12	825051	380	40.13212866	-73.61025787
9/6/12	825052	341	40.13136012	-73.61152939
9/6/12	825053	353	40.13121023	-73.61180239
9/6/12	825054	340	40.13108808	-73.61213352
9/6/12	825055	380	40.13100997	-73.61238158
9/6/12	825056	330	40.13759704	-73.65293202
9/6/12	825057	348	40.14005706	-73.65530158
9/6/12	825058	353	40.14071876	-73.65720194
9/6/12	825059	315	40.14070429	-73.65750743
9/6/12	825060	296	40.1407167	-73.65780066
9/6/12	825061	326	40.14072747	-73.65795305
9/6/12	825062	315	40.14074671	-73.65805832
9/6/12	825063	335	40.1408808	-73.65952302
9/6/12	825064	355	40.14249271	-73.66101741
9/6/12	825065	341	40.14421257	-73.65705097
9/6/12	825066	351	40.15690334	-73.68424086
9/6/12	825067	362	40.15690334	-73.68424086
9/6/12	825068	353	40.15690334	-73.68424086
9/6/12	825069	358	40.15690334	-73.68424086
9/6/12	825070	352	40.15690334	-73.68424086
9/6/12	825071	357	40.15690334	-73.68424086
9/6/12	825072	364	40.15690334	-73.68424086
9/6/12	825073	328	40.15690334	-73.68424086
9/6/12	825074	366	40.15690334	-73.68424086
9/6/12	825075	375	40.15690334	-73.68424086
9/6/12	825076	367	40.15690334	-73.68424086
9/6/12	825077	351	40.15690334	-73.68424086
9/6/12	825078	336	40.15690334	-73.68424086
9/6/12	825079	330	40.15537495	-73.68690041
9/6/12	825080	355	40.15530476	-73.68706614

9/6/12	825081	368	40.15525191	-73.68717283
9/6/12	825082	355	40.15518092	-73.68726812
-	825083	-	-	-
9/6/12	825084	325	40.15510092	-73.6873636
9/6/12	825085	369	40.15500304	-73.68747115
9/6/12	825086	340	40.15500304	-73.68747115
5/9/14	825087	365	39.508878	-74.324622
5/9/14	825088	350	39.508878	-74.324622
9/6/12	825089	370	40.15481628	-73.68768609
9/6/12	825090	360	40.15476291	-73.68774582
9/6/12	825091	380	40.15466476	-73.6878299
9/6/12	825092	339	40.15454846	-73.68790258
9/6/12	825093	318	40.15440488	-73.68795231
9/6/12	825094	324	40.15435084	-73.68795335
9/6/12	825095	335	40.15424288	-73.68796717
9/6/12	825096	338	40.15416209	-73.68799221
9/6/12	825097	335	40.15412632	-73.68801638
9/6/12	825098	330	40.15402804	-73.68808872
9/6/12	825099	338	40.15394777	-73.68816071
9/6/12	825100	342	40.15389413	-73.68819696
9/6/12	825101	310	40.1538226	-73.6882453
9/6/12	825102	328	40.15368816	-73.99362671
9/6/12	825103	375	40.15369757	-73.68834164
9/6/12	825104	333	40.15364406	-73.68838963
9/6/12	825105	331	40.15359055	-73.68843762
9/6/12	825106	380	40.15354657	-73.6885324
9/6/12	825107	374	40.15351054	-73.68853309
9/6/12	825108	345	40.15349399	-73.68866256
9/6/12	825109	325	40.15345002	-73.68875733
9/6/12	825110	311	40.15335227	-73.68887662
9/6/12	825111	341	40.15332578	-73.6889241
9/6/12	825112	333	40.15326353	-73.68899574
9/6/12	825113	348	40.1531924	-73.68907929
9/6/12	825114	340	40.15151292	-73.67214644
9/6/12	825115	323	40.15158404	-73.67206287
9/6/12	825116	369	40.151637	-73.67196791
9/6/12	825117	354	40.15171685	-73.67186069
9/6/12	825118	373	40.15181512	-73.67178833
9/6/12	825119	330	40.15192133	-73.67162189
9/6/12	825120	330	40.15197443	-73.67153867
9/6/12	825121	359	40.1520563	-73.67160752
9/7/12	825122	381	40.14528644	-73.67361774
9/7/12	825123	361	40.14553851	-73.6736011
9/7/12	825124	369	40.14571811	-73.67355065
9/7/12	825125	410	40.14585322	-73.67354802
9/7/12	825126	257	40.1459523	-73.67354609
9/7/12	825127	370	40.14618675	-73.67356501
9/7/12	825128	373	40.14632172	-73.67355064
9/7/12	825129	371	40.14649286	-73.67354731
9/7/12	825130	372	40.14634696	-73.67103786
9/7/12	825131	381	40.16348336	-73.67033969

9/7/12	825132	355	40.16621298	-73.67268202
9/7/12	825133	370	40.17457788	-73.7113466
9/7/12	825134	389	40.17094639	-73.71127437
9/7/12	825135	392	40.17120512	-73.71104634
9/7/12	825136	392	40.17150927	-73.71085268
9/7/12	825137	370	40.17179476	-73.71060065
9/7/12	825138	355	40.17206144	-73.71027851
9/7/12	825139	340	40.17231155	-73.71008587
9/7/12	825140	359	40.17267823	-73.70984404
9/7/12	825141	372	40.17302559	-73.70948513
9/7/12	825142	349	40.17323927	-73.70925794
9/7/12	825143	346	40.17364185	-73.70900368
9/7/12	825144	393	40.1739101	-73.70882243
9/7/12	825145	385	40.17423057	-73.70847576
9/7/12	825146	382	40.17446266	-73.70828345
9/7/12	825147	336	40.17476641	-73.70805454
9/7/12	825148	350	40.17496208	-73.70782768
9/7/12	825149	385	40.17601786	-73.70717343
9/7/12	825150	368	40.17594147	-73.7067873
9/7/12	825151	406	40.18548571	-73.70630064
9/7/12	825152	355	40.17645798	-73.70624898
9/7/12	825153	355	40.17684188	-73.70593631
9/7/12	825154	470	40.17717996	-73.70555405
9/7/12	825155	372	40.17748358	-73.70531338
9/7/12	825156	372	40.17777884	-73.70513159
9/7/12	825157	394	40.17792033	-73.70489399
9/7/12	825158	383	40.17815163	-73.7046312
9/7/12	825159	325	40.17856228	-73.70429452
10/11/12	825160	398	40.40038333	-73.95585
10/11/12	825161	406	40.25156667	-73.83585
10/11/12	825162	370	40.25156667	-73.83585
10/11/12	825163	254	40.25156667	-73.83585
10/11/12	825164	296	40.22221667	-73.82765
10/11/12	825165	355	40.22221667	-73.82765
10/11/12	825166	330	40.22221667	-73.82765
10/11/12	825167	255	40.22221667	-73.82765
10/16/13	825168	342	40.08869952	-74.00121874
1/23/13	825169	270	40.23471667	-73.92705
1/23/13	825170	360	40.26381667	-73.61138333
1/23/13	825171	390	40.26381667	-73.61138333
1/23/13	825172	385	40.26381667	-73.61138333
1/23/13	825173	400	40.26381667	-73.61138333
1/23/13	825174	330	40.26381667	-73.61138333
1/23/13	825175	340	40.26381667	-73.61138333
1/23/13	825176	390	40.26381667	-73.61138333
1/23/13	825177	400	40.26381667	-73.61138333
1/23/13	825178	370	40.26381667	-73.61138333
1/23/13	825179	400	40.27128333	-73.63525
1/23/13	825180	345	40.27128333	-73.63525

1/23/13	825181	295	40.27128333	-73.63525
1/23/13	825182	395	40.27128333	-73.63525
1/23/13	825183	320	40.27128333	-73.63525
1/23/13	825184	298	40.27128333	-73.63525
1/23/13	825185	340	40.27128333	-73.63525
1/23/13	825186	385	40.27128333	-73.63525
1/23/13	825187	370	40.27128333	-73.63525
1/23/13	825188	382	40.27128333	-73.63525
1/23/13	825189	383	40.27128333	-73.63525
1/23/13	825190	320	40.27128333	-73.63525
1/23/13	825191	380	40.34688333	-73.91433333
1/23/13	825192	383	40.34688333	-73.91433333
1/23/13	825193	344	40.34688333	-73.91433333
1/23/13	825194	395	40.34688333	-73.91433333
1/23/13	825195	420	40.34688333	-73.91433333
1/23/13	825196	290	40.34688333	-73.91433333
1/23/13	825197	405	40.34688333	-73.91433333
1/23/13	825198	380	40.34688333	-73.91433333
1/23/13	825199	380	40.34688333	-73.91433333

Table 4. Winter flounder gonad data was collected on Sept. 6, 2012 at the Mud Hole and used to identify the sex of the winter flounder and the proportion of mature individuals. This was determined by visual inspection of the gonad and weighing the total body mass of the individual and the gonad mass separate from the body. A gonadosomatic index (GSI) in addition to comparing the individual's length to literature defining size at maturing for the Mid-Atlantic Bight and Southern New England sector was used to determine maturity.

Date Caught	Length (mm)	Weight (g)	Gonad weight (g)	GSI	Sex
9/6/12	364	653	33.7	5.16	Female
9/6/12	422	1004	35.9	3.58	Female
9/6/12	335	547	8.8	1.61	Female
9/6/12	335	500	7.8	1.56	Female
9/6/12	295	342	0.7	0.20	Male
9/6/12	320	404	1.8	0.45	Male
9/6/12	387	774	17.8	2.30	Female
9/6/12	370	669	20.1	3.00	Female
9/6/12	342	483	1.9	0.39	Male
9/6/12	377	817	37	4.53	Female
9/6/12	390	773	37.4	4.84	Female
9/6/12	355	593	22.2	3.74	Female
9/6/12	347	536	23.7	4.42	Female
9/6/12	370	643	25.9	4.03	Female
9/6/12	370	683	18.5	2.71	Female
9/6/12	414	904	24.3	2.69	Female
9/6/12	386	766	40.6	5.30	Female
9/6/12	311	365	1.3	0.36	Male
9/6/12	357	538	11.8	2.19	Female
9/6/12	431	1155	56.9	4.93	Female
9/6/12	435	1044	57.1	5.47	Female
9/6/12	395	823	50.8	6.17	Female
9/6/12	357	604	19.6	3.25	Female
9/6/12	365	661	16.9	2.56	Female
9/6/12	388	729	16.5	2.26	Female
9/6/12	427	1058	45.5	4.30	Female
9/6/12	350	549	18.5	3.37	Female
9/6/12	325	476	16.7	3.51	Female
9/6/12	348	598	34.2	5.72	Female
9/6/12	315	400	7.1	1.78	Female
9/6/12	328	445	2	0.45	Male
9/6/12	315	403	1.9	0.47	Male
9/6/12	340	487	3.9	0.80	Male
9/6/12	310	414	8.3	2.00	Female
9/6/12	306	375	1.2	0.32	Male
9/6/12	330	452	2	0.44	Male
9/6/12	296	353	7.3	2.07	Female
9/6/12	321	413	10	2.41	Female
9/6/12	250	221	2.8	1.27	Unknown

LIST OF FIGURE CAPTIONS

Figure 1. Distribution of tagged winter flounder released during 2012-2013 (see Tables 1, 2, and 3 for addition details) including American Littoral Society (ALS), Archival, and Acoustic tags. The bathymetry is shaded in blue with dark blue denoting deeper and light blue denoting shallower and the coastline marked in green. The Mud Hole is a portion of the Hudson Shelf Valley. The hydrophones (denoted by purple stars) were set near the mouths of the Manasquan River, Navesink River, and Shark River to detect movement into New Jersey estuaries.

Figure 2. The length (cm) frequency distributions for winter flounder by each tag type including American Littoral Society (ALS), Archival, and Acoustic tags.

Figure 3. (A) An example of the search pattern to track acoustically tagged winter flounder used for the AUV (red) as well as the search pattern used by the boat (blue) on Sept. 7, 2012. (B) A subset map includes the initial acoustic tag distribution in relation to the release point (green) and the boat GPS track, which is used to pinpoint position. Fish are denoted in pink with tag identification number underneath.

Figure 4. Recovered winter flounder with archival tag (ID no. 6663), dorsal and ventral views.

Figure 5. Graph of a spectral analysis used to determine the most influential tidal state experienced by the fish so that tide can be removed from the archival tag depth data. The period is in hours and the power determines the dominant signal.

Figure 6. Graph of a depth record from a winter flounder tagged with an archival tag. The raw depth data (in blue) and the depth data with the tidal signal removed (in green), using a nyquist frequency (ns) of 24 to maintain as much of the time series as possible.

Figure 7. The daily averaged and raw temperature recorded of a winter flounder with archival tag ID no. 6663. This tag was release and recaptured out near the Mud Hole in September 2012.

Figure 8. The daily averaged salinity observed by a winter flounder with archival tag ID no. 6663. This tag was release and recaptured out near the Mud Hole in September 2012.

Figure 9. Temperature range experienced by tag ID no. 6663 as recorded every 24 minutes, with error of ±0.1°C. This tag was release and recaptured out near the Mud Hole in September 2012.

Figure 10. Salinity range experienced by tag ID no. 6663 as recorded every 24 minutes, with error of ±1. This tag was release and recaptured out near the Mud Hole in September 2012.

Figure 1.

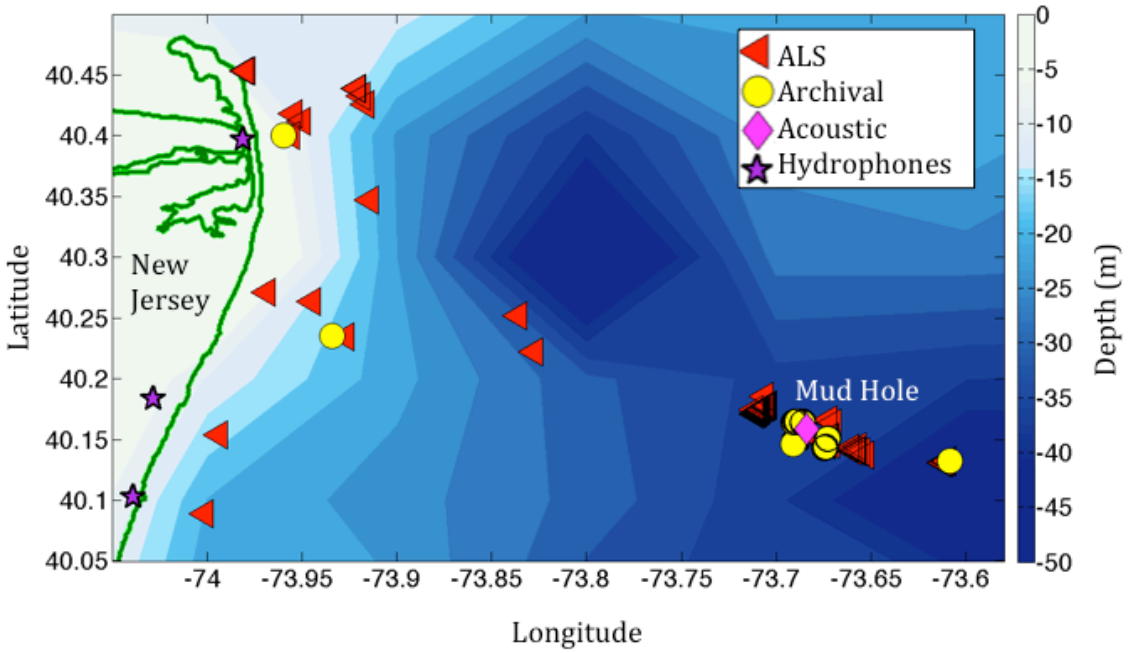
ALS
Archival
Acoustic
Hydrophones
New Jersey
Mud Hole
Latitude
Longitude
Depth (m)
40.45
40.4
40.35
40.3
40.25
40.2
40.15
40.1
40.05
-74
-73.95
-73.9
-73.85
-73.8
-73.75
-73.7
-73.65
-73.6
0
-5
-10
-15
-20
-25
-30
-35
-40
-45
-50

Figure 2.

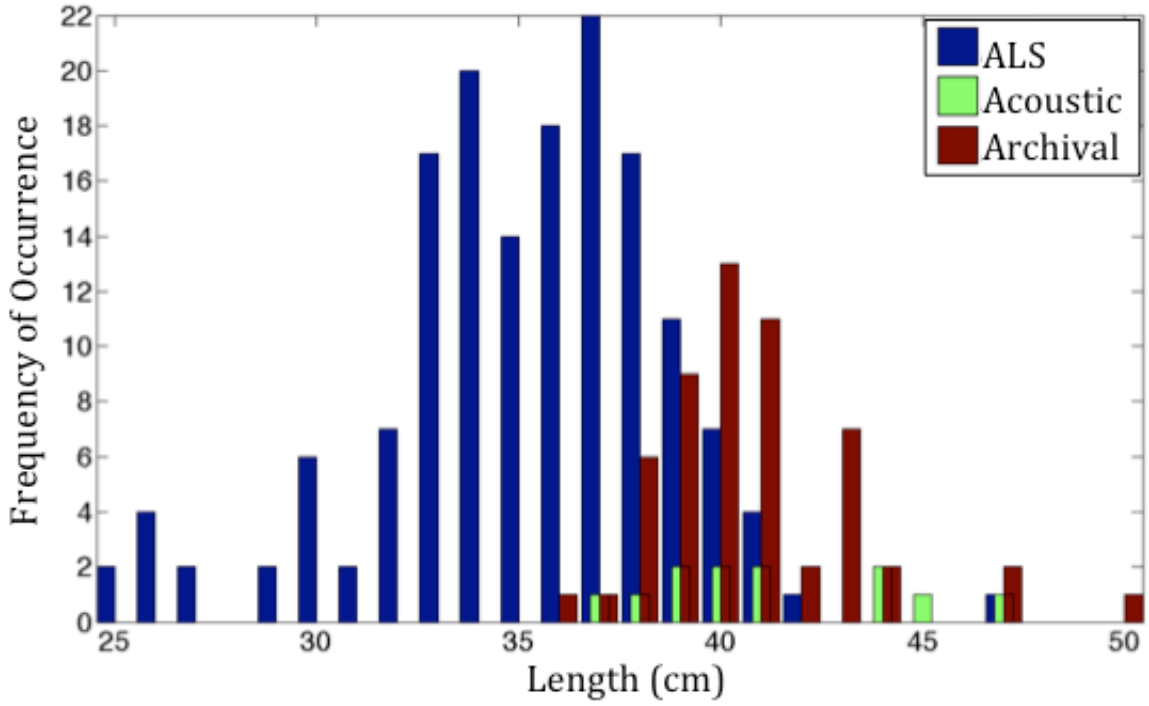
ALS
Acoustic
Archival
Frequency of Occurrence
Length (cm)
0
2
4
6
8
10
12
14
16
18
20
22
25
30
35
40
45
50

Figure 3.

A.

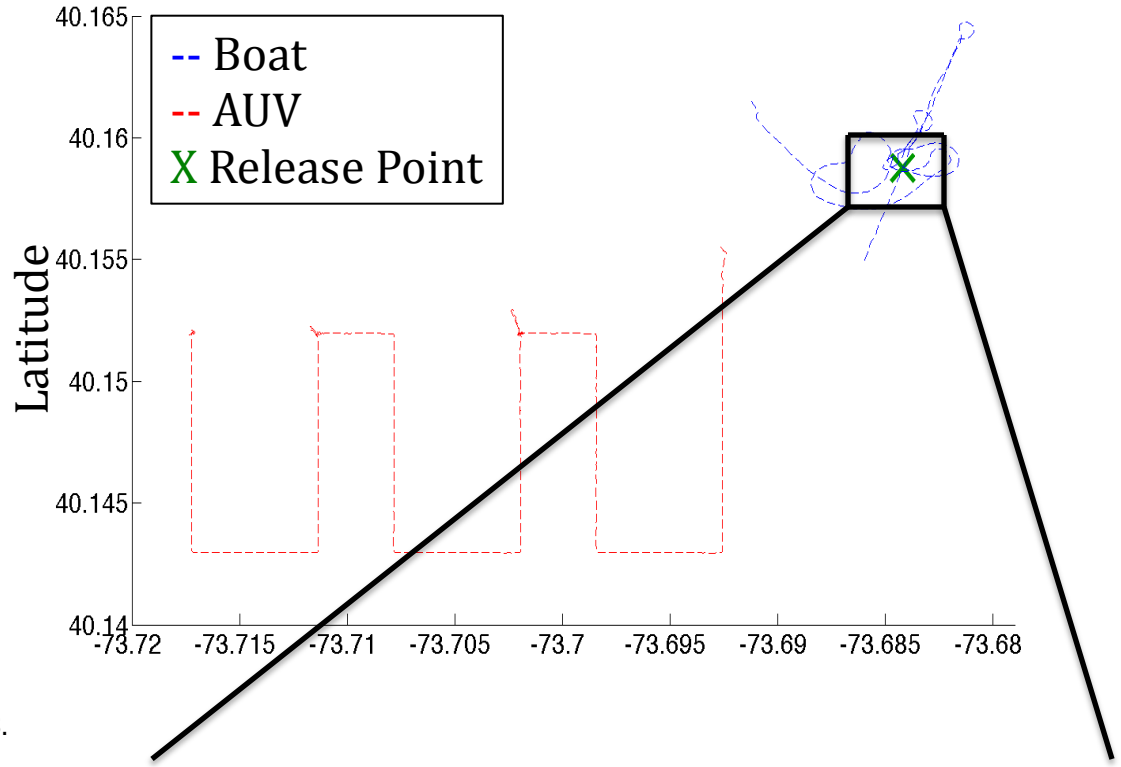
-- Boat
-- AUV
X Release Point
Latitude
40.165
40.16
40.155
40.15
40.145
40.14
-73.72
-73.715
-73.71
-73.705
-73.7
-73.695
-73.69
-73.685
-73.68

B.

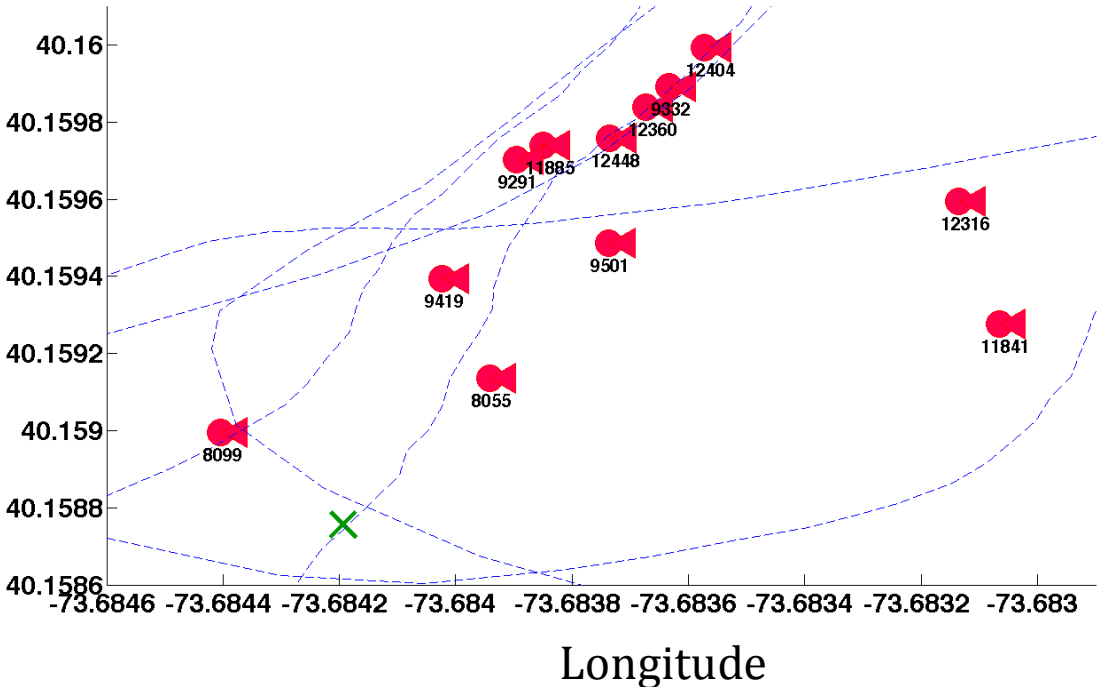
40.16
40.1598
40.1596
40.1594
40.1592
40.159
40.1588
40.1586
12404
9332
12360
11885
12448
9291
12316
9501
9419
11841
8055
8099
-73.6846
-73.6844
-73.6842
-73.684
-73.6838
-73.6836
-73.6834
-73.6832
-73.683
Longitude

Figure 4.

Figure 5.

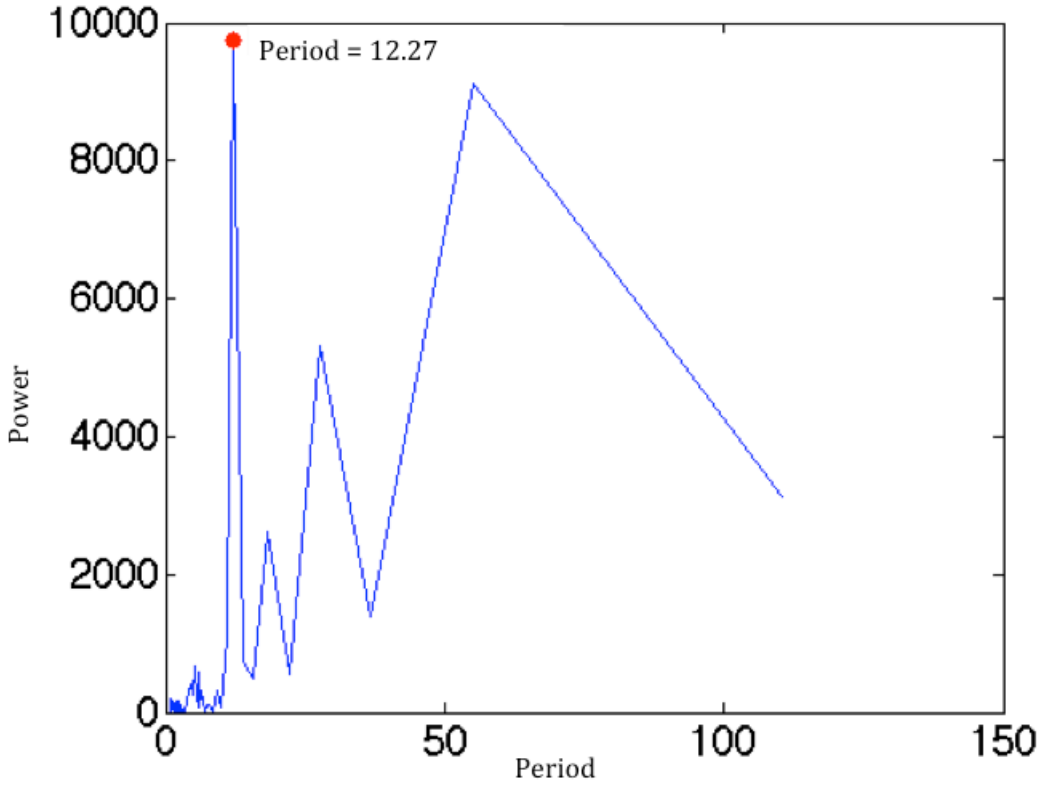
Period = 12.27
10000
8000
6000
4000
2000
0
Power
0
50
100
150
Period

Figure 6.

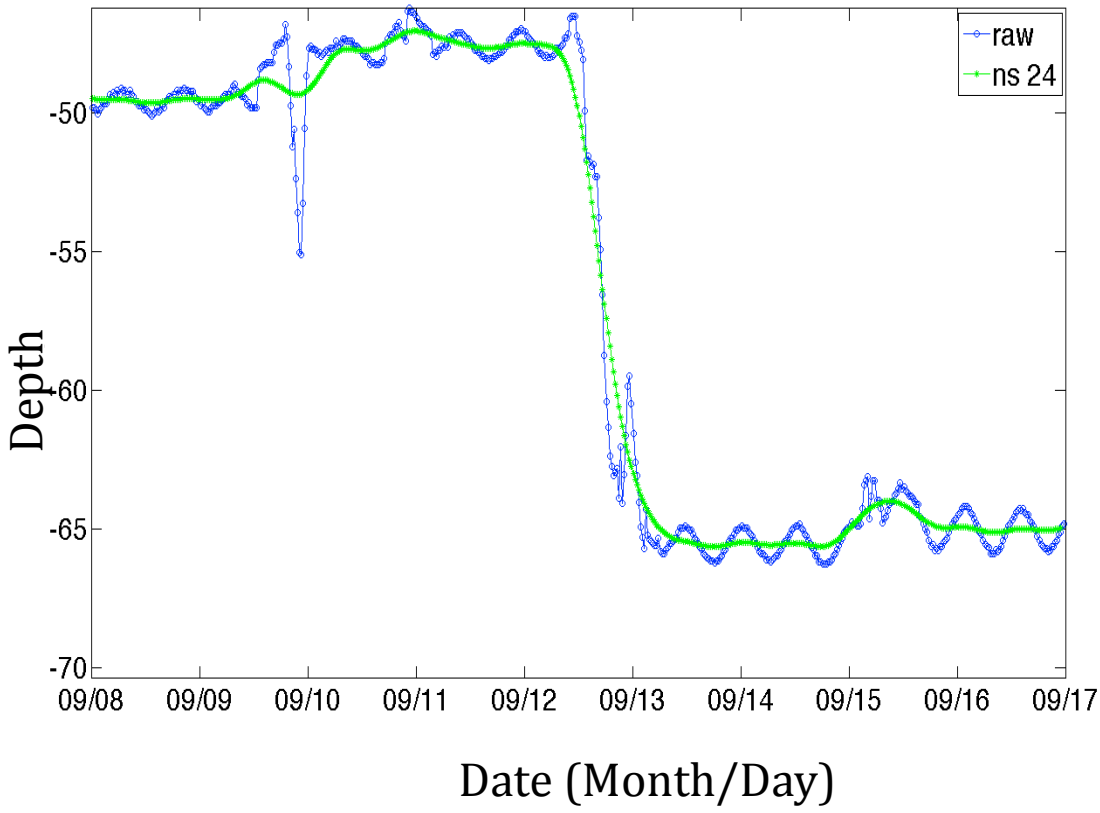
raw
ns 24
-50
-55
-60
-65
-70
Depth
09/08
09/09
09/10
09/11
09/12
09/13
09/14
09/15
09/16
09/17
Date (Month/Day)

Figure 7.

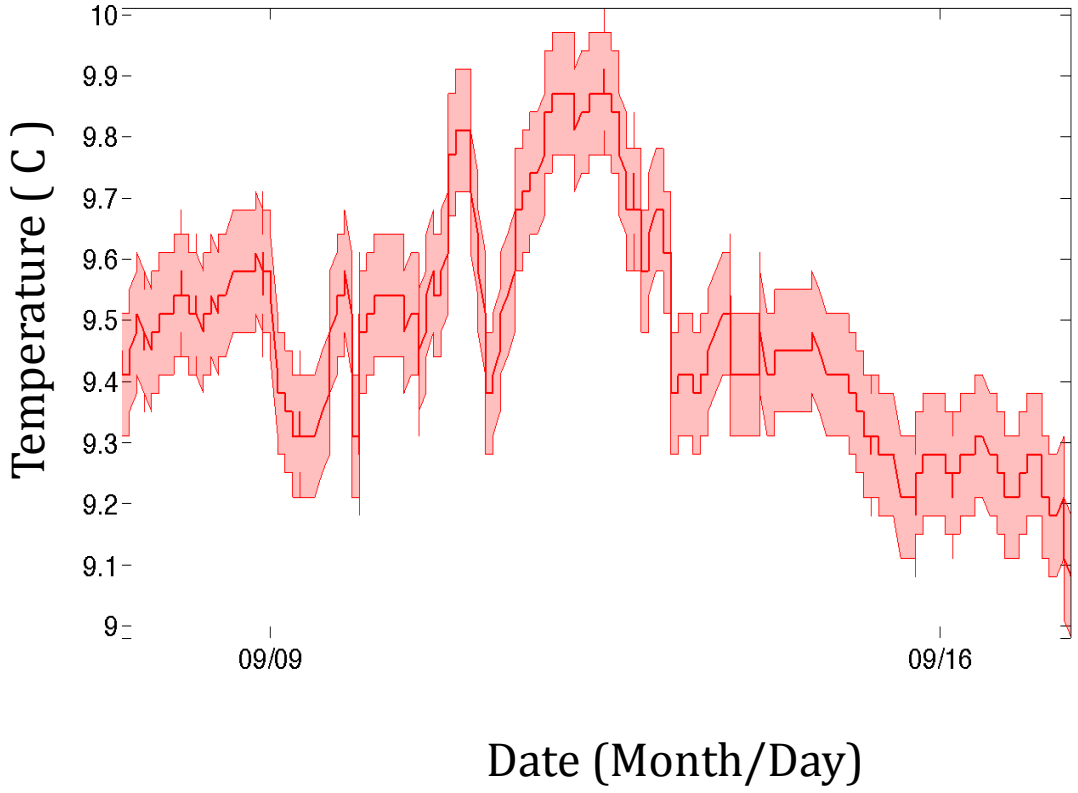
10
9.9
9.8
9.7
9.6
9.5
9.4
9.3
9.2
9.1
9
Temperature (C)
09/09
09/16
Date (Month/Day)

Figure 8.

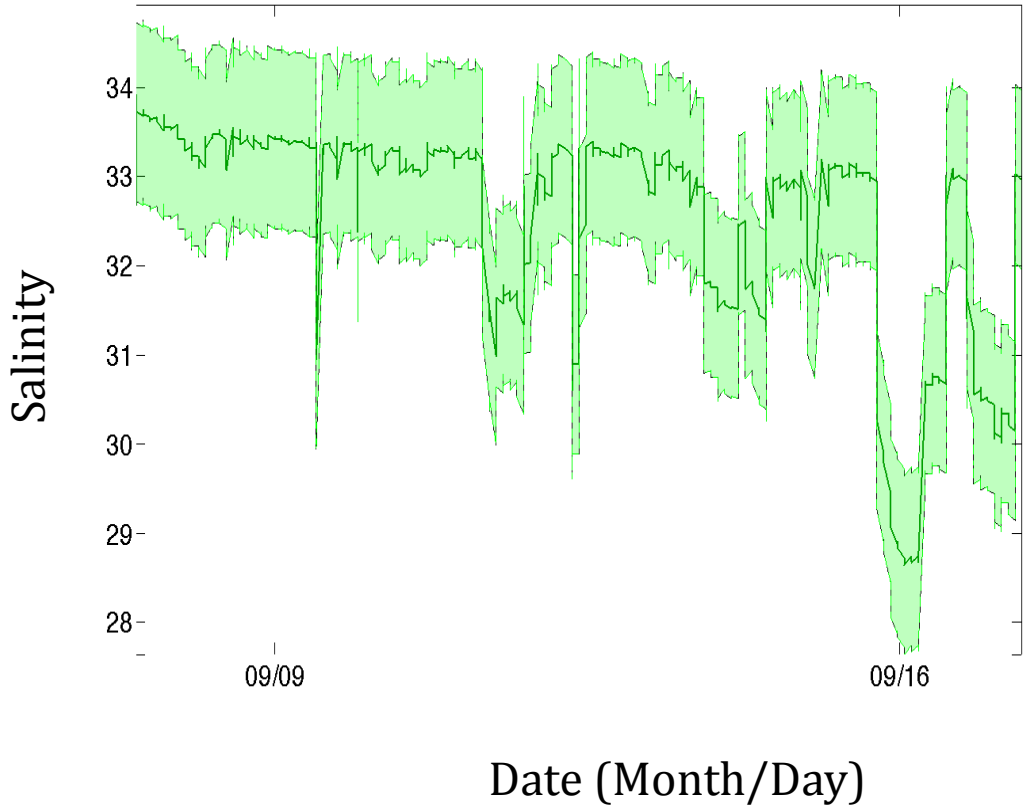

Figure 9.

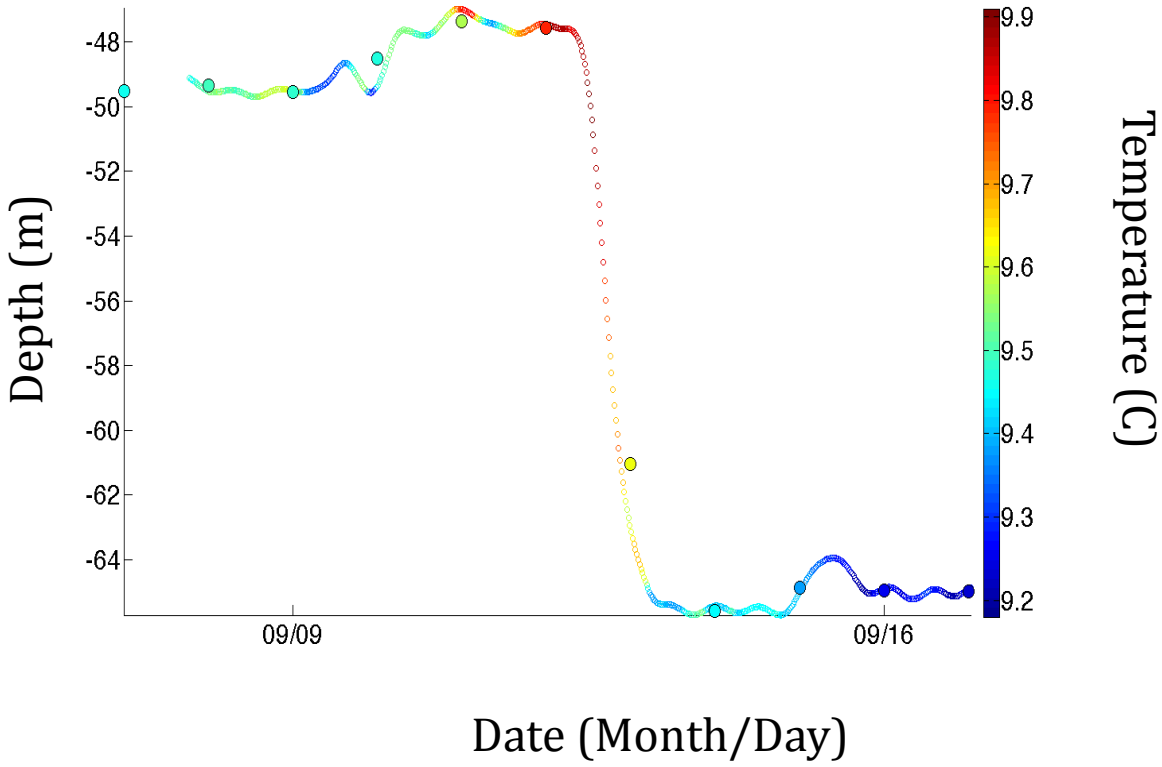
Depth (m)
-48
-50
-52
-54
-56
-58
-60
-62
-64
09/09
09/16
Date (Month/Day)
9.9
9.8
9.7
9.6
9.5
9.4
9.3
9.2
Temperature (C)

Figure 10.

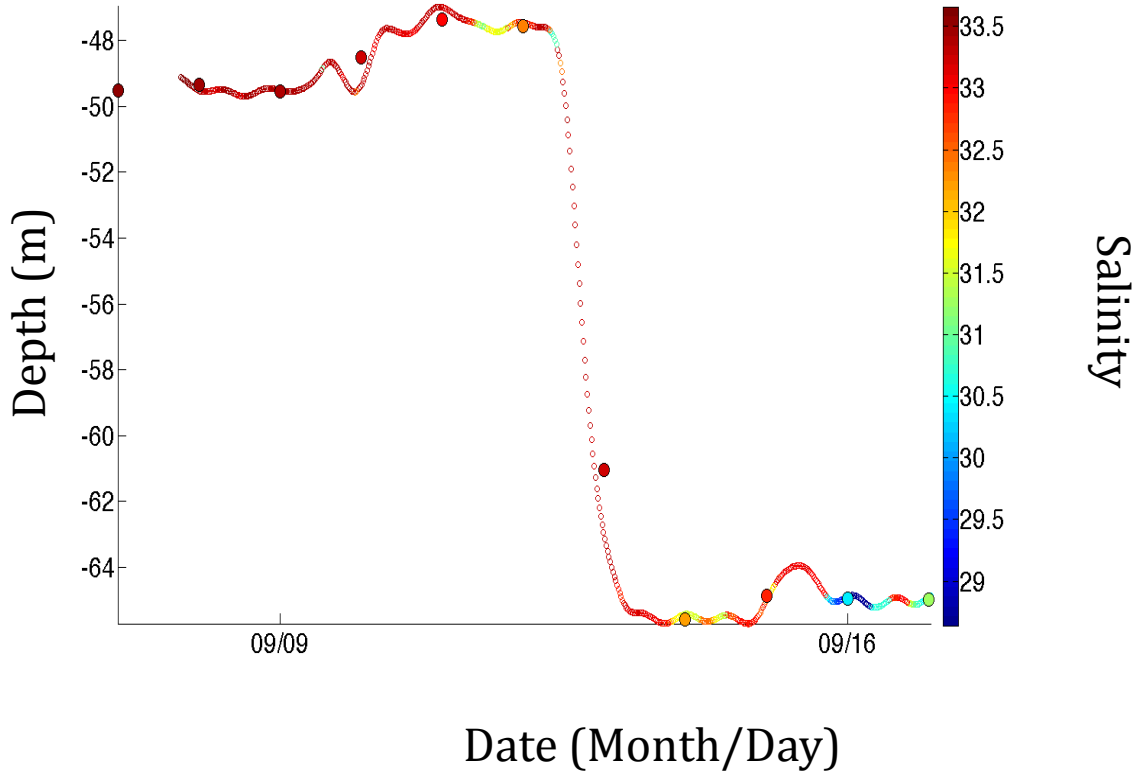
Depth (m)
-48
-50
-52
-54
-56
-58
-60
-62
-64
09/09
09/16
Date (Month/Day)
33.5
33
32.5
32
31.5
31
30.5
30
29.5
29
Salinity

– Chapter 4 –

PATH RECONSTRUTION FOR TAGGED MID-ATLANTIC BIGHT FISH

Abstract

Since archival tags record the environmental parameters of an individual but not the location, the goal of this project was to test three state space models at three different time scales and find one that most efficiently reconstructed a known simulated winter flounder path. I used two data matching and simulation state space models and one particle filter model to reconstruct fish location. All of the models were tested on simulated known fish paths created using hydrodynamic model data and informed with winter flounder movement metrics and archival tag data from one recovered winter flounder. While the state space models performed similarly reconstructing simulated fish paths at short time scales of 11 and 31 days, at a larger time scale reconstructing a 92 day fish path the particle filter outperformed the data matching and simulation state space models. Despite not being user friendly and having the longest model run time, the particle filter is our best state space model choice.

4.1 Introduction

Over the last several decades there have been rapid advancements in animal tagging and tracking technology (Bridge *et al.*, 2011), especially in aquatic habitats (Ehrenberg and Steig, 2003; Cooke *et al.*, 2013). One such advancement is the archival (a.k.a. digital/data storage) tag. An archival tag collects and logs environmental data from onboard-sensors, allowing the researcher to learn about the conditions that a tagged fish experienced. Unlike conventional tags that only provide start and end locations or acoustic tags that provide high resolution over a short period of time, archival tags record the environmental

parameters of an individual to provide continuous basin-scale location and give insight into complex life history questions and interactions between an individual and its environment. The biggest limitations of archival tag use are their cost, size, and the fact that they must be retrieved to access the data.

Archival tags come in a variety of types and have been used successfully for a variety of relatively large fishes including salmon (Ishida *et al*., 2001), sailfishes (Hoolihan and Luo, 2011), tunas (Schaefer and Fuller, 2010), white marlin (Graves and Horodysky, 2005), sharks (Wilson *et al.*, 2007), cow nose rays (Grusha and Patterson, 2005), eels (Jellyman and Tsukamoto, 2002) striped bass (Graves *et al.*, 2009), cod (Heffernan, 2004; Gröger *et al.*, 2007; Neuenfeldt, 2007; Pedersen, 2008; Le Bris *et al.,* 2013), halibut (Loher and Blood, 2009; Loher and Rensmeyer, 2011), yellowtail flounder (Cadrin and Westwood, 2004; Cadrin and Moser, 2006), and plaice (Hunter *et al*., 2003; Hunter *et al.,* 2004) as well as turtles (Flemming *et al.*, 2010) and marine mammals (Dowd and Joy, 2011).

Archival tags offer several advantages over both mark-recapture tagging and telemetry techniques (Gröger *et al.*, 2007), mainly due to the fact that the archival tag is experiencing the same environmental conditions as the individual carrying it. There is a growing range of environmental parameters that an archival tag can record to reconstruct behavior, habitat use, or position. Position can be back calculated from archived light data using the timing and duration of sun-up and sun-down inclination (Nielsen and Sibert, 2007), or from the co-occurrence over time of temperature, salinity (conductivity), pressure (depth), and tidal state (inferred from pressure amplitude and phase) (Hunter *et al.,* 2003; Le Bris *et al*., 2013). Acceleration or turning angle (Albert and Lambert, 2011), magnetic field strength (Seitz and Nielsen, 2013) or a combination of several parameters can also be used. The behavior of the study species often constrains the choice of which the environmental variable would be most practical. Light sensors are commonly used with

pelagic species; however, these are problematic for species that live in deep and murky water, and which may bury, because light readings will be inaccurate (Evans *et al.*, 2013).

Path reconstruction of a tagged individual is the process of finding the most parsimonious environmental parameter match over space and time between the tag data and a temporally and spatially explicit record of those same parameters for the area that comprises the potential habitat. Path reconstruction can be accomplished through a range of heuristic (Domeier and Kiefer, 2005; Neuenfeldt *et al.,* 2007) and state space models (SSMs), including but not limited to: Kalman filters (Kalman, 1960; Sibert *et al.,* 2003), particle filters (Andersen *et al.*, 2007), Bayesian filters, hidden Markov models, and data matching and simulation models (Righton and Mills, 2008; Ådlandsvik *et al.*, 2007). Most of these SSMs begin with a sequential first order Markov process and differ on the parameters prior to the state that is sought. Stochastic simulations then attempt to approximate state probability densities (Pedersen *et al.*, 2011) combined with a process model such as a random walk to advance the state forward in time (Jonsen *et al.*, 2013). For a review on available SSMs for individual animal movement and behavior see Patterson and Thomas (2008), Schick *et al.,* (2008), and Jonsen *et al*., (2013).

The species of interest for our study is the winter flounder. It is an ideal candidate for the use of an archival tag because they are targeted in the fisheries and they exhibit an across shelf seasonal spawning migration, which provides clear environmental identifiers for position (ocean or estuary). Additionally since winter flounder are mainly a demersal fish, this facilitates the use of a SSM by constraining the possible states in which the flounder could be located.

4.2. Methods

For the current application studying winter flounder migration, the archival tag

recorded conductivity (salinity), temperature, and pressure (depth and tidal location) (Star-Oddi, DST CTD, 15 mm x 46 mm, user specified conductivity and temperature range). The tag data may be used in two ways; first to directly measure the qualities of occupied habitat (demonstrated in Chapter 3), and secondly to reconstruct paths based on what places had those qualities over different times (e.g. state-space model) (Nichol and Somerton, 2009; Thygesen and Nielsen, 2009). Connectivity between ocean and estuarine habitats is the emphasis of this study and thus can be addressed on the basis of exclusive combinations of salinity, temperature, and depth (template fit, e.g. Metcalfe and Arnold, 1997) without precise knowledge of latitude and longitude. To obtain location, observed tag data is then compared to a hydrodynamic model, circulation model, tidal model, bathymetry, or sea surface temperature (Nielsen *et al*., 2006; Neuenfeldt *et al*., 2007). In the Mid-Atlantic Bight, collected data for the bottom water over the huge potential range of these individuals is sparse. Instead, I used hydrodynamic model output from the Rutgers Regional Ocean Modeling System (ROMS 4DVAR assimilation analysis/forecast) using the ESPreSSO (Experimental System for Predicting Shelf and Slope Optics) ocean model to find the state spaces over time. Such a method has been used to estimate the paths of fish tagged with temperature-salinity or pressure tags alone (e.g. Nichol and Somerton, 2009 for rock sole in the Bering Sea) and is sensitivity tested through groundtruthing with "known" synthesized data (Thygesen *et al.*, 2009). Uncertainty that applies to pelagic fish species for such a method is mitigated for winter flounder, which have a primarily benthic habit, further constraining the modeled possibilities.

This approach relies on knowledge about the environmental parameters, which are our observations (temperature, salinity, and depth) at a particular state (latitude and longitude) unknown to us at a given time (t). A SSM bridges the gaps between the inferences of habitat occupied at a particular time (ocean or estuary) and allows us to georectify those

habitats. The paths and habitat residency can be further resolved by filtering the possible locations to those that maximize the fit between the tag data and ocean conditions as constrained by time and place in a formal SSM model. The "place" or virtual space in such a model is defined as cells within a latitude, longitude, depth coordinate system, each of which is assigned a particular conductivity and temperature value varying in time. I restricted a number of different possible sequential cell occupations, or possible reconstructed paths, by the range in which a fish could swim (e.g. maximum swim radius, MSR). Further, reconstructed paths are limited to places connected to the last occupied state of the fish; e.g. the most likely fish path is the one that minimizes the number or magnitude of "jumps", for example between two cold deep spots, without showing data for a warm shallow spot that lies in between. Still, a number of paths remain possible and these must be filtered to the most parsimonious options. These connectivity constraints are handled by use of a sequential first order Markov process, which moves from one state to an adjacent state as allowed by the best fit between the data on the archival tag and the best estimated conditions from a hydrodynamic model for the surrounding cells. An error estimate is also produced because a number of possibilities may result, so that the confidence bounds can be described.

A SSM has the inputs of the observation model (archival tag data), the transition model (moving from one state to the next), and an environmental history (hydrodynamic model), from which I calculated plausible states for each time step, and then found the most likely explanation through the state space. The differences between models are often the decision process of how the plausible states (filtering), reconstructed paths (prediction and smoothing), and most likely reconstructed path made up of belief states are calculated. Two SSMs were used in this study, a data matching and simulation method, modeled after Righton and Mills (2008) and Ådlandsvik *et al.,* (2007), and a particle filter method,

modeled after Andersen *et al.,* (2007) with methods from Russel and Norvig (2010), and Klaas *et al.,* (2006). Tidal constituents were not used in these models since daily average of environmental parameters was used, which tends to smear tidal estimate. However, tidal state can be used in future revisions of these models if I use a bihourly time scale. These models are made up of two coupled stochastic models: the process model and the observation model. Additionally there are several methods to smooth plausible paths (Briers *et al.,* 2010, Klaas *et al*., 2006).

The transition model here is defined by average swim rate and this parameter is best populated from observation. Several authors have defined swim rate at 0.5 body lengths (bl) per second (s^{-1}) (e.g. for cod, Neuenfeldt *et al.,* 2007 and demersal fish, Righton and Mills, 2008). However, in a flume winter flounder are capable of swimming at 0.65 ± 0.06 bl s^{-1} at 4 °C and 0.73 ± 0.07 bl s^{-1} at 10 °C (Joaquim *et al.*, 2004). For 75 minutes winter flounder were able to swim comfortably at < 0.4 bl s^{-1} (Joaquim *et al.*, 2004). In the wild He (2003) found an average swimming speed of 0.52 bl s^{-1} at −1.2 °C and 0.95 bl s^{-1} at 4.4 °C. At extremely high temperatures winter flounder become inactive and often bury (Olla *et al*., 1969; He, 2003). Temperature positively correlates with time spent swimming in the water column (He, 2003).

Distance traveled was estimated from acoustic telemetry (Grothues *et al.*, 2012) at an average daily movement of 100 meters (standard deviation 125 meters) in a New Jersey estuary from winter into spring, with greater distances assumed in the ocean or while migrating. In Barnegat Bay, New Jersey study, minimum movement was seen in May-June at 0.9 m/d with maximum movement of 587.5 m/d in early February, but overall movements were frequently less than 200 m/d in the bay (Pravatiner, 2010). Winter flounder acoustically tagged by Fairchild *et al.,* (2013) in the Gulf of Maine and detected by hydrophones located inshore and offshore during the spawning season showed an average

linear daily movement of tags recovered to be 208 ± 401 m, and a maximum daily movement of 1733 m and minimum of 1 m.

Linear distance between release and recapture is an underestimation of how far a winter flounder could travel in a day but these numbers allowed creation of a probability distribution for the transition model. I did not use a transition model that accounted seasonally for greater distances traveled during migrations because movement strategies would be different for a bay resident, offshore fish, or ocean spawning fish. Therefore the transition model stayed consistent over time. Additionally there is still confusion on how winter flounder behave during migration and if they are active at night outside of the spawning season (Grothues *et al.,* 2012; Grothues and Bochenek, 2010), but I am assuming they are active at night.

I analyzed these data in MATLAB (version 2014a). To enhance performance, when applicable, I divided the computational process between cores/workers using parallel loop iteration (function *parfor*). This boosts computational speed, however the initial designation of the loops into parallel clusters (using function *parpool*) itself takes approximately one to two minutes to execute prior to running the model and should be accounted for when comparing model run times. All parallel (*parfor)* loops were assigned to use 3-4 workers depending on availability of computing resources. I ran the models on a Macbook Pro with a 2.6 GHz Intel Quad-Core i7 processor.

Hydrodynamic Model

The Rutgers Regional Ocean Modeling System (ROMS), ESSPreSSO domain encompasses the Mid-Atlantic Bight from the center of Cape Cod, MA, southward to Cape Hatters, NC (Figure 1), with a 5-6 km horizontal and 36 level vertical grid from the coast to beyond the shelf break and shelf/slope front (myroms.org/espresso/). Model data was loaded into Matlab through an OPeNDAP server

(http://tds.marine.rutgers.edu:8080/thredds/roms/espresso/catalog.html). Since the only recovered archival tag was located in 2012, I chose the historic daily average data option (from 2009-2013) from the THREDDS data server (OPeNDAP: /thredds/dodsC/roms/espresso/2009_da/his). Loading and parameterization applied John Evans' snctools tools (http://mexcdf.sourceforge.net/downloads/) and MATLAB toolboxes created by John Wilkin of the Rutgers Ocean Modeling Group (http://romsmatlab.tiddlyspot.com/). I used the environmental data from the center of each grid point (longitude = lon_rho, latitude = lat_rho) and from Level 1 (the seafloor level). Level 1 encompasses roughly the bottom few meters for that location and varies with water column depth.

Model Assumptions

Model assumptions were based on observations of adult (> 30 cm) winter flounder, however they can easily be altered for application to any tagged Mid-Atlantic marine animal. I only used data from when the fish was in the water (> 0 m depth), not including its transition to or from the seafloor when tagged or recovered. A visual inspection of the data allowed us to decide when to cut the data, however since our archival tag recorded data every 24 minutes, the first and last few points are the ones under inspection. While winter flounder do swim in the water column, the majority of their time is spent < 0.6 m off of the sea floor (He, 2003) and thus I used output from level 1 of the ROMS model. In both models I composed an index for temperature, salinity, and depth for each day of the time series prior to running the SSM so that they were available in MATLAB as the model stepped through each day. An alternative to level 1 is to use *in situ* depth.

I removed the tidal signal (inertial and M2) from the data using an inverse Fourier transform lowpass filter to get a more accurate bathymetric depth (function *lowpass,* R.

Chant), however since the fish is not stationary there is still some uncertainty in depth due to smoothing.

Throughout the SSM, I assume a simple first-order Markov process dependent only on the state prior and transition from that state to determine the next state (Figure 2).

The recovery position has a large error radius due to the fact that the fish could enter the bottom trawl at any point along tow and would then be traveling at vessel speed rather than under its own power negating the transition distance assumed in the model. The transition model here is based on the theoretical maximum distance of a winter flounder traveling at 0.4 bl s^{-1} that remains active at night (Eq. 1)

Maximum swim distance = (length of fish in meters*0.4) * seconds/day (*Eq. 1*)

Since winter flounder spend large periods of time on the seafloor (He, 2003) with little movement influenced by water flow, I did not use a passive distribution algorithm for the transition model. I then converted maximum distance traveled to radians (function *distdim*) to get the maximum swim radius (MSR).

To infer a state I assume a static world at each time step sampled at regular intervals. The time intervals in ROMS can be 2 hours or daily average while the archival tag records a measurement every 24 minutes, and thus is interpolated for hours or averaged for day. I used a daily average for the tag data. The choice of time interval also affects the transition model, or how far a fish could move given that time step. A daily interval is used here to maximize computational speed. This choice was made due to the size of the grid squares in the ROMS ESPreSSO hindcast in relation to the winter flounder MSR, yet at the daily scale tidal state, often used in geolocation of demersal fish (Hunter *et al.*, 2003), is not used. If the two-hour time interval is used instead of daily average, tidal state calculated

from pressure can be used to help bolster belief state (the most likely state at a given time) accuracy since tidal variables are readily available in the ROMS ESPreSSO hindcast. A maximum daily depth has successfully been used in previous studies (Pedersen, 2008; Le Bris *et al.*, 2013), but I am using a daily average depth.

Simulating Known Paths to Test Model Performance

To test for accuracy, I created 20 known (i.e. simulated) paths that I then attempted to reconstructed using the SSMs and only the "data" gathered during progression of the simulated fish through the model domain. To generate the simulated paths, I used a biased random walk, where the probability to move in a certain defined direction is higher than another. The transition from each state was chosen within the MSR with a normal probability density function (pdf) with a mean of 200 m and variance of 2 km, including no-movement in a given time step as an option. Additionally, temperature preference was accounted for within 0 °C to 20 °C with a normal pdf of mean of 9.5 °C (the average temperature of occurrence off of New Jersey, Winton *et al.*, 2014) and of variance of 6 °C (the average error when compared to the archival tag data for the ROMS ESPReSSO bottom temperature). All paths were generated from the same start point, which was the ROMS grid square center (lat_rho, lon_rho) closest to where I released our tagged winter flounder (40.1440, -73.6740) on Sept. 6, 2012. Paths were simulated for time scales of 92 days for proof of concept (Figure 3). Environmental data for level 1 across the grid space were pulled out of ROMS ESPReSSO and then error was added to these data to match the observed archival tag data error. From the single archival tag recovered (released at 40.1440, -73.6740), the first at-depth reading reported a depth of 48.68 m, temperature of 9.51 °C, and salinity of 32.67 on Sept. 6, 2012 at 10:36am. The closest ROMS position to this point is located at 40.1772, -73.6650 with a depth of 36.26 m and had a temperature of 16.31°C, and salinity of 32.43 on Sept. 6, 2012 at 10 am. Error for temperature was added

from a normal probability density function with a mean of 6 °C and variance of 2 °C. Error for salinity was added from a normal pdf with a mean of 0.15 and variance of 0.15.

Data Matching and Simulation Models

This data matching and simulation SSM draws from the methods of Righton and Mills (2008). The beauty of a data matching and simulation model is that is it simple to understand and faster than a computationally expensive SSM. Additionally, since I am using a gridded hydrodynamic model, implementation is easy (Table 1). A caveat to this model is that the decisions lacks a measurement of probability between plausible states to make a choice since the transition model stays consistent and states are randomly chosen within an error range.

The first step is to match the data from the archival tag to the hydrodynamic model (ROMS ESPReSSO) considering error. I started off by defining the standard error of our environmental variables based on the ability of ROMS ESPReSSO to match the bottom temperature at a known location. Temperature had an error of approximately ±7 ^{o}C. Salinity had an error of ±1. Depth is assumed to be bottom depth, so depth had an error of ±4 m. Since bathymetry in ROMS ESPReSSO is an average of the depths in the cell (and even then interpolated from infrequent soundings), error from fish being close to but not on the bottom becomes negligible.

For each day, I then found plausible locations based on the errors for each variable across the ROMS ESPReSSO grid. I did this for as many time steps as the path included. Here I used 11, 31, and 92-day time series pulled from the simulated paths. I found the state that matches temperature, salinity, and depth from the tag within these bounds. If this could not be accomplished, I then matched the state to salinity and depth from the tag as a secondary measure. If there was still no match, I then took a step back to the prior state in time and chose a different state for the time step prior as a tertiary measure. I chose not to use the

method of staying at the current position if a match was not found, because while it did reveal possible paths the data did not match tag observation.

Starting at the grid center closest to the release point, I then commenced a random walk for each time step choosing one state within the MSR from the state prior that was a plausible location based on the environmental data for that day. The transition model here gives equal weight to staying in the same state as moving the maximum distance or any distance in between. If the last state was at or within 2 km of the recapture point I kept that set of states, if not that path was discarded. This buffer zone around the recapture point was the smallest possible without causing particle starvation (the condition where so few particles survive filtering that the model cannot proceed). I reiterated this process from the release state to the recovery state 100,000 times across the state space (using the function *parpool).*

Each path that reached the end point (either the recapture location or simulation path end) was saved, and each state that was part of that reconstructed path was assigned a weight of +1. After the iterations were complete, all plausible states thus were cumulatively weighted by the frequency at which they had been crossed. Lastly using these weights I estimated the most likely path that was used to cross the state space. I did this by creating a kernel density (function *ksdensity*) for both latitude and longitude, then (using the functions *meshgrid* and *max)* found the maximum probability of being at a state given time. Residuals between the known test path and the path generated by the model were calculated (using the function *distance)* to get the distance between a state at $time_t$ in meters.

This basic matching scheme is the same as for the Ådlandsvik *et al.,* (2007) model, yet the path starts at both ends (from the release and recapture states) and works toward the center. At the center time point, if states are less than the maximum distance per day, their reconstructed paths are combined. Once several plausible reconstructed paths are

found, I calculated a simple mean of the plausible states for each time point instead of a weighting and kernel density approach. For the Ådlandsvik *et al.,* (2007) model I used 10,000 iterations rather than the 100,000 iterations used in Righton and Mills (2008).

Particle Filter Model

A particle filter uses probability theory to quantify if any given belief state is likely or unlikely (Russell and Norvig, 2010). The state where the fish was released is known, so out of all the possible states that position gets a probability of 1. Two constants that remain in the model are the MSR and the pdfs for temperature, salinity, and the transition between states. The pdf for the transition model here is a normal curve giving more weight to moving slightly and the least weight to moving the maximum distance (10368 m for a particle with an assigned 300 mm bl). Status quo is less likely than moving slightly but more likely than moving the maximum distance from the state before, $\mathbf{X}_{t-1}$. I assumed the transition probability between states is independent of time. Temperature and salinity are both normal distributions based on the difference between the observed variable and ROMS variable. Thus, an error with difference of 6 ^{o}C and salinity 0.15 is most probable and is weighted highest.

Error is taken into account for both archival tag error and ROMS ESPreSSO error. ROMS ESPreSSO error is calculated using the average difference between observations at the start and end positions compared to the archival tag data. Archival tag mechanical error is negligible compared to ROMS ESPReSSO error but listed in methods for reference in Chapter 3. The pdf for depth is uniform. Thus, given that I am using daily average depth, a difference between the observed depth and the hydrodynamic model depth of less than 4 m would be assigned a probability of 1 while a greater difference would be assigned a probability of 0.

Possible states for $\mathbf{X}_t$ (latitude and longitude at level 1 at a given time) are within the MSR (found using the functions *scircle1* and *inpolygon)* from $\mathbf{X}_{t-1}$. I used the ROMS land mask to avoid locations on land. I saved *n* states consistently, at each time step. These states are not unique and can be duplicated. A sample (n) of at least 10,000 states is recommended to avoid particle starvation, yet I tested performance at *n* = 100 and n = 1,000 to cut down on the model run time.

The following equations (Eq. 2 and 3) are outlined in Russell and Norvig (2010). In the particle filter, where **P** denotes probability, the observation model is defined as (Eq. 2),

$$\mathrm{P}(\mathbf{O}_t|\mathbf{X}_t) = \mathrm{P}(\mathbf{O}_t|\mathbf{e}_{0:t}, \mathbf{O}_{0:t-1}) \qquad (Eq.\ 2)$$

In this case, the observation model includes temperature, salinity, and depth observed by the archival tag compared to the observations in the ROMS ESPReSSO model at a given time. To calculate $\mathrm{P}(\mathbf{O}_t|\mathbf{X}_t)$, residuals are calculated between the tag observation and ROMS ESPReSSO model values at possible states and time *t*. Values from the pdf curves are assigned to each state given the residual at that state. A random vector generator (*randsample*) function chooses one of the possible states. The distance in meters is calculated between $\mathbf{X}_{t-1}$ and $\mathbf{X}_t$, and a value from the pdf for depth is assigned to that state given the difference. I calculated the probability of being at the belief state, $P(\mathbf{X}_t|\mathbf{O}_t)$ (Eq. 3)

$$P(\mathbf{X}_t|\mathbf{O}_t) = \alpha * P(\mathbf{O}_t|\mathbf{X}_t) * \int_{X_{t-1}} P(\mathbf{X}_t|\mathbf{X}_{t-1}) * P(\mathbf{X}_{t-1}|\mathbf{O}_{1:t-1}) \qquad (Eq.\ 3)$$

where α is a normalizing agent so that the sum is 1, and the transition model is defined at $P(\mathbf{X}_t|\mathbf{X}_{t-1})$. I normalized $P(\mathbf{X}_t|\mathbf{O}_t)$ for all *n* states to get a weight for those states at that

time. Random resampling based on the weight values yielded the best possible combination of *n* states for that time (using the *randsample* function with weight set as true).

The recapture point is known to only about 5 km precision in the case of trawl recaptures so it is weighted highly in the backward smoothing step but the probability of being at that state (the weight) is not equal to 1 like the release point. The algorithm then checks that the recapture state is within the time_t vector for possible states, if not, it is added and highly weighted with final weight between 0 (no confidence) and 1 (high confidence/precision).

Once the forward filtering is accomplished, I move to the backward smoothing process. New states are not calculated in the backward smoothing step, but the existing states are reweighted as (Eq. 4)

$$w_{\mathrm{t|T}}^{(\boldsymbol{i})} = w_t^{(\mathrm{i})} \left[\sum_{j=1}^{n} w_{t+1|T}^{(j)} \frac{p(x_{t+1}^{(j)} | x_t^{(i)})}{\sum_{k=1}^{n} w_t^{(k)} p(x_{t+1}^{(j)} | x_t^{(k)})} \right] \qquad (Eq.\ 4)$$

where *i, j,* and *k* = 1:*n*, T = time_t, and t = $\text{time}_{1:t-1}$ (defined in Klaas *et al*., 2006). The denominator is calculated as the transition distance between the scalar $\mathbf{X}_t^{(j)}$ and each scalar in vector $\mathbf{X}_{t+1}^{(k)}$. A value from the pdf of transitions is then assigned as the probability of transitioning to that space. Next I multiplied the pdf values for transitioning between those states by the weight vector $\mathbf{w}_t^{(k)}$ (the probability of being at that state calculated in the forward pass) and took the sum from $k_{1:n}$. To calculate the numerator in (*Eq. 4*) I calculated the transition distance from the state scalar $\mathbf{X}_t^{(i)}$ to all of the scalars in the state vector $\mathbf{X}_{t+1}^{(j)}$ and assigned pdf values for those transitions. I then multiplied this answer by the weight vector $\mathbf{w}_{t+1|T}^{(j)}$ (the string of probabilities of being at those states calculated in the forward pass) and took the sum from $j_{1:n}$. I calculated a new smoothed weight for the state scalar $\mathbf{X}_t^{(i)}$

by multiplying the weight scalar $\mathbf{w}_t^{(i)}$ by the numerator divided by the denominator. Doing this equation in this order is computationally important since it uses multiple 'for' loops and also saves time.

Once the forward filter and backward smoothing are complete I calculated a weighted mean at each time step for the *n* possible paths, using the probability calculated in the backward pass for being at that state at the weight. Residuals between the known test path and the simulated path were calculated as the shortest of either rhumb line or great circle (function *distance*) between states at a time$_t$.

4.3 Results

Both the Particle filtering and data matching models were capable of reconstructing simulated paths between the start to end location at small time scales (11 and 31 days).

Data Matching and Simulation Models

The Righton and Mills (2008) data matching and simulation model, which uses a kernel density to reconstruct the path and is calculated from release to recovery point, ran on average 715.54 s for a 31-day-long data set (Table 3). Eight out of 20 simulated known paths were successfully reconstructed with an average distance from the known path of 14 ± 4 km, averaging 312.75 successful paths out of 100,000 iteration attempts. With a break function inserted into the path reconstruction loop, unsuccessful path reconstructions on average ran 208.35 s. For simulated known paths subset at an eleven-day time series, ten out of 20 path reconstruction attempts were successful, averaging 413.62 s with a deviation of 9 ± 5 km in length from that of the simulated known path. Unsuccessful path reconstruction attempts ran for 209.94 seconds on average. For path reconstruction attempts of simulated tracks using a 92 day-long time series for the Righton and Mills

(2008) method no paths reconstructions were successful, and averaged 473.82 seconds to run the model.

The Ådlandsvik *et al.,* (2007) data matching and simulation model, which uses a mean to reconstruct the path and runs from both the release and recapture point, ran on average 121.46 s for 31 day-long simulated known track when path reconstruction was successful and ran for 75.26 seconds when unsuccessful (Table 4). Eleven out of 20 simulated known path reconstruction attempts were successful, averaging a distance of 13±7 km from the known path. For simulated known data from an 11 day-long time series, to reconstruct the paths a successful model ran for an average of 262.66 s while an unsuccessful model ran 31.82 seconds. Fourteen out of 20 path reconstruction attempts were successful, averaging a deviation of 7±4 km from the known path. The Ådlandsvik *et al.,* (2007) method does produce an impressive number of possible paths with 12,894,625 plausible reconstructed paths for an 11 day-long time series and 503,090 plausible reconstructed paths for a 31 day-long time series at 10,000 iterations forward and 10,000 backward. When reconstructing a simulated path composed of a 92 day-long time series, there were no simulated paths that were successfully reconstructed, averaging 290.23 s to run the model with zero yield. Reconstructions of simulated paths were attempted using 100,000 iterations (instead of 10,000 iterations) for 31 daylong paths (n = 1, 1187 s) and 92 daylong paths (n = 3, 1270.74 s) but were also unsuccessful.

Combining the Ådlandsvik *et al.,* (2007) path creation method (starting from both ends) with the Righton and Mills (2008) weighting and kernel density method (instead of taking the arithmetic means for all plausible states at each time step) did not advance the SSM model performance. These path reconstruction attempts had similar residuals and standard deviations from the known path (e.g., 15 ± 7 km for the 11 day time series) but the kernel density method took longer to run. This combination of methods had a flaw where if

there were millions of plausible reconstructed paths it took hours to weight the states without any increase in path reconstruction accuracy.

Particle Filter Model

The particle filter, which is more computationally expensive, ran on the order of days for 10,000 states saved in an attempt to reconstruct a simulated known path subset into a 31 day-long time series. Yet with fewer particles where less states are saved, the model runs much faster and is the fastest when n = 100 states saved. When n = 1000 states saved and above it becomes the longest running model. While saving few particles suites speed, it does not converge at a solution (rerunning the model can reveal a different reconstructed path). When I ran the model on the same simulated known path multiple times, there was no solution through the state space the first time but there was a solution a second time, and running it a third time revealed a slightly different reconstructed path still within similar error of the reconstructed path prior.

For 100 states saved, when attempting to reconstruct a known path subset into an 11 day-long time series 16 out of 20 path reconstruction attempts were successful, averaging 10 ± 4 km (or 8 ± 3 km smoothing with a mean) from the known path (Table 5). It took an average of 30.99 s for successful attempts and 13.13 s for unsuccessful attempts. For a sample of 1000 states saved, when attempting to reconstruct a known path subset into an 11 day-long time series, 18 out of 20 path reconstruction attempts were successful, averaging a deviation of 11 ± 4 km (9 ± 4 km using a mean to smooth) from the know path. Successful path reconstructions ran 1716.65 s, while unsuccessful path reconstructions ran 1782.61 s. For a sample of 100 particles, when attempting to reconstruct a known path subset into an 31 day-long time series 9 out of 20 path reconstructions were successful, averaging 11 ± 3 km (or 9 ± 4 km smoothing with a mean) from the known path. Successful paths ran 89.19 s, while unsuccessful paths ran 54.26 s. For a sample of 1000 states saved,

when attempting to reconstruct a known path subset into an 31 day-long time series 15 out of 20 paths were successful, averaging a distance of 13 ± 9 km (same as using a mean to smooth) from the know path. Successful paths ran 5644.69 s, while unsuccessful paths ran 1782.61 s. Only two simulated known paths were tested on the scale of a 92 daylong time series with 100 states saved. One reconstruction attempt was successful (20 ± 11 km or 19 ± 10 km using a mean, 204.9 s) while the other attempt was not (60.63 s). One reconstruction attempt was tested at the 92 daylong scale saving 1000 states at each time step, yet due to the computer restarting over night the path was not completed but ran on the order of days. The majority of the failures in the particle filter SSM were due to the last state $\mathbf{X}_{T-1}$ not being within the MSR from the recovery position $\mathbf{X}_{T}$.

Consistently Unsuccessful Reconstruction Attempts

Neither the Ådlandsvik *et al.,* (2007) or Righton and Mills (2008) SSM could solve for simulated known path numbers 3, 5, 11, 12, 15 and 16 for either the 11 or 31 daylong time series. There was no immediately discernable pattern that would stand out as a reason why these paths were not solved. Additionally the particle filter SSM was unable to reconstruct simulated known path number 15.

4.4 Discussion

State space models are growing in popularity with ecologists over the last two decades as a tool for understanding complex life history questions, however they can be difficult to understand, implement, and choose. A growing literature base is making these decisions easier (Patterson and Thomas, 2008; Schick *et al,.* 2008; Jonsen *et al,.* 2013), however it is still a complicated process.

In making the choice to use a hydrodynamic model to investigate environmental history, ROMS ESPReSSO has its own constraints. The greatest limitation in using ROMS

ESPReSSO is that due to a large error in the environmental parameters at its bottom layer, it can either a) provide too many states at each time step and thus inhibit a great number of paths from reaching the end recovery point or b) provide no plausible states. The Ocean Observation Laboratory at Rutgers University is actively fine-tuning the ESPreSSO model and has recently achieved better model data, especially in decreasing the temperature error (John Wilkin, personal communication). This will refine our future state space models. Considering the size of the grid squares used in ROMS ESPReSSO (5-6 km) and the swimming behavior of winter flounder (assumed maximum of 10 km day^{-1} with a high probability of moving 2 km day^{-1} or less), there will most likely be a high probability of staying in the same state due to winter flounder not moving past grid boundaries. If I used the 2-hour resolution this probability of staying in the same grid square would increase. Possibly using a model with finer scale resolution might help accuracy of path reconstruction since especially outside of the migration season winter flounder are not as mobile.

The data matching and simulation SSM additionally has it own limitations, such as that the lack of a weighting process leaves all states within the full MSR as viable choices as long as they match the observed tag data (given error). This allows for less likely reconstructed paths to be explored and for those reconstructed paths to carry the same weight as higher probability paths. Another caveat is that the data matching and simulation model performs best at short time scales and worse at longer time scales. Therefore if the tag record is long, since the state space grows with time, the number of iterations through the state space needs to increase in order to reconstruct the path. This increases the model run time, without the guarantee that the increase in iterations will create a reconstructed path.

Even for the particle filter SSM, the residuals from the known path increased as time-at-liberty increased. Additionally, since I used a particle set of 100 or 1000 rather than 10,000 or higher as suggested, this was problematic for path reconstruction. Saving 100 particles at each time step allowed for particle starvation and was thus not reliable, even if it did create a reconstructed path. Increasing to 1000 particles saved at each time step did not increase path accuracy but did increase the time it takes to run the model.

None of the reconstructed paths were better from each other for 11 and 31 daylong time scales, yet at longer time scales (92 days) the particle filter out-performed the data matching and simulation SSMs. When it came to the last step in reconstructing the path, between the kernel density method (outlined in Righton and Mills, 2008) or taking the arithmetic mean, taking the mean proved to be a better choice when considering model run time. The particle filter method does not perform more accurately when reconstructing the path than the data matching and simulation methods despite the increase in model run time; however, it reconstructed more paths than the other models and successfully reconstructed paths at longer time scales. Although Ådlandsvik *et al.,* (2007) and Righton and Mills (2008) were able to perform their SSMs for year time scales, I was unable to do so using the parameters above and ROMS ESPReSSO model. Longer time scales still need to be tested since the tags can record up to four years of data at a rate of one record every 24 minutes.

The transition distance pdf proved to be very important in the particle filter; altering this did change accuracy when reconstructing the path, however it was still within the error of other paths. Also, for all SSMs the transition distance is linear but needs to be corrected for obstructions like land, islands, etc. so that it accounts for the distance to move around an obstruction such as out of a bay through the mouth. Using the ROMS land mask

assisted with this slightly but not completely. In general, if I am able to inform the model better to cut down on the transition MSR then I can hone in on plausible locations.

Future work is planned to delve further into SSM performance based on parameter choices unique to the ROMS ESPReSSO model and to winter flounder. Changing the transition model according to season to account for increased activity during migration both with swim rate and activity at night would be one of these choices. Since swim rates are temperature dependent (Joaquim *et al.*, 2004) with decreased rates at high and low extremes and fastest observed rates at optimal temperatures (Olla *et al.,* 1969; He, 2003), the transition model could be conditional on temperature. The amount of time that winter flounder spend swimming in the water column opposed to resting on the seafloor, which is also temperature and spawning dependent (He, 2003), can be factored into the model as well. Additionally, I am assuming winter flounder are active during the day and night, which would influence how far a winter flounder could travel. As is, this is an overestimation of the distance in which a winter flounder could travel in one day and could be decreased to assist with finding plausible states. Additional research should be done to investigate the swim rates of migrating winter flounder opposed to winter flounder outside of the spawning season because assuming a constant swim rate year round could also be an overestimation.

Overall this work revealed specific items for improvement of the SSMs in path reconstruction, but at small time scales did not divulge a best-fit model out of the three tested. However, the particle filter method was able to reconstruct the most paths and reconstructed paths at the largest time scale; therefore, despite its complexity and long model run time, it is currently the most useful model to apply.

LIST OF TABLES

Table 1. Pseudocode for the data matching and simulation model

for $time_2$:$time_t$
    find states in environmental history that match the observed tag data given error for each day
    build a matrix of plausible states for each day
for *n* iterations
    for $time_2$:$time_t$
        random walk through primary matched states restricted by maximum swim radius
        if there are no matches try secondary matches
        if there are no matches take a step back and try again
        if there are still no matches break the loop here to save time
    if the recovery point is successfully reached
        give each state crossed in that path a weight of +1
for $time_2$:$time_t$
    do a kernel density to estimate the most likely plausible state at each step

Table 2. Pseudocode for particle filter model

for $time_2$:$time_t$
    find states in ROMS that match the observed tag data given error for each day
    build a matrix of plausible states for each day
Forward Filter:
for $time_1$:$time_t$
    for *i* = 1:*n* replicates
        find states within the MSR
        subtract the tag variables from state environmental variables
        calculate the observation model P($\mathbf{O}_t|\mathbf{X}_t$), or *pdf* value at each state
        randomly chose one of the available states $\boldsymbol{X}_t^i$
        calculate the transition model $P(\mathbf{X}_t|\mathbf{X}_{t-1})$
        calculate $P(\mathbf{X}_t|\mathbf{O}_t)$
    Normalize $P(\mathbf{X}_t|\mathbf{O}_t)$ for all states $\boldsymbol{X}_t^{1:N}$ to get a weight for each state $\boldsymbol{X}_t^i$
    Resample based on the weights to get *n* states at time *t*
Backward Smoothing:
for $time_t$:$time_1$
    for *k* = 1:*n* replicates
        Calculate the denominator in (*Eq. 4*)
    Sum *k* = 1:*n* to get a scalar for the denominator
    for *j* = 1:*n* replicates
        Calculate the numerator in (*Eq. 4*)
        Sum *j* = 1:*n* to get a scalar for the numerator
        Calculate new smoothed weight for $\mathbf{X}_t^{(i)}$

Table 3. Path reconstruction results using the data matching and simulation Righton and Mills (2008) method. I defined each simulated known path by the path number (1-20) and the subsample of the time series used is denoted by days (11, 31, or 92). The residuals and standard deviation (STDEV) here are calculated using the kernel density method. The number of successfully reconstructed paths is out of 100,000 possible paths. The time in which the model took to run (successful or not) is recorded in seconds.

Path #	Days	Kernel Density Residuals	Kernel Density STDEV	Num. of Paths	Model run time
1	11	11624.36	8969.42	39	373.98
2	11	7739.96	4813.89	3989	484.45
3	11				175.06
4	11				118.75
5	11				117.33
6	11	18329.97	12752.94	7	212.36
7	11	6417.01	5765.44	27534	515.82
8	11	5064.24	3574.85	23132	491.54
9	11				401.65
10	11	7833.71	6654.86	3061	269.22
11	11				360.61
12	11				117.39
13	11	3811.6	2758.17	7060	461.35
14	11	5618.07	4226	11171	487.4
15	11				43.68
16	11				43.54
17	11				469.35
18	11	13356.46	11802.72	2571	386
19	11	11662.7	8567.46	1561	454.03
20	11				252.08
1	31				351.53
2	31	11233.93	6619.31	1158	920.91
3	31				123.92
4	31				120.12
5	31				220.31
6	31				217.86
7	31	22106.50	16130.86	8	775.28
8	31	11263.55	9060.2	723	1224.43
9	31	14198.40	9294.36	28	634.97
10	31	9447.08	5325.41	318	441.95
11	31				289.13
12	31				109.87
13	31				114.36
14	31				627.62
15	31				43.59
16	31				46.26
17	31	17474.08	13269.70	10	703.81
18	31	12178.06	8522.74	247	418.24
19	31	9518.22	5919.03	10	604.72
20	31				235.59
1	92				399.58
2	92				984.88

3	92				177.18
4	92				118.86
5	92				117.32
6	92				208.54
7	92				766.58
8	92				1355.81
9	92				608.89
10	92				513.52
11	92				326.24
12	92				617.68
13	92				628.48
14	92				689.37
15	92				53.56
16	92				53.79
17	92				656.03
18	92				412.43
19	92				552.69
20	92				235.05
Avg.	11	9145.81	4512.44	8012.5	>0 paths: 413.62
					0 paths: 209.94
Avg.	31	13427.48	4383.02	312.75	>0 paths: 715.54
					0 paths: 208.35
Avg.	92				0 paths: 473.82

Table 4. Path reconstruction results using the data matching and simulation Ådlandsvik *et al.,* (2007) method. I defined each simulated known path by the path number (1-20) and the subsample of the time series used is denoted by days (11, 31, or 92). The residuals and standard deviation (STDEV) here are calculated using the kernel density and the arithmetic mean method. The number of successfully reconstructed paths is out of 10,000 or 100,000 possible paths. The time in which the model took to run (successful or not) is recorded in seconds.

Path	Days	Kernel Density Residuals	STDEV	Mean Residuals	Mean STDEV	No. of iterations	No. of Paths	Model run time
1	11	12817.12	6454.47			10000	808	96.65
2	11					10000	2749576	Stopped at 5286.04
3	11					10000		87.53
4	11					10000		96.12
5	11					10000		78.86
6	11					10000		65.75
7	11	20284.98	13488.05			10000	50015	337.44
8	11					10000	4265934	Stopped at 1350.43
9	11	15216.77	9375.20			10000	16465	199.44
10	11					10000	594625	Stopped at 2006.85
11	11					10000		104.42
12	11					10000		68.81
13	11	9700.44	8023.63			10000	100961	582.20
14	11					10000		79.6
15	11					10000		23.97
16	11					10000		67.97
17	11	27416.14	15612.59			10000	347318	1684.05
18	11	13107.69	8890.42			10000	62455	390.5
19	11	8170.87	5290.36			10000	28227	255.2
20	11					10000	1354687	Stopped at 2680.25
1	11			12030.59	9539.11	10000	117010	43.63
2	11			5532.58	4204.99	10000	3360064	82.93
3	11					10000		38.04
4	11			9656.58	7272.01	10000	13818455	167.68
5	11					10000		36.04
6	11			15892.73	12191.9	10000	10093	45.18
7	11			5425.02	5470.54	10000	46096474	1645.67
8	11			5589.48	3656.74	10000	28540076	590.1
9	11			3617.58	3249.18	10000	1565963	70.22
10	11			7318.19	5936.34	10000	4381380	78.41
11	11					10000		39.46
12	11					10000		20.34
13	11			2885.1	2058.31	10000	20101333	210.37
14	11			4534.71	3789.21	10000	17921381	197.44
15	11					10000		29.38

16	11					10000		27.67
17	11			6894.19	4698.21	10000	19149685	190.59
18	11			12070.13	10561.51	10000	2703212	76
19	11			4629.07	2663.2	10000	4212554	86.03
20	11			3728.27	3953.48	10000	18547072	193.55
1	31			11930.29	6794.89	10000	529	86.12
2	31			11367.24	6988.36	10000	2616670	166.8
3	31					10000		88.32
4	31					10000		96.12
5	31					10000		78.86
6	31					10000		65.75
7	31			20720.95	13781.92	10000	57576	116.45
8	31					10000		80.2
9	31			13407.87	8371.51	10000	18789	110.13
10	31					10000		129.2
11	31					10000		68.81
12	31					10000		73.6
13	31			10125.95	7100.36	10000	103028	125.16
14	31					10000		79.6
15	31					10000		23.97
16	31					10000		68.31
17	31			26915.69	7100.36	10000	337409	139.91
18	31			12052.87	7761.99	10000	69839	117.66
19	31			6624.67	3751.81	10000	20801	132.88
20	31			6683.32	4112.8	10000	1303171	98.01
1	92					10000		284.51
2	92					10000		539.38
3	92					10000		301.88
4	92					10000		377.13
5	92					10000		376.89
6	92					10000		100.97
7	92					10000		312.54
8	92					10000		475.77
9	92					10000		374.18
10	92					10000		359.72
11	92					10000		377.13
12	92					10000		295.79
13	92					10000		393.18
14	92					10000		284.98
15	92					10000		242.32
16	92					10000		68.77
17	92					10000		141.66
18	92					10000		177.38
19	92					10000		295.79
20	92					10000		135.82
10	31					100000		1186.6
4	92					100000		1185.77
19	92					100000		1623.75
20	92					100000		1002.7
Avg.	11	15244.86	6643.13			10000	86607	>0 paths: 506.50
								0 paths: 74.78 plus
Avg.	11			7128.87	3867.33	10000	13291179.46	>0 paths: 262.66
								0 paths: 31.82
Avg.	31			13314.32	6576.94	10000	503090	>0 paths:

								121.46
								0 paths: 77.52
Avg.	92					10000		0 paths: 295.79
Avg.	92					100000		0 paths: 1249.71

Table 5. Path reconstruction results using the particle filter method. I defined each simulated known path by the path number (1-20) and the subsample of the time series used is denoted by days (11, 31, or 92). The residuals and standard deviation (STDEV) here are calculated using the kernel density and the arithmetic mean method. The number of successfully reconstructed paths is out of 100 or 1,000 plausible states kept at each time step. The time in which the model took to run (successful or not) is recorded in seconds.

Path	Days	Kernel Density Residuals	Kernel Density STDEV	Means Residuals	Means STDEV	Num. of States	Num. of Paths	Model Run Time
1	11	15322.79	14853.22			100	100	186.06
2	11	8568	6160.06	9498.49	7903.15	100	100	20.09
3	11	11687.96	14431.59	9519.08	7228.05	100	100	21.6
4	11	5106.46	4265.01	6111.4	5600.42	100	100	21.48
5	11	8089.51	7290.38	6668.87	5760.64	100	100	18.65
6	11	7085.84	7621.96	5374.97	5027.07	100	100	21.17
7	11	7731.96	7653.53	5806.8	5477.77	100	100	20.9
8	11	6674.65	5916.55	5443.29	3927.64	100	100	18.55
9	11					100		13.34
10	11	7231.58	7327.48	4268.17	4654.96	100	100	18.94
11	11	10348.6	9404.9	9304.42	7061.26	100	100	19.66
12	11	13977.64	8886.39	12796.3	8392.14	100	100	19.83
13	11	5632.19	4808.86	5221.21	4794.47	100	100	23.61
14	11					100		12.79
15	11					100		14.53
16	11	11692.7	11491	11062.53	9624.77	100	100	19.84
17	11	5396.67	4857.87	5370.58	4759.49	100	100	19.61
18	11	15181.01	9101.69	14072.76	9061.06	100	100	25.43
19	11	13828.07	10879.20	11733.71	8173.64	100	100	20.35
20	11					100		11.87
1	11	17875.15	11034.42			1000	1000	1660.89
2	11	10418.69	10020.11	10252.96	7446.01	1000	1000	1770.93
3	11	11426.89	10228.85	10194.63	8343.93	1000	1000	1454.07
4	11	5198.34	6991.10	5848.49	5167.81	1000	1000	1706.77
5	11	7670.59	9750.12	7019.75	6269.38	1000	1000	1551.24
6	11	11171.51	9209.62	5915.14	5192.19	1000	1000	2371.01
7	11	7317.79	8362.48	4623.45	4576.22	1000	1000	1843.12
8	11	7024.27	6529.05	5019.52	3926.36	1000	1000	1533.3
9	11	19558.74	12651.44	18488.80	11243.76	1000	1000	1599.53
10	11	5754.00	5078.94	4354.68	3576.51	1000	1000	1387.97
11	11	13065.55	7204.21	9851.29	5833.52	1000	1000	1623.04
12	11	14712.12	9583.62	13652.1	8107.81	1000	1000	1505.14
13	11	7256.51	6272.28	5368.49	4660.02	1000	1000	1799.67
14	11					1000		1019.43
14	11	11286.96	8933.42	11286.96	8933.42	1000	1000	1752.24
15	11					1000		1273.95
16	11	5120.66	3550.95	3486.15	2668.86	1000	1000	1768.83
17	11	9636.98	8248.1	4968.60	4918.15	1000	1000	1817.32
18	11	14394.25	8001.39	15446.46	9199.5	1000	1000	1801.95
19	11	12729.20	8002.83	12712.89	7456.77	1000	1000	1952.74
20	11					1000		993.14

1	31					100		48.65
2	31					100		47.7
3	31	11432.95	7982.3	9753.52	7641.98	100	100	125.7
4	31	8658.35	6277.48	8883.59	6391.45	100	100	90.25
5	31					100		50.81
6	31	9314.66	6007.22	9711.59	5822.71	100	100	83.8
7	31					100		53.9
8	31					100		54.37
9	31					100		65.46
10	31	8126.76	5783.4	5668.63	4556.81	100	100	105.68
11	31					100		55.96
12	31					100		57.41
13	31	11304.18	8858.8	11497.73	8729.96	100	100	81.42
14	31	12231.66	9279.4	13179.86	8636.52	100	100	103
15	31					100		54.3
16	31	8968.63	7720.97	8298.67	5983.05	100	100	69.31
17	31					100		59.15
18	31	12673.6	9611.23	12149.07	7956.76	100	100	65.66
19	31					100		49.15
20	31	18941.7	11650.29	18538.87	11264.9	100	100	77.9
1	31					1000		2992.82
2	31	9712.10	7721.07	9137.45	5373.16	1000	1000	6188.76
3	31	9259.5	8554.8	8739.0	6438.3	1000	1000	5402.77
4	31	10967.54	7850.75	9255.69	6716.3	1000	1000	5509.94
5	31					1000		1782.61
6	31	10833.59	7142.14	8597.06	4890.57	1000	1000	5775.65
7	31	6600.85	5432.66	5247.8	3868.38	1000	1000	5798.82
8	31					1000		1782.61
9	31					1000		5920.21
10	31	7812.4	6041.75	5198.7	3271.77	1000	1000	4979.16
11	31	1315	8817.9	11242	6855	1000	1000	5674.38
12	31	13151	9046.7	12559	6961.6	1000	1000	5585.67
13	31					1000		1782.61
14	31	14898.58	10064.17	12962.63	8273.44	1000	1000	6350.76
15	31	12135	9281.3	13672	8763.1	1000	1000	5651.71
16	31	11250	8374.9	10029	6650.8	1000	1000	5135.97
17	31	19377	12705	19979	13070	1000	1000	5525.18
18	31	13083.71	8310.43	12727.01	7998.80	1000	1000	6527.64
19	31	40120	26425	41054	25937	1000	1000	3264.05
20	31	18613.68	11180.36	18846.20	10438.92	1000	1000	7299.82
1	92	19529.27	10625.4	18560.61	10201.01	100	100	204.79
18	92					100		60.63
Avg.	11	9597.18	3569.96	8150.17	3176.45	100	100	>0 paths: 30.99
								0 paths: 13.13
Avg.	11	10645.46	4225.37	8734.73	4434.01	1000	1000	>0 paths: 1716.65
								0 paths: 1095.51
Avg.	31	11294.72	3308.94	10853.50	3646.49	100	100	>0 paths: 89.19
								0 paths: 54.26
Avg.	31	13275.33	8668.53	13283.10	8738.36	1000	1000	>0 paths: 5644.69
								0 paths: 1782.61

Avg.	92	19529.27	10625.4	18560.61	10201.01	100	100	>0 paths: 204.79
								0 paths: 60.63

LIST OF CAPTIONS

Figure 1. The model domain on the Northeastern U.S. shelf for the ROMS ESPreSSO data, including grid and bathymetry. This image is from http://www.myroms.org/espresso/espresso_grid.png.

Figure 2. An illustration of the State Space Model framework used, including the measurements (Y), our unknown (X) across time (T).

Figure 3. Simulated paths for 11, 31, and 92 days in the New York Bight (off of New Jersey and below Long Island, New York) with the New Jersey coastline, different paths are denoted by the change in color. Release was on Sept. 6, 2012.

LIST OF FIGURES

Figure 1.

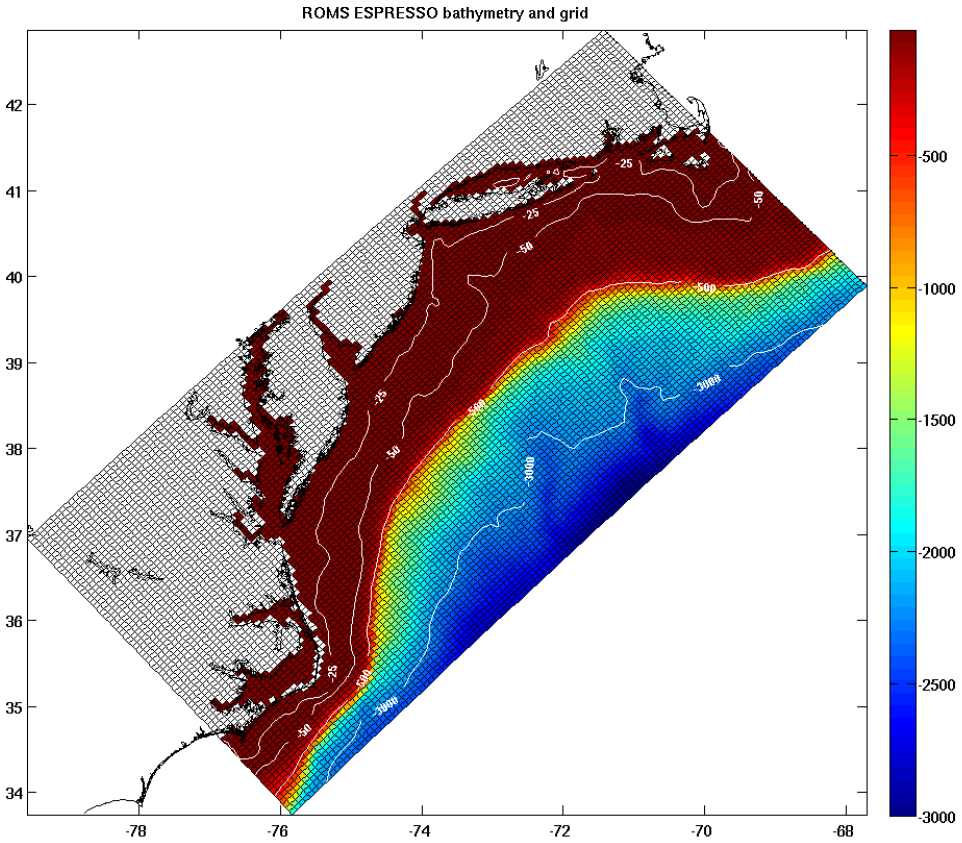

Figure 2.

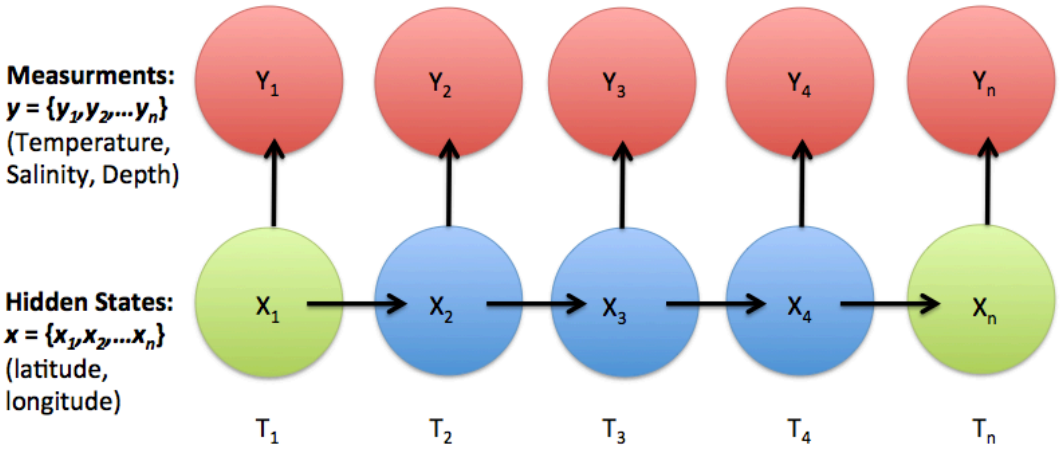
Measurments:
$y = \{y_1, y_2, \ldots y_n\}$
(Temperature, Salinity, Depth)
Hidden States:
$x = \{x_1, x_2, \ldots x_n\}$
(latitude, longitude)
Y_1
Y_2
Y_3
Y_4
Y_n
X_1
X_2
X_3
X_4
X_n
T_1
T_2
T_3
T_4
T_n

Figure 3

Simulated known paths (1-20) at 11 days..

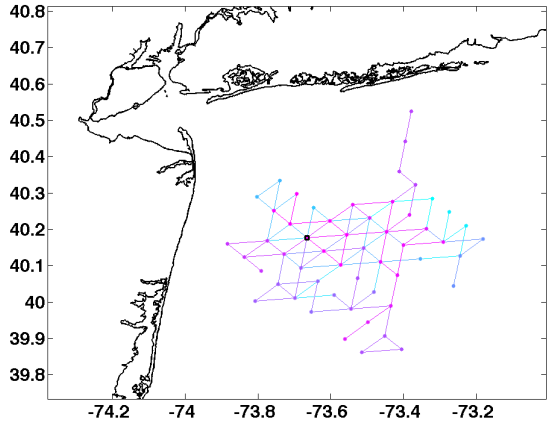

Simulated known paths (1-20) at 31 days.

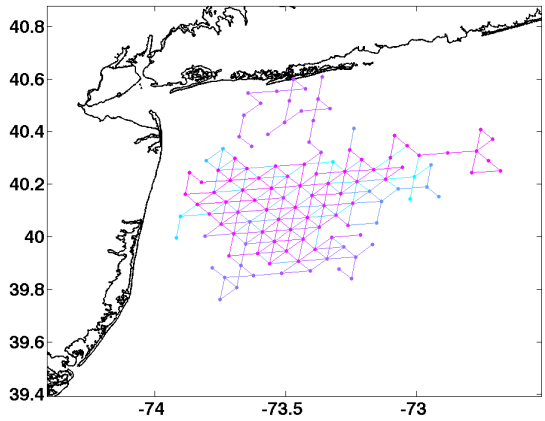

Simulated known paths (1-20) at 92 days.

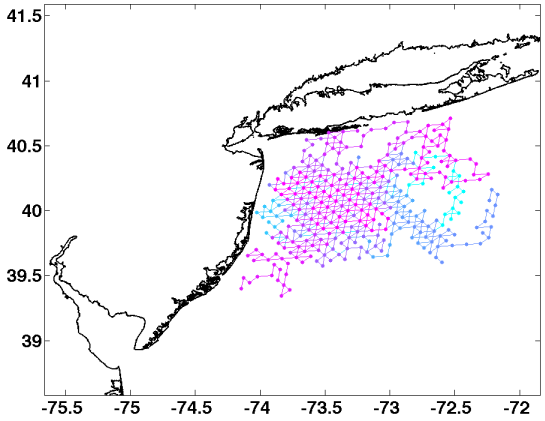

– Chapter 5 –

GENERAL CONCLUSIONS

Winter flounder is a commercially and recreationally important species that is in decline. While increasing ocean temperatures and overfishing have been blamed, management based on a poor understanding of life history and an inaccurate stock model is another possibility. This would be the case if winter flounder, historically known to migrate into estuaries in the fall/winter to spawn and back offshore in the spring, were also spawning offshore. The goal of this study was to enhance our understanding of winter flounder connectivity between estuarine and continental shelf habitats and thus address issues related to the decline of winter flounder and management of its habitats. Specifically I 1) evaluated the decline in abundance and the distributional response over time and to temperature using historical trawl data sets from the Northeastern United States (NMFS and NEAMAP) and off the coast of New Jersey (NJDEP), 2) I tagged and in some instances tracked winter flounder, and 3) created and tested models to determine connectivity between estuarine and continental shelf habitats for adults using state-of-the-art archival tags.

Limitations of this study are detailed in each chapter, yet an overarching problem is burial by winter flounder, here and in all previous studies. Burial hinders capture in trawl surveys but also inhibits detection in surveys for acoustic tags. In addition, most winter flounder are seasonally available in spatially separate areas, such as on the continental shelf and estuaries. Thus, sampling in only the major habitat type would inhibit understanding trends but also make for difficult decisions on where to actively search for tagged fish.

In analyzing the historic NEFSC, DEP, and NEAMAP bottom trawl groundfish surveys I found several trends. The bottom water temperature along with the spatial distribution of winter flounder in the southern Mid-Atlantic Bight has changed over the last few decades.

The relationship between bottom water temperature and winter flounder abundance was important but did not appear to have a direct influence on abundance. In addition, temperature did not correlate with the shifts in spatial distribution for most seasons. Winter flounder in this region did seasonally see an increase in bottom water temperature, but on average, remained within suitable temperature ranges. The shift in spatial distribution was predominately northward across most surveys for most seasons. Yet, trends differed across surveys and seasons, most likely due to the temporal and spatial differences between them, but this highlights the importance of interpreting data in more than one scale and season. There also appeared to be a range shift with fish no longer found as close to shore as they historically were but a shift in biomass occurred inshore for most surveys and most seasons. Only two surveys (NEFSC inshore and DEP) demonstrated a decrease in depth where winter flounder occurred. The geometric mean catch per tow decreased in these same two surveys, yet this was seasonal for the NEFSC inshore survey, which also saw a seasonal increase in geometric mean catch per tow.

In analyzing the current winter flounder population off of New Jersey, especially at the Mud Hole, part of the Hudson Valley shelf canyon, I was able to find mature animals that demonstrated different behaviors. The subsample of females captured were not far in the annual maturation cycle in September, but still within the range of median length at annual maturation in the Mid-Atlantic; therefore, it is safe to assume that the majority of fish I tagged were mature. Through the use of acoustic and archival tags, two behavioral subgroups were observed in the fall with two fish moving inshore and two offshore, yet connectivity associated with seasonal spawning was not observed at these time scales. Historic ALS (marker) tags confirmed the existence of small home ranges for the majority of tagged fish. Environmental data from the recovered archival tag enabled us to observe

habitat preference and bolster our state space models built to reconstruct tagged fish location.

I was successfully able to reconstruct a known simulated fish path using environmental data through the use of three state space models, and these methods could easily be modified for use of any archivally tagged Mid-Atlantic fish. Two types of state space models were tested, a data matching and simulation model (addressed in two separate ways) and a particle filter model. All three models were able to reconstruct a known simulated path at small time scales (11 and 31 days) with similar accuracy, yet at larger time scales (92 days) the particle filter model outperformed the data matching and simulation models. Additionally the particle filter model was able to reconstruct the most known simulated fish paths. In the future, I hope to obtain more recovered archival tags and further evaluate our particle filter SSM. In addition, I would also like to test other forms of SSMs such as Kalman filters and hidden Markov models to make sure I am using the best SSM for this tag data given the scope of the study.

While I was unable to work out estuary to ocean connectivity due to our low tag recovery rate, I have established a useful skill set to do so in the future. In addition, with a shift in distribution over the last few decades, communities have requested that southern estuaries (e.g., Cape May) be removed from the available winter flounder essential fish habitat to allow for winter dredging. With a better understanding of where winter flounder are, I might be able to influence management plans to sustain the winter flounder population in addition to commerce.

Literature Cited:

Able, K. W. 2005. A re-examination of fish estuarine dependence: Evidence for connectivity between estuarine and ocean habitats. Estuarine, Coastal and Shelf Science, 64: 5–17.

Able, K.W., and Fahay, M.P. 1998. The First Year in the Life of Estuarine Fishes in the Middle Atlantic Bight. Rutgers University Press, New Brunswick. 342 pp.

Able, K. W. and Fahay, M. P. 2010. Ecology of Estuarine Fishes: Temperate Waters of the Western North Atlantic. Johns Hopkins University Press, Baltimore, MD. 566 p.

Able, K. W., Grothues, T. M., Morson, J. M., and Coleman, K. E. 2014. Temporal variation in winter flounder recruitment at the southern margin of their range: is the decline due to increasing temperatures? ICES Journal of Marine Science, 71: 2186–2197.

Able, K. W. and Hagan, S.M. 1995 Fishes in the vicinity of Beach Haven Ridge: annual and seasonal patterns of abundance during the early 1970s. IMCS Technical Report 95-24.

Able, K. W., Witting, D. A., McBride, R. S., Rountree, R. A., and Smith, K. J. 1996 Fishes of polyhaline estuarine shores in Great Bay Little Egg Harbor, New Jersey: a case study of seasonal and habitat influences, pp. 335-353 In: Nordstrom, K.F. and C.T. Roman (eds.) Estuarine Shores: Evolution, Environments and Human Alterations. John Wiley & Sons, Chichester, England.

Ådlandsvik, B., Huse, G., and Michalsen, K. 2007. Introducing a method for extracting horizontal migration patterns from data storage tags. Hydrobiologia, 582: 187–197. http://link.springer.com/10.1007/s10750-006-0556-7 (Accessed 12 January 2015).

Albert, O., and Lambert, Y. 2011. Distinguishing pelagic and demersal swimming of deepwater flatfish by recording of body angles. American Fisheries Society Symposium: 1–22. http://bioeng.fisheries.org/proofs/tag/Albert.pdf (Accessed 12 January 2015).

Allison, E., Perry, A., Badjeck, M., Adger, W., Brown, K., Conway, D., Halls, A., Pilling, G. M., Reynolds, J. D., Andrew, N. L., and Dulvy, N. K. 2009. Vulnerability of national economies to the impacts of climate change on fisheries. Fish and Fisheries, 10: 173–196. http://doi.wiley.com/10.1111/j.1467-2979.2008.00310.x (Accessed 12 January 2015).

ALS. *American Littoral Society*. Aug. 2012. <http://www.littoralsociety.org/>

Andersen, K., Nielsen, A., Thygesen, U., Hinrichsen, H., and Neuenfeldt, S. 2007. Using the particle filter to geolocate Atlantic cod (Gadus morhua) in the Baltic Sea, with special emphasis on determining uncertainty. Can. J. Fish. Aquat. Sci., 64: 618–627. http://www.nrcresearchpress.com/doi/abs/10.1139/f07-037 (Accessed 12 January 2015).

Bell, R. J., Hare, J. A., Manderson, J. P., and Richardson, D. E. 2014a. Externally driven changes in the abundance of summer and winter flounder. ICES Journal of Marine Science, 71: 2416–2428.

Bell, R. J., Richardson, D. E., Hare, J. A., Lynch, P. D., and Fratantoni, P. S. 2014b. Disentangling the effects of climate, abundance, and size on the distribution of marine fish: an example based on four stocks from the Northeast US shelf. ICES Journal of Marine Science. doi: 10.1093/icesjms/fsu217.

Bigelow, H.B., and Schroeder W.C. 1953. Fishes of the Gulf of Maine. US. Fish Wildl. Serv. Fish. Bull. 53. 577p.

Bridge, E. S., Thorup, K., Bowlin, M. S., Chilson, P. B., Diehl, R. H., Fléron, R. W., Hartl, P., Kays, R., Kelly, J. F., Robinson, D., and Wikelski, M. 2011. Technology on the Move: Recent and Forthcoming Innovations for Tracking Migratory Birds. American Institute of Biological Sciences, 61: 689–698. http://www.jstor.org/stable/info/10.1525/bio.2011.61.9.7\nISI:000295711200007.

Briers, M., Doucet, A., and Maskell, S. 2010. Smoothing algorithms for state–space models. Ann. Inst. Stat. Math., 62: 61–89. http://link.springer.com/10.1007/s10463-009-0236-2 (Accessed 12 January 2015).

Brown, S., Buja, K., Jury, S., Monaco, M., and Banner, A. 2000. Habitat Suitability Index Models for Eight Fish and Invertebrate Species in Casco and Sheepscot Bays, Maine. North American Journal of Fisheries Management: 37–41. http://www.tandfonline.com/doi/abs/10.1577/1548-8675(2000)020%3C0408%3AHSIMFE%3E2.3.CO%3B2 (Accessed 13 January 2015).

Buckley, L., Collie, J., Kaplan, L., and Crivello, J. 2008. Winter flounder larval genetic population structure in Narragansett Bay, RI: recruitment to juvenile young-of-the-year. Estuaries and Coasts: 745–754. http://link.springer.com/article/10.1007/s12237-008-9065-4 (Accessed 12 January 2015).

Burton, M. P. M. 1991. Induction and reversal of the non-reproductive state in winter flounder, *Pseudopleuronectes americanus* Walbaum, by manipulating food availability. Journal of Fish Biology 39:909–910.

Burton, M. P., and Idler, D. R. 1984. The reproductive cycle in winter flounder, Pseudopleuronectes americanus (Walbaum). Can. J. Zool., 62: 2563–2567.

Burton, M. P., and Idler, D. R. 1987a. An experimental investigation of the non- reproductive, post-mature state in winter flounder. Journal of Fish Biology 30:643–650.

Burton, M. P., and Idler, D. R. 1987b. Variability of reproductive status in a population of *Pseudopleuronectes americanus*. Pages 207–212 *in* S. O. Kullander and B. Fernaholm, editors. Proceedings of the 5th Congress of European ichthyologists. Swedish Museum of Natural History, Stockholm.

Byrne, D.M., 1989. New Jersey trawl surveys. In: Azarovitz, T.R., McGurrin, J., Seagraves, R. (Eds.), Proceedings of a Workshop on Bottom Trawl Surveys, pp. 46-48.

Cadrin, S., and Moser, J. 2006. Partitioning On-bottom and Off-bottom Behavior: a case study with yellowtail flounder off New England. ICES CM: 1–26. http://nefsc.noaa.gov/cooperative-tagging/PDF/Cadrin_Moser2006.pdf (Accessed 12 January 2015).

Cadrin, S., and Westwood, A. 2004. The Use of Electronic Tags to Study Fish Movement: a case study with yellowtail flounder off New England. ICES CM: 1–34. http://scholar.google.com/scholar?hl=en&btnG=Search&q=intitle:The+Use+of+Electronic+Tags+to+Study+Fish+Movement:+a+case+study+with+yellowtail+flounder+off+New+England#0 (Accessed 12 January 2015).

Chambers, R., Rose, K., and Tyler, J. 1995. Recruitment and recruitment processes of winter flounder, Pleuronectes americanus, at different latitudes, implications of an individual-based simulation model. Netherlands Journal of Sea Research, 34: 19–43. http://www.sciencedirect.com/science/article/pii/0077757995900128 (Accessed 12 January 2015).

Chambers, R., Witting, D., and Lewis, S. 2001. Detecting critical periods in larval flatfish populations. Journal of Sea Research, 45. http://www.sciencedirect.com/science/article/pii/S1385110101000582 (Accessed 12 January 2015).

Chant, R. J., Curran, M. C., Able, K. W., and Glenn, S. M. 2000. Delivery of Winter Flounder (Pseudopleuronectes americanus) Larvae to Settlement Habitats in Coves Near Tidal Inlets. Estuarine, Coastal and Shelf Science, 51: 529–541. http://linkinghub.elsevier.com/retrieve/pii/S0272771400906942.

Cheung, W., Close, C., Lam, V., Watson, R., and Pauly, D. 2008. Application of macroecological theory to predict effects of climate change on global fisheries potential. Marine Ecology

Progress Series, 365: 187–197. http://www.int-res.com/abstracts/meps/v365/p187-197/ (Accessed 7 January 2015).

Cheung, W., Lam, V., Sarmiento, J. L., Kearney, K., Watson, R., and Pauly, D. 2009. Projecting global marine biodiversity impacts under climate change scenarios. Fish and Fisheries, 10: 235–251. http://doi.wiley.com/10.1111/j.1467-2979.2008.00315.x (Accessed 13 January 2015).

Cheung, W., Sarmiento, J., Dunne, J., Frolicher, T. L., Lam, V. W. Y., Palomares, M. L. D., Watson, R., and Pauly, D. 2013. Shrinking of fishes exacerbates impacts of global ocean changes on marine ecosystems. Nature Climate Change, 3: 254–258. Nature Publishing Group. http://www.nature.com/doifinder/10.1038/nclimate1691 (Accessed 13 January 2015).

Clark , S.H., and Brown, B.R. 1977. Changes in biomass of fin fishes and squids from the Gulf of Maine to Cape Hatteras, 1963–1974, as determined from research vessel survey data. Fish Bull US 75:1–21

Coates P., and Howe A. 1975. Winter Flounder Movements, Growth, and Mortality off Massachusetts. Transatlantic of The American Fisheries Society; 104(1):13. Available from: Supplemental Index, Ipswich, MA. Accessed February 21, 2015

Collette, B. B., and Klein-MacPhee, G. 2002. Righteye Flounders: Family Pleuronectidae. In: Bigelow and Schroeder's Fishes of the Gulf of Maine, 3rd edn, pp. 560-587. Ed. by B. B. Collette, and G. Klein- MacPhee. Smithsonian Institution Press, Washington. 748 pp.

Cooke, S. J., Midwood, J. D., Thiem, J. D., Klimley, P., Lucas, M. C., Thorstad, E. B., Eiler, J., Holbrook, C., and Ebner, B. C. 2013. Tracking animals in freshwater with electronic tags: past, present and future. Animal Biotelemetry, 1: 1–19. http://www.animalbiotelemetry.com/content/1/1/5.

Crawford, R. 1990. Winter flounder in Rhode Island coastal ponds. Rhode Island Sea Grant Publication RIU-G-90-001.

Crawford, R.E., and Carey, C.G. 1985. Retention of winter flounder within a Rhode Island salt pond. Estuaries 8: 217-227.

Crivello, J., Danila, D., and Lorda, E. 2004. The genetic stock structure of larval and juvenile winter flounder larvae in Connecticut waters of eastern Long Island Sound and estimations of larval entrainment. Journal of fish …: 62–76. http://onlinelibrary.wiley.com/doi/10.1111/j.0022-1112.2004.00424.x/full (Accessed 13 January 2015).

Curran, C. M., and Able, K. W. 2002. Annual Stability in the Use of Coves Near Inlets as Settlement Areas for Winter Flounder (Pseudopleuronectes americanus). Coastal and Estuarine Research Federation, 25: 227–234. http://www.jstor.org/stable/1353312.

DeCelles, G. R., and Cadrin, S. X. 2010. Movement patterns of winter flounder (Pseudopleuronectes americanus) in the southern Gulf of Maine: observations with the use of passive acoustic telemetry. Fishery Bulletin, 108: 408–420.

DeCelles, G. R., and Cadrin, S. X. 2011. An Interdisciplinary Assessment of Winter Flounder (Pseudopleuronectes americanus) Stock Structure. Journal of Northwest Atlantic Fishery Science, 43: 103–120. http://journal.nafo.int/43/decelles/8-decelles.pdf (Accessed 7 January 2015).

Despres-Patanjo, L. 1988. Twenty five years of fish surveys in the northwest Atlantic: The NMFS Northeast Fisheries Center's bottom trawl survey program. Marine Fisheries …, 50. http://spo.nmfs.noaa.gov/mfr504/mfr50418.pdf (Accessed 12 January 2015).

Diaz, R. J., Cutter, G. R., and Hobbs, C. H. 2004. Potential Impacts of Sand Mining Offshore of Maryland and Delaware: Part 2—Biological Considerations. Journal of Coastal Research, 20: 61–69.

Domeier, M., Kiefer, D., Nasby-Lucas, N., Wagschal, A., and O'Brien, F. 2005. Tracking Pacific bluefin tuna (Thunnus thynnus orientalis) in the northeastern Pacific with an automated algorithm that estimates latitude by matching sea-surface-temperature data from satellites with temperature data from tags on fish. Fishery Bulletin, 103: 292–306. http://aquaticcommons.org/9615/ (Accessed 12 January 2015).

Dowd, M., and Joy, R. 2011. Estimating behavioral parameters in animal movement models using a state-augmented particle filter. Ecology, 92: 568–575. http://www.esajournals.org/doi/abs/10.1890/10-0611.1 (Accessed 12 January 2015).

Drinkwater, K. 2005. The response of Atlantic cod (Gadus morhua) to future climate change. ICES Journal of Marine Science, 62: 1327–1337. http://icesjms.oxfordjournals.org/cgi/doi/10.1016/j.icesjms.2005.05.015 (Accessed 6 August 2014).

Dulvy, N. K., Rogers, S. I., Jennings, S., Stelzenmller, V., Dye, S. R., and Skjoldal, H. R. 2008. Climate change and deepening of the North Sea fish assemblage: a biotic indicator of warming seas. Journal of Applied Ecology, 45: 1029–1039. http://doi.wiley.com/10.1111/j.1365-2664.2008.01488.x (Accessed 1 October 2014).

Ehrenberg, J. E., and Steig, T. W. 2003. Improved technigues for studying the temporal and spatial behavior of fish in a fixed location. ICES Journal of Marine Science, 60: 700–760.

Evans, K., Lea, M., and Patterson, T. 2013. Recent advances in bio-logging science: Technologies and methods for understanding animal behaviour and physiology and their environments. Deep Sea Research Part II: Topical Studies in Oceanography, 88-89: 1–6. http://linkinghub.elsevier.com/retrieve/pii/S0967064512001865 (Accessed 12 January 2015).

Fairchild, E. A., Siceloff, L., Howell, W. H., Hoffman, B., and Armstrong, M. P. 2013. Coastal spawning by winter flounder and a reassessment of Essential Fish Habitat in the Gulf of Maine. Fisheries Research, 141: 118–129.

Fairchild, E., Sulikowski, J., Rennels, N., Howell, W. H., and Gurshin, C. W. 2008. Distribution of Winter Flounder, Pseudopleuronectes americanus, in the Hampton–Seabrook Estuary, New Hampshire: Observations from a Field Study. Estuaries and Coasts, 31: 1158–1173. http://link.springer.com/article/10.1007/s12237-008-9091-2 (Accessed 12 January 2015).

Flemming, J., Jonsen, I., Myers, R., and Field, C. 2010. Hierarchical state-space estimation of leatherback turtle navigation ability. PloS one, 5: e14245. http://www.pubmedcentral.nih.gov/articlerender.fcgi?artid=3010992&tool=pmcentrez&rendertype=abstract (Accessed 12 January 2015).

Fletcher, G. L. 1977. Circannual cycles of blood plasma freezing point and Na+ and Cl- concentrations in Newfoundland winter flounder (*Pseudopleuronectes americanus*) correlation with water temperature and photoperiod. Can. J. Zool. 55: 789-795

Fogarty, M. J., and Murawski, S. A. 1998. Large-Scale Disturbance and the Structure of Marine Systems: Fishery Impacts on Georges. Ecological Applications, 8: S6–S22.

Frank, K.T. and W.C. Leggett. 1983. Multispecies larval fish associations: Accident of adaptation? Can. J. Fish. Aquat. Sci. 40: 754-762.

Friedland, K. D., and Hare, J. A. 2007. Long-term trends and regime shifts in sea surface temperature on the continental shelf of the northeast United States. Continental Shelf Research, 27: 2313–2328.

Frisk, M., Jordaan, A., and Miller, T. 2014. Moving beyond the current paradigm in marine population connectivity: are adults the missing link? Fish and Fisheries: 242–254. http://onlinelibrary.wiley.com/doi/10.1111/faf.12014/full (Accessed 12 January 2015).

Fry, F. E. J. 1947. Effects of the environment on animal activity. The University of Toronto Press. http://scholar.google.com/scholar?hl=en&btnG=Search&q=intitle:EFFECTS+OF+THE+ENVIRONMENT+ON+ANIMAL+ACTIVITY#0 (Accessed 13 January 2015).

Fry, F. E. J. 1971. The effect of environmental factors on animal activity. In *Fish Physiology*, Vol. 6 (Hoar, W. S. & Randall, D. J., eds), New York, NY: Academic Press. pp. 1–98.

Garrison, L. P., and Link, J. S. 2000. Fishing effects on spatial distribution and trophic guild structure of the fish community in the Georges Bank region. ICES Journal of Marine Science, 57: 723–730.

Genner, M. J., Sims, D. W., Wearmouth, V. J., Southall, E. J., Southward, A. J., Henderson, P. A., and Hawkins, S. J. 2004. Regional climatic warming drives long-term community changes of British marine fish. Proc. R. Soc. Lond., 271: 655–61. http://www.pubmedcentral.nih.gov/articlerender.fcgi?artid=1691641&tool=pmcentrez&rendertype=abstract (Accessed 13 January 2015).

Gibson, M. R. 2013. Assessing the local population of winter founder with a two-era biomass dynamic model: a narrower view of Southern New England. Draft Report, RI Division of Fish and Wildlife.

Gift, J. J. and Westman, J. R. 1971. Responses of some estuarine fish to increasing thermal gradients. Dept. Environ. Sci., Rutgers University, New Brunswick, N.J., Mimeo

Goldberg, R., Phelan, B., Pereira, J., and Hagan, S. 2002. Variability in habitat use by young-of-the-year winter flounder, Pseudopleuronectes americanus, in three northeastern US estuaries. Estuaries. http://link.springer.com/article/10.1007/BF02691309 (Accessed 12 January 2015).

Graves, J. E., and Horodysky, A. Z. 2005. Application of pop-up satellite archival tag technology to estimate postrelease survival of white marlin (Tetrapturus albidus) caught on circle and straight-shank (' J ') hooks in the western North Atlantic recreational fishery . Fish. Bull., 103: 84–96.

Graves, J., Horodysky, A., and Latour, R. 2009. Use of pop-up satellite archival tag technology to study postrelease survival of and habitat use by estuarine and coastal fishes: An application to striped bass (Morone saxatilis). Fishery Bulletin, 107: 373–383. http://aquaticcommons.org/8793/ (Accessed 12 January 2015).

Gröger, J., Rountree, R., Thygesen, U., Jones, D., Martins, D., Xu, Q., and Rothschild, B. 2007. Geolocation of Atlantic cod (Gadus morhua) movements in the Gulf of Maine using tidal information. Fisheries Oceanography, 16: 317–335. http://doi.wiley.com/10.1111/j.1365-2419.2007.00433.x (Accessed 12 January 2015).

Grosslein, M. D. 1969. Groundfish Survey Methods. Woods Hole Laboratory Reference, 69-2: 1–34.

Grothues, T.M. 2009. A Review of Acoustic Telemetry Technology and a Perspective on its Diversification Relative to Coastal Tracking Arrays

Grothues, T. M., Able, K. W., and Pravatiner, J. H. 2012. Winter flounder (Pseudopleuronectes americanus Walbaum) burial in estuaries: Acoustic telemetry triumph and tribulation. Journal of Experimental Marine Biology and Ecology, 438: 125–136.

Grothues, T. M. and Bochenek, E. A. 2010. Winter Flounder Telemetry in the Navesink River Estuary, New Jersey, During the 2009 Spawning Season. Final Report to New Jersey Department of Transportation Office of Maritime Resources I Boat New Jersey

Grothues, T. M., and Davis, W. C. 2013. Sound pressure level weighting of the center of activity method to approximate sequential fish positions from acoustic telemetry. Canadian Journal Of Fisheries And Aquatic Sciences, 70: 1359–1371. <Go to ISI>://WOS:000323758200010.

Grothues, T. M., Dobarro, J., and Eiler, J. 2010. Collecting, interpreting, and merging fish telemetry data from an AUV: Remote sensing from an already remote platform. 2010 IEEE/OES Autonomous Underwater Vehicles, AUV 2010.

Grusha, D., and Patterson, M. 2005. Quantification of drag and lift imposed by pop-up satellite archival tags and estimation of the metabolic cost to cownose rays (Rhinoptera bonasus). Fishery Bulletin, 103: 63–70. http://aquaticcommons.org/9641/ (Accessed 12 January 2015).

Harden Jones, F.R., 1968. Fish Migration. St. Martin's Press, New York.

Hare, J. *Ecology of the Northeast U.S. Continental Shelf, Oceanography*. Feb. 2014. <http://www.nefsc.noaa.gov/ecosys/ecology/Oceanography/>

Hare, J. A., Alexander, M. A., Fogarty, M. J., Williams, E. H., and Scott, J. D. 2010. Forecasting the dynamics of a coastal fishery species using a coupled climate-population model. Ecological Applications, 20: 452–464.

Hare, J. A., and Able, K. W. 2007. Mechanistic links between climate and fisheries along the east coast of the United States: explaining population outbursts of Atlantic croaker (Micropogonias. Fisheries Oceanography, 16: 31–45. http://doi.wiley.com/10.1111/j.1365-2419.2006.00407.x (Accessed 12 January 2015).

He, P. 2003. Swimming behaviour of winter flounder (Pleuronectes americanus) on natural fishing grounds as observed by an underwater video camera. Fisheries Research, 60: 507–514. http://www.sciencedirect.com/science/article/pii/S0165783602000863 (Accessed 12 January 2015).

Heffernan, O. 2004. Use of data storage tags to quantify vertical movements of cod: effects on acoustic measures. ICES Journal of Marine Science, 61: 1062–1070. http://icesjms.oxfordjournals.org/cgi/doi/10.1016/j.icesjms.2004.07.003 (Accessed 12 January 2015).

Hoolihan, J., and Luo, J. 2011. Vertical habitat use of sailfish (Istiophorus platypterus) in the Atlantic and eastern Pacific, derived from pop-up satellite archival tag data. Fisheries …, 20: 192–205. http://doi.wiley.com/10.1111/j.1365-2419.2011.00577.x (Accessed 12 January 2015).

Howe, A. B., Coates, P. G., and Pierce, D. E. 1976. Winter flounder estuarine year-class abundance, mortality, and recruitment. Transactions of the American Fisheries Society 105: 647-657.

Howell, P.T., and Molnar, D.R. 1995. A study of marine recreational fisheries in Connecticut. Inshore survey of juvenile winter flounder. Job 3. p. 55-78. Federal Aid to Sport Fish Restoration F54R. Final Report. March 1, 1989-Febuary 28, 1995. Connecticut Dep. Enviro. Prot. Fish. Div. Old Lyme, CT.

Hunter, E., Metcalfe, J., Holford, B., Arnold, G., and Aldridge, J. 2004. Geolocation of free-ranging fish on the European continental shelf as determined from environmental variables. Marine Biology, 144: 787–798. http://link.springer.com/article/10.1007/s00227-002-0984-5 (Accessed 12 January 2015).

Hunter, E., Metcalfe, J., and Reynolds, J. 2003. Migration route and spawning area fidelity by North Sea plaice. Proc. R. Soc. Lond. B, 270: 2097–2103. http://rspb.royalsocietypublishing.org/content/270/1529/2097.short (Accessed 12 January 2015).

Hutchings, J. A., and Myers, R. A. 1994. Timing of cod reproduction - Interannual variability and the influence of temperature. Marine Ecology Progress Series, 108: 21–32.

Ishida, Y., Yano, A., Ban, M., and Ogura, M. 2001. Vertical movement of a chum salmon Oncorhynchus keta in the western North Pacific Ocean as determined by a depth-

recording archival tag. Fisheries Science, 67: 1030–1035. http://onlinelibrary.wiley.com/doi/10.1046/j.1444-2906.2001.00358.x/full (Accessed 12 January 2015).

Jeffries, H.P., and W.C. Johnson. 1974. Seasonal distributions of bottom fishes in the Narragansett Bay area: seven-year variations in the abundance of winter flounder (*Pseudopleuronectes americanus*). J. Fish. Res. Board Can. 31: 1057-1066

Jellyman, D., and Tsukamoto, K. 2002. First use of archival transmitters to track migrating freshwater eels Anguilla dieffenbachii at sea. Marine Ecology Progress Series, 233: 207–215.

Joaquim, N., Wagner, G. N., and Gamperl, A. K. 2004. Cardiac function and critical swimming speed of the winter flounder (Pleuronectes americanus) at two temperatures. Comparative Biochemistry and Physiology, 138: 277–285.

Jonsen, I., Basson, M., and Bestley, S. 2013. State-space models for bio-loggers: A methodological road map. Deep Sea Research II, 88-89: 34–46. Elsevier. http://linkinghub.elsevier.com/retrieve/pii/S096706451200094X (Accessed 12 January 2015).

Kalman, R. E. 1960. A New Approach to Linear Filtering and Prediction Problems. Transactions of the ASME-Journal of Basic Engineering, 82: 35–45. http://fluidsengineering.asmedigitalcollection.asme.org/article.aspx?articleid=1430402.

Kämpf, J., Payne, N., and Malthouse, P. 2010. Marine Connectivity in a Large Inverse Estuary. Journal of Coastal Research, 26: 1047–1056.

Keller, A. A., and Klein-MacPhee, G. 2000. Impact of elevated temperature on the growth, survival, and trophic dynamics of winter flounder larvae: A mesocosm study. Canadian Journal of Fisheries and Aquatic Sciences 57: 2382-2392.

Kelley, S. W., Ramsey, J. S., and Byrnes, M. R. 2004. Evaluating Shoreline Response to Offshore Sand Mining for Beach Nourishment. Journal of Coastal Research, 20: 89–100.

Kemp, P. F., Falkowski, P. G., Flagg, C. N., Phoel, W. C., Smith, S. L., Wallace, D. W. R., and Wirick, C. D. 1994. Modeling vertical oxygen and carbon flux during stratified spring and summer conditions on the continental shelf, Middle Atlantic Bight, eastern U.S.A. Deep Sea Research Part II: Topical Studies in Oceanography, 41: 629–655.

Klaas, M., Briers, M., and Freitas, N. De. 2006. Fast particle smoothing: If I had a million particles. Proceedings of the 23rd International Conference on Machine Learning, Pittsburgh, PA, 2006: 481–488.http://portal.acm.org/citation.cfm?id=1143844.1143905\npapers2://publication/uuid/55BDE85E-A59C-4191-867A-5DBB276B2B9E (Accessed 12 January 2015).

Klein-MacPhee, G. 2002. Righteye Flounders: Family pleuronectidae. In Fishes of the Gulf of Maine. 3rd ed. Edited by B.B. Collette and G. Klein-MacPhee. Smithsonian Institution Press, Washington, D.C.

Kraus, R. T., and Secor, D. H. 2004. Dynamics of white perch Morone americana population contingents in the Patuxent River estuary, Maryland, USA. Marine Ecology Progress Series, 279: 247–259.

Le Bris, A., Fréchet, A., Galbraith, P., and Wroblewski, J. 2013. Evidence for alternative migratory behaviors in the northern Gulf of St Lawrence population of Atlantic cod (Gadus morhua L.). ICES Journal of Marine Science.

Liebhold, A., Koenig, W., and Bjørnstad, O. 2004. Spatial synchrony in population dynamics. Annu. Rev. Eco. Evol. Syst., 35: 467–490. http://www.annualreviews.org/doi/abs/10.1146/annurev.ecolsys.34.011802.132516 (Accessed 12 January 2015).

Link, J., Nye, J., and Hare, J. 2011. Guidelines for incorporating fish distribution shifts into a fisheries management context. Fish and Fisheries, 12: 461–469. http://doi.wiley.com/10.1111/j.1467-2979.2010.00398.x (Accessed 12 January 2015).

Lobell, M.J. 1939. A biological survey of the salt waters of Long Island, 1938. Report on certain fishes. Winter flounder (*Pseudopleuronectes americanus*). Supplement to the 28th Annual Report of the New York State Conservation Department, Part 1:63-96

Loher, T., and Blood, C. 2009. Seasonal dispersion of Pacific halibut (Hippoglossus stenolepis) summering off British Columbia and the US Pacific Northwest evaluated via satellite archival tagging. Canadian Journal of Fisheries and Aquatic Sciences, 66: 1409–1422. http://www.nrcresearchpress.com/doi/abs/10.1139/F09-093 (Accessed 13 January 2015).

Loher, T., and Rensmeyer, R. 2011. Physiological responses of Pacific halibut, Hippoglossus stenolepis, to intracoelomic implantation of electronic archival tags, with a review of tag implantation. Reviews in Fish Biology and Fisheries, 21: 97–115. http://link.springer.com/10.1007/s11160-010-9192-4 (Accessed 12 January 2015).

Lucey, S., and Nye, J. 2010. Shifting species assemblages in the northeast US continental shelf large marine ecosystem. Marine Ecology Progress Series, 415: 23–33. http://www.pices.int/publications/presentations/2010-Climate-Change/B2/B2-6198-Lucey_Nye.pdf (Accessed 12 January 2015).

Maa, J. P.-Y., Hobbs, C. H., Kim, S. C., and Wei, E. 2004. Potential Impacts of Sand Mining Offshore of Maryland and Delaware: Part 1-Impacts of Physical Oceanographic Processes. Journal of Coastal Research, 20: 44–60.

MacPhee, G.K. (Ed.), 1978. Synopsis of biological data for the winter flounder, *Pseudopleuronectes americanus* (Walbaum). NOAA (National Oceanographic Atmospheric Administration) Technical Report. NMFS (National Marine Fisheries Service), Circular 414.

Metcalfe, J. 2006. Fish population structuring in the North Sea: understanding processes and mechanisms from studies of the movements of adults. Journal of Fish Biology, 69: 48–65. http://doi.wiley.com/10.1111/j.1095-8649.2006.01275.x (Accessed 12 January 2015).

Maddock, D. M., and M. P. M. Burton. 1994. Some effects of starvation on the lipid and skeletal muscle layers of the winter flounder, *Pleuronectes americanus*. Canadian Journal of Zoology 72:1672–1679.

Manderson, J. 2006. Dynamics of early juvenile winter flounder predation risk on a North West Atlantic estuarine nursery ground. Marine Ecology Progress Series, 328: 249–265. http://scholarworks.umass.edu/nrc_faculty_pubs/197/ (Accessed 12 January 2015).

Manderson, J. 2008. The spatial scale of phase synchrony in winter flounder (Pseudopleuronectes americanus) production increased among southern New England nurseries in the 1990s. Canadian Journal of Fisheries and Aquatic Sciences, 351: 340–351. http://www.nrcresearchpress.com/doi/abs/10.1139/f07-169 (Accessed 12 January 2015).

Manderson, J. P., Phelan, B. A., Stoner, a. W., and Hilbert, J. 2000. Predator-prey relations between age-1+ summer flounder (Paralichthys dentatus, linnaeus) and age-0 winter flounder (Pseudopleuronectes americanus, walbaum): Predator diets, prey selection, and effects of sediments and macrophytes. Journal of Experimental Marine Biology and Ecology, 251: 17–39.

Manderson, J., and Pessutti, J. 2004. Shallow water predation risk for a juvenile flatfish (winter flounder; Pseudopleuronectes americanus, Walbaum) in a northwest Atlantic

estuary. Journal of Experimental Marine Biology and Ecology, 304: 137–157. http://www.sciencedirect.com/science/article/pii/S0022098103005768 (Accessed 12 January 2015).

Mayo, R. K., and Terceiro, M. 2005. Assessment of 19 Northeast Groundfish Stocks through 2004 2005 Groundfish Assessment Review Meeting (2005 GARM), Northeast Fisheries Science Center , Woods Hole , Massachusetts , 15-19 August 2005. U.S. Dep. Commer. Northeast Fish. Sci. Cent. Ref. Doc., 05-13: 1–499.

McBride, R., Wuenschel, M., Nitschke, P., Thornton, G., and King, J. R. 2013. Latitudinal and stock-specific variation in size-and age-at-maturity of female winter flounder , *Pseudopleuronectes americanus*, as determined with gonad histology. Journal of Sea Research, 75: 41–51. doi:10.1016/j.seares.2012.04.005 (Accessed 12 January 2015).

McCay, B. J. 2012. Anthropology: Shifts in fishing grounds. Nature Climate Change, 2: 840–841. Nature Publishing Group. http://www.nature.com/doifinder/10.1038/nclimate1765 (Accessed 5 January 2015).

McCracken, F.D, 1963. Seasonal movements of the winter flounder, *Pseudopleuronectes americanus* (Walbaum) on the Atlantic coast. J. Fish. Res. Board Can. 20: 551-586.

McElroy, W., Wuenschel, M., and Press, Y. 2013. Differences in female individual reproductive potential among three stocks of winter flounder, *Pseudopleuronectes americanus*. Journal of Sea Research, 75: 52–61. Elsevier B.V. http://dx.doi.org/10.1016/j.seares.2012.05.018 (Accessed 12 January 2015).

Metcalfe, J. 2006. Fish population structuring in the North Sea: understanding processes and mechanisms from studies of the movements of adults. Journal of Fish Biology, 69: 48–65. http://doi.wiley.com/10.1111/j.1095-8649.2006.01275.x (Accessed 12 January 2015).

Metcalfe, J., and Arnold, G. 1997. Tracking fish with electronic tags. Nature, 387: 665–666.

Miles, T., Glenn, S. M., and Schofield, O. 2013. Temporal and spatial variability in fall storm induced sediment resuspension on the Mid-Atlantic Bight. Continental Shelf Research, 63: S36–S49. Elsevier. http://dx.doi.org/10.1016/j.csr.2012.08.006.

Mills, K., Pershing, A., and Brown, C. 2013. Fisheries Management in a Changing Climate Lessons from the 2012 ocean Heat Wave in the Northwest Atlantic. Oceanography, 26: 191–195. http://dx.doi.org/10.5670/oceanog.2011.80. (Accessed 12 January 2015).

Mueter, F., and Litzow, M. 2008. Sea ice retreat alters the biogeography of the Bering Sea continental shelf. Ecological Applications, 18: 309–320. http://www.esajournals.org/doi/abs/10.1890/07-0564.1 (Accessed 12 January 2015).

Murawski, S. A. 1993. Climate change and marine fish distributions: forecasting from historical analogy. Transactions of the American Fisheries Society, 122: 647–658. http://www.tandfonline.com/doi/abs/10.1577/1548-8659(1993)122%3C0647%3ACCAMFD%3E2.3.CO%3B2 (Accessed 12 January 2015).

Nairn, R., Johnson, J. A., Hardin, D., and Michel, J. 2004. A Biological and Physical Monitoring Program to Evaluate Long-term Impacts from Sand Dredging Operations in the United States Outer Continental Shelf. Journal of Coastal Research, 20: 126–137.

NEFSC. *NEAMAP – Mid Atlantic @ VIMS.* 2006. Web. Feb. 2014. <http://www.nefsc.noaa.gov/groundfish/meetings/neamap.pdf>

Nelson, D., Miller, J., Rusanowsky, D., Greig, R.A., Sennefelder, G.R., Mercaldo-Allen, R., Kuropat, C., Gould, E., Thurberg, F.P., and Calabrese, A. 1991. Comparative Reproductive Success of Winter Flounder in Long Island Sound: A Three-Year Study (Biology, Biochemistry, and Chemistry). Estuaries. 318.

Neuenfeldt, S., Hinrichsen, H., Nielsen, A., and Andersen, K. 2007. Reconstructing migrations of individual cod (Gadus morhua L.) in the Baltic Sea by using electronic data storage tags. Fisheries Oceanography, 16: 526–535. http://www.blackwell-synergy.com/doi/abs/10.1111/j.1365-2419.2007.00458.x (Accessed 12 January 2015).

Nichol, D., and Somerton, D. 2009. Evidence of the selection of tidal streams by northern rock sole (Lepidopsetta polyxystra) for transport in the eastern Bering Sea. Fishery Bulletin, 107: 221–234. http://aquaticcommons.org/8804/ (Accessed 13 January 2015).

Nielsen, A., Bigelow, K., Musyl, M., and Sibert, J. 2006. Improving light-based geolocation by including sea surface temperature. Fisheries Oceanography, 15: 314–325. http://doi.wiley.com/10.1111/j.1365-2419.2005.00401.x (Accessed 13 January 2015).

Nielsen, A., and Sibert, J. R. 2007. State–space model for light-based tracking of marine animals. Canadian Journal of Fisheries and Aquatic Sciences, 64: 1055–1068.

Nissling, a, Westin, L., and Hjerne, O. 2002. Reproductive success in relation to salinity for three flatfish species, dab (Limanda limanda), plaice (Pleuronectes platessa), and flounder (Pleuronectes flesus), in the brackish water Baltic Sea. Ices Journal of Marine Science, 59: 93–108. <Go to ISI>://000173358800008.

Nissling, A., and Dahlman, G. 2010. Fecundity of flounder, Pleuronectes flesus, in the Baltic Sea - Reproductive strategies in two sympatric populations. Journal of Sea Research, 64: 190–198. Elsevier B.V. http://dx.doi.org/10.1016/j.seares.2010.02.001.

Nye, J. A., Baker, M. R., Bell, R., Kenny, A., Kilbourne, K. H., Friedland, K. D., Martino, E., *et al.* 2014. Ecosystem effects of the Atlantic Multidecadal Oscillation. Journal of Marine Systems, 133: 103–116. Elsevier B.V. http://linkinghub.elsevier.com/retrieve/pii/S0924796313000316 (Accessed 25 November 2014).

Nye, J. A., Bundy, A., Shackell, N., Friedland, K. D., and Link, J. S. 2010. Coherent trends in contiguous survey time-series of major ecological and commercial fish species in the Gulf of Maine ecosystem. ICES Journal of Marine Sciences, 67: 26–40.

Nye, J. A., Link, J. S., Hare, J. A., and Overholtz, W. J. 2009. Changing spatial distribution of fish stocks in relation to climate and population size on the Northeast United States continental shelf. Marine Ecology Progress Series, 393: 111–129. http://www.int-res.com/abstracts/meps/v393/p111-129/ (Accessed 5 December 2014).

Oberhauser, K., and Peterson, a T. 2003. Modeling current and future potential wintering distributions of eastern North American monarch butterflies. Proceedings of the National Academy of Sciences of the United States of America, 100: 14063–8. http://www.pubmedcentral.nih.gov/articlerender.fcgi?artid=283546&tool=pmcentrez&rendertype=abstract (Accessed 7 January 2015).

O'Brien, L., J. Burnett, and R.K. Mayo. 1993. Maturation of nineteen species of finfish off the northeast coast of the United States, 1985-1990. NOAA Tech. Report. NMFS 133. 66.

Olla, L.B., R. Wicklund & S. Wilk. 1969. Behavior of winter flounder in a natural habitat. Trans. Amer. Fish. Soc. 98: 717–720.

Overholtz, W. J., Hare, J. A., and Keith, C. M. 2011. Impacts of Interannual Environmental Forcing and Climate Change on the Distribution of Atlantic Mackerel on the U.S. Northeast Continental Shelf. Marine and Coastal Fisheries, 3: 219–232. http://www.tandfonline.com/doi/abs/10.1080/19425120.2011.578485 (Accessed 12 January 2015).

Oviatt, C. A. 2004. The changing ecology of temperate coastal waters during a warming trend. 714 Estuaries 27(6): 895-904.

Patterson, T., and Thomas, L. 2008. State–space models of individual animal movement. Trends in Ecology & Evolution, 23: 87–94. http://www.ncbi.nlm.nih.gov/pubmed/18191283 (Accessed 13 January 2015).

Pearcy, W.G. 1962. Ecology of an estuarine population of winter flounder, *Pseudopleuronectes americanus* (Walbaum). Parts I-IV. Bull. Bingham Oceanogr. Collection. 18(1): 5-78.

Pedersen, M., Righton, D., Thygesen, U., Andersen, K., and Madsen, H. 2008. Geolocation of North Sea cod (Gadus morhua) using hidden Markov models and behavioural switching. Can. J. Fish. Aquat. Sci., 65: 2367–2377. http://www.nrcresearchpress.com/doi/abs/10.1139/F08-144 (Accessed 13 January 2015).

Pedersen, M. W., Berg, C. W., and Thygesen, U. H. 2011. Estimation methods for nonlinear state-space models in ecology. Ecological Modelling, 222: 1394–1400. Elsevier B.V. http://linkinghub.elsevier.com/retrieve/pii/S0304380011000299 (Accessed 13 January 2015).

Pereira, J. J., Goldberg, R., Ziskowski, J. J., Berrien, P. L., Morse, W. W., and Johnson, D. L. 1999. Essential fish habitat source document: Winter Flounder, *Pseudopleuronectes amicanus*, Life History and Habitat Characteristics.

Perlmutter, A. 1947. The blackback flounder and its fishery in New England and New York. Bull. Bingham Oceanogr. Collect. 11(2): 92 p.

Perry, A., Low, P., Ellis, J., and Reynolds, J. 2005. Climate change and distribution shifts in marine fishes. Science, 308: 1912–1915. http://www.ncbi.nlm.nih.gov/entrez/query.fcgi?db=pubmed&cmd=Retrieve&dopt=AbstractPlus&list_uids=000230120000041\nhttp://links.isiglobalnet2.com/gateway/Gateway.cgi?GWVersion=2&SrcAuth=mekentosj&SrcApp=Papers&DestLinkType=FullRecord&DestApp=WOS&KeyUT=0002.

Phelan, B., Manderson, J., Stoner, A., and Bejda, A. 2001. Size-related shifts in the habitat associations of young-of-the-year winter flounder (*Pseudopleuronectes americanus*): field observations and laboratory experiments with sediments and prey. Journal of Experimental Marine Biology and Ecology, 257: 297–315. http://linkinghub.elsevier.com/retrieve/pii/S0022098100003403.

Phelan, B. A. 1992. Winter Flounder Movements in the Inner New York Bight. Transactions of the American Fisheries Society, 121: 777–784.

Phelan, B. A., Goldberg, R., Bejda, A. J., Pereira, J., Hagan, S., Clark, P., Studholme, A. L., Calabrese, A., Able, K. W. 2000. Estuarine and habitat-related differences in growth rates of young-of- the-year winter flounder (*Pseudopleuronectes americanus*) and tautog (Tautoga onitis) in three northeastern US estuaries. Journal of Experimental Marine Biology and Ecology, 247: 1–28.

Pinsky, M. M. L., and Fogarty, M. 2012. Lagged social-ecological responses to climate and range shifts in fisheries. Climate Change, 115: 883–891. http://link.springer.com/10.1007/s10584-012-0599-x (Accessed 13 January 2015).

Pinsky, M. M. L., Worm, B., Fogarty, M. M. J., Sarmiento, J. L., and Levin, S. A. 2013. Marine taxa track local climate velocities. Science, 341: 1239. http://www.sciencemag.org/content/341/6151/1239.short (Accessed 15 July 2014).

Pörtner, H., and Knust, R. 2007. Climate Change Affects Marine Fishes Through the Oxygen Limitation of Thermal Tolerance. Science, 315: 95–97. http://www.sciencemag.org/content/315/5808/95.short (Accessed 12 January 2015).

Pravatiner, J. H. 2010. Estuarine fabitat and behavior of winter flounder (Peudopleuronectes americanus): an approach using acoustic telemetry in Barnegat Bay, NJ, USA.

Press, Y. K., McBride, R. S., and Wuenschel, M. J. 2014. Time course of oocyte development in winter flounder *Pseudopleuronectes americanus* and spawning seasonality for the Gulf of Maine , Georges Bank and southern New England stocks. Journal of fish biology, 85: 421–45. http://www.ncbi.nlm.nih.gov/pubmed/24942788 (Accessed 7 January 2015).

Radlinski, M. K., Sundermeyer, M. A., Bisagni, J. J., and Cadrin, S. X. 2013. Spatial and temporal distribution of Atlantic mackerel (Scomber scombrus) along the nrotheast coast of the United States, 1985-1999. ICES Journal of Marine Science, 70: 1151–1161.

Ray, G. C. 2005. Connectivities of estuarine fishes to the coastal realm. Estuarine, Coastal and Shelf Science, 64: 18–32.

Rice, J. A., Quinlan, J. A., Nixon, S. W., Hettler, W. F. J., Warlen, S. M., and Stegmann, P. M. 1999. Spawning and transport dynamics of Atlantic menhaden: inferences from characteristics of immigrating larvae and predictions of a hydrodynamic model. Fisheries Oceanography, 8: 93–110.

Rideout, R. M., Rose, G. a., and Burton, M. P. M. 2005. Skipped spawning in female iteroparous fishes. Fish and Fisheries, 6: 50–72.

Rideout, R. M., and Tomkiewicz, J. 2011. Skipped spawning in fishes: more common than you might think. Marine and Coastal Fisheries: Dynamics, Management, and Ecosystem Science, 3: 176–189.

Righton, D., and Mills, C. 2008. Reconstructing the movements of free-ranging demersal fish in the North Sea: a data-matching and simulation method. Marine Biology, 153: 507–521. http://link.springer.com/10.1007/s00227-007-0818-6 (Accessed 13 January 2015).

Rikardsen, A., and Thorstad, E. 2006. External attachment of data storage tags increases probability of being recaptured in nets compared to internal tagging. Journal of fish biology: 963–968. http://onlinelibrary.wiley.com/doi/10.1111/j.0022-1112.2006.00974.x/full (Accessed 12 January 2015).

Rose, G. 2005. On distributional responses of North Atlantic fish to climate change. ICES Journal of Marine Science, 62: 1360–1374. http://icesjms.oxfordjournals.org/cgi/doi/10.1016/j.icesjms.2005.05.007 (Accessed 13 January 2015).

Russell, S. and P. Norvig. 2010. Artificial Intelligence: A Modern Approach. Prentice-Hall Series in Artificial Intelligence. Prentice-Hall Englewood Cliffs, NJ. 3rd edition. pp. 510-648

Sagarese, S., and Frisk, M. 2011. Movement Patterns and Residence of Adult Winter Flounder within a Long Island Estuary. Marine and Coastal Fisheries: 37–41. http://www.tandfonline.com/doi/abs/10.1080/19425120.2011.603957 (Accessed 13 January 2015).

Sailia, S.B. 1961. A study of winter flounder movements. Limnol. Oceanogr. 6: 292-298.

Scarlett, P. G. 1991a. Relative abundance of winter flounder (*Pseudopleuronectes americanus*) in nine inshore areas of New Jersey. Bulletin of the New Jersey Academy of Science 36(2): 1-5.

Scarlett, P.G. 1991b. Temporal and spatial distribution of winter flounder, *Pseudopleuronectes americanus*, spawning in the Navesink and Shrewsbury Rivers, New Jersey. New Jersey Dep. Environ. Prot. Div. Fish, Game and Wildl. Mar. Fish. Adm. Bur. Of Mar. Fish., Trenton, NJ. 12p.

Scarlett, P. G., and Allen, R. L. 1992. Temporal and spatial distribution of winter flounder (Pleuronectes americanus) spawning in Manasquan River, New Jersey. Bulletin of the New Jersey Academy of Science 37(1): 13-17.

Schaefer, K., and Fuller, D. 2010. Vertical movements, behavior, and habitat of bigeye tuna (Thunnus obesus) in the equatorial eastern Pacific Ocean, ascertained from archival tag data. Marine biology, 157: 2625–2642. http://link.springer.com/10.1007/s00227-010-1524-3 (Accessed 13 January 2015).

Schick, R., Loarie, S., and Colchero, F. 2008. Understanding movement data and movement processes: current and emerging directions. Ecology Letters, 11: 1338–1350. http://www.ncbi.nlm.nih.gov/pubmed/19046362 (Accessed 13 January 2015).

Secor, D. H. 1999. Specifying divergent migrations in the concept of stock: The contingent hypothesis. *In* Fisheries Research, pp. 13–34.

Secor, D. H. 2007. The year-class phenomenon and the storage effect in marine fishes. Journal of Sea Research, 57: 91–103.

Secor, D. H., and Rooker, J. R. 2005. Connectivity in the life histories of fishes that use estuaries. Estuarine, Coastal and Shelf Science, 64: 1–3.

Seitz and Nielsen. 2007. Web. Feb. 2014 <http://www.nps.gov/glba/learn/nature/upload/Seitz-2013-Highlight-FINAL-web.pdf>

Sheaves, M. 2009. Consequences of ecological connectivity: The coastal ecosystem mosaic. Marine Ecology Progress Series, 391: 107–115.

Sibert, J., Musyl, M., and Brill, R. 2003. Horizontal movements of bigeye tuna (Thunnus obesus) near Hawaii determined by Kalman filter analysis of archival tagging data. Fisheries Oceanography, 12: 141–151. http://onlinelibrary.wiley.com/doi/10.1046/j.1365-2419.2003.00228.x/full (Accessed 13 January 2015).

Sims, D., and Wearmouth, V. 2004. Low-temperature-driven early spawning migration of a temperate marine fish. Journal of Animal Ecology, 73: 333–341. http://onlinelibrary.wiley.com/doi/10.1111/j.0021-8790.2004.00810.x/full (Accessed 13 January 2015).

Sogard, S.M. and Able, K. W. 1994. Diel variation in immigration of fishes and decapod crustaceans to artificial seagrass habitat. Estuaries 17(3): 622-630.

Sogard, S., Able, K., and Hagan, S. 2001. Long-term assessment of settlement and growth of juvenile winter flounder (*Pseudopleuronectes americanus*) in New Jersey estuaries. Journal of Sea Research, 45. http://www.sciencedirect.com/science/article/pii/S138511010100048X (Accessed 13 January 2015).

Stansbury, A., Gotz, T., Deecke, V., and Janik, V. 2015. Grey seals use anthropogenic signals from acoustic tags to locate fish: evidence from a simulated foraging task. Proc. R. Soc. B, 282: 1–9. http://classic.rspb.royalsocietypublishing.org/content/282/1798/20141595.abstract (Accessed 12 January 2015).

Stoner, A., Manderson, J. P., and Pessutti, J. P. 2001. Spatially explicit analysis of estuarine habitat for juvenile winter flounder: combining generalized additive models and geographic information systems. Marine Ecology Progress Series, 213: 253–271. ftp://205.193.112.140/pub/ocean/Shackell_Nancy/ACCASP_HabitatAvailability/stonerGAMSGIS.pdf (Accessed 13 January 2015).

Stoner, A. W., Bejda, A. J., Manderson, J. P., Phelan, B. A., Stehlik, L. L., and Pessutti, J. P. 1999. Behavior of winter flounder, pseudopleuroonectes americanus, during the

reproductive season: labratory and field observations on spawning, feeding, and locomotion. Fishery Bulletin, 97.

Ter Hofstede, R., Hiddink, J., and Rijnsdorp, A. 2010. Regional warming changes fish species richness in the eastern North Atlantic Ocean. Marine Ecology Progress Series, 414: 1–9. http://www.scopus.com/inward/record.url?eid=2-s2.0-77957729376&partnerID=tZOtx3y1 (Accessed 13 January 2015).

Ter Hofstede, R., and Rijnsdorp, A. D. 2011. Comparing demersal fish assemblages between periods of contrasting climate and fishing pressure. ICES Journal of Marine Science, 68: 1189–1198. http://www.scopus.com/inward/record.url?eid=2-s2.0-79959492760&partnerID=tZOtx3y1 (Accessed 13 January 2015).

Thygesen, U. H., and Nielsen, A. 2009. Lessons from a Prototype Geolocation Problem. Media: 257–276.

Thygesen, U. H., Pedersen, M., and Madsen, H. 2009. Geolocating fish using hidden Markov models and data storage tags. *In* Tagging and Tracking of Marine Animals with Electronic Devices, pp. 277–293. http://www.springerlink.com/index/10.1007/978-1-4020-9640-2\nhttp://www.springerlink.com/index/W74738N630T07016.pdf.

Tyler A., Dunn R. Ration, growth, and measures of somatic and organ condition in relation to meal frequency in winter flounder, *Pseudopleuronectes americanus*, with hypotheses regarding population homeostasis. Journal Of The Fisheries Research Board of Canada [serial online]. January 1976; 33(1): 63. Available from: Supplemental Index, Ipswich, MA. Accessed February 21, 2015.

Warner, R. R., and Chesson, P. L. 1985. Coexistence mediated by recruitment fluctuations: A field guide to the storage effect.

Weinberg, J. R. 2005. Bathymetric shift in the distribution of Atlantic surfclams: response to warmer ocean temperature. ICES Journal of Marine Science, 1453: 1444–1453. http://icesjms.oxfordjournals.org/cgi/doi/10.1016/j.icesjms.2005.04.020 (Accessed 12 January 2015).

Wilber, D. H., Davis, D., Clarke, D. G., Alcoba, C. J., and Gallo, J. 2013. Winter flounder (*Pseudopleuronectes americanus*) estuarine habitat use and the association between spring temperature and subsequent year class strength. Estuarine, Coastal and Shelf Science, 133: 251–259. Elsevier Ltd. http://dx.doi.org/10.1016/j.ecss.2013.09.004.

Wilson, S. G., Stewart, B. S., Polovina, J. J., Meekan, M. G., Stevens, J. D., and Galuardi, B. 2007. Accuracy and precision of archival tag data: A multiple-tagging study conducted on a whale shark (Rhincodon typus) in the Indian Ocean. Fisheries Oceanography, 16: 547–554. http://doi.wiley.com/10.1111/j.1365-2419.2007.00450.x (Accessed 7 January 2015).

Winton, M., Wuenschel, M. J., and Mcbride, R. S. 2014. Investigating spatial variation and temperature effects on maturity of female winter flounder (*Pseudopleuronectes americanus*) using generalized additive models. Canadian Journal of Fisheries and Aquatic Sciences, 71: 1279–1290. http://www.nrcresearchpress.com/doi/abs/10.1139/cjfas-2013-0617 (Accessed 13 January 2015).

Wirgin, I., Maceda, L., Grunwald, C., Roy, N. K., and Waldman, J. R. 2014. Coastwide Stock Structure of Winter Flounder Using Nuclear DNA Analyses. Transactions of the American Fisheries Society, 143: 240–251. http://www.tandfonline.com/doi/abs/10.1080/00028487.2013.847861.

Witting, D. a., and Able, K. W. 1995. Predation by sevenspine bay shrimp Crangon septemspinosa on winter flounder Pleuronectes americanus during settlement: Laboratory observations. Marine Ecology Progress Series, 123: 23–32.

Witting, D. A., Able, K. W., and Fahay, M. P. 1999. Larval fishes of a Middle Atlantic Bight estuary: assemblage structure and temporal stability.

Wuenschel, M. J., Able, K. W., and Byrne, D. 2009. Seasonal patterns of winter flounder *Pseudopleuronectes americanus* abundance and reproductive condition on the New York Bight continental shelf. Journal of Fish Biology, 74: 1508–1524. http://onlinelibrary.wiley.com/doi/10.1111/j.1095-8649.2009.02217.x/full (Accessed 13 January 2015).

Yergey, M. E., Grothues, T. M., Able, K. W., Crawford, C., and DeCristofer, K. 2012. Evaluating discard mortality of summer flounder (Paralichthys dentatus) in the commercial trawl fishery: Developing acoustic telemetry techniques. Fisheries Research, 115-116: 72–81. Elsevier B.V. http://dx.doi.org/10.1016/j.fishres.2011.11.009.

Young, T.A., Daly, A.M., and K.R. Cooper. 2004. Pure compound and sediment elutriate embryo larval assay of winter flounder from the Hudson/ Raritan Estuary and Long Island Sound. Marine Environmental Research. 50: 243-246